High Frequency Transformer for Switching Mode Power Supplies

by

Fu Keung Wong

B. Eng. and M. Phil.

School of Microelectronic Engineering

Faculty of Engineering and Information Technology

Griffith University, Brisbane, Australia

Submitted in fulfillment of the requirements of the degree of

Doctor of Philosophy

March 2004

The material in this thesis has not been previously submitted for a degree or diploma in any university. To the best of my knowledge and belief, the thesis contains no material previously published or written by another person except where due reference is made in the thesis itself.

_____

Fu Keung Wong

Acknowledgments

In loving memory of my mother.

Firstly, thanks to my Principle Supervisor, Prof. Junwei Lu and Associate Supervisor, Prof. David Thiel for their supervision and many innovative suggestions. Without their constant guidance, encouragement and support, this thesis could not have been completed. I am also greatly appreciated to the faith they have both shown in my abilities.

I wish to thank the Dean, Prof. Barry Harrison for his suggestion of thesis writing.

Many thanks go to Dr. Dennis Sweatman, Mr. Raymond Sweatman and Dr. Jisheng Han for their support and helpful advice in the “Clean Room”. I am also thankful to Dr. Eddie Tse and Dr. Kuan Yew Cheong for their invaluable suggestions and encouragement.

A sincere gratitude is extended to Mr. Wat, Kai Sau for the provision of printed circuit board materials and precise fabrication with nothing for return. It is a true friendship.

Special thanks to my father for his long-lasting support and guidance.

Finally, my deep gratitude goes to my wife Lai-Ching, for her understanding and continuous support with love. She is patiently looking after the children to free me from domestic chores. Her spiritual inspiration and encouragement are always an important

part of my life. Also not forgetting my daughters, Tin-Yan and Sze-Yan, they make my headache disappeared and put happiness in my mind.

Contents

List of Figures

List of Tables

List of Publications

Journal Paper:

1. Fu Wong, Jun Lu and David Thiel, **"Design Consideration of High Frequency Planar Transformer"**, *IEEE Transactions on Magnetics*. (accepted)

2. Fu Wong, Jun Lu and David Thiel, **"Characteristics of High Frequency Planar Transformer with Helical Winding Structure"**, *Series of Japan Society of Applied Electromagnetism and Mechanics (JSAEM)*, vol. 14, 2003. pp. 213-217.

3. Jun Lu and Fu Wong, **"Faraday Shielding in Coaxial Winding Transformer"**, *International Journal Of Applied Electromagnetics and Mechanics*, Vol. 11, No. 4. July 2001. pp. 261-267.

4. Fu Wong and Jun Lu, **"High Frequency Planar Transformer with Helical Winding Structure"**, *IEEE Transactions.. on Magnetic*, September 2000. pp.3524-3526.

Conference Paper:

1. Fu Wong**, "Power Performance of Planar Transformer with Helical Winding Structure"**, Microelectronic Engineering Research Conference, 2003.

2. Fu Wong and Jun Lu**, "Design Consideration for High Frequency Planar Transformer"**, IEEE Intermag 2002.

3. Fu Wong and Jun Lu, **"Characteristics of High Frequency Planar Transformer with Helical Winding Structure"**, JANZS Japan, January 2002.

4. Jun Lu and Fu Wong, **"Effectiveness of Shielded High Frequency Coaxial Transformer for Switching Power Supplies"**, 2002 International Symposium & Technical Exhibition on Electromagnetic Compatibility.

5. Fu Wong, **"New Design Rule for High Frequency Planar Transformer"**, Microelectronic Engineering Research Conference, 2001.

6. Fu Wong and Jun Lu**, "High Frequency Planar Transformer with Helical Winding Structure"**, IEEE Intermag 2000.

7. Jun Lu and Fu Wong, **"High Frequency Coaxial Transformer with Faraday Shield"**, IEEE Intermag 2000.

8. Fu Wong and Jun Lu, **"Helical Printed Circuit Winding for High Frequency Planar Transformers"**, 9th MAGDA Conference of Electromagnetic Phenomena and Dynamics, 2000.

9. Jun Lu and Fu Wong, **"Effectiveness of Shielding Coil in High Frequency Coaxial Transformer"**, 9th MAGDA Conference of Electromagnetic Phenomena and Dynamics, 2000.

10. Fu Wong and Jun Lu, **"Helical Winding Structure for High Frequency Planar Transformers"**, MERC99.

Abstract

A power supply is an essential part of all electronic devices. A switching mode power supply is a light weight power solution for most modern electronic equipment. The high frequency transformer is the backbone of modern switched mode power supplies. The skin effect and proximity effects are major problems in high frequency transformer design, because of induced eddy currents. These effects can result in transformers being destroyed and losing their power transferring function at high frequencies. Therefore, eddy currents are unwanted currents in high frequency transformers. Leakage inductance and the unbalanced magnetic flux distribution are two further obstacles for the development of high frequency transformers.

Winding structures of power transformers are also a critical part of transformer design and manufacture, especially for high frequency applications.

A new planar transformer with a helical winding structure has been designed and can maintain the advantages of existing planar transformers and significantly reduce the eddy currents in the windings. The maximum eddy current density can be reduced to 27% of the density of the planar transformer with meander type winding structure and 33% of the density of the transformer with circular spiral winding structure at an operating frequency of 1MHz. The voltage ratio of the transformer with helical winding structure is effectively improved to 150% of the voltage ratio of the planar transformer with circular spiral coils.

With the evenly distributed magnetic flux around the winding, the planar transformer with helical winding structure is excellent for high frequency switching mode power supplies in the 21st Century.

Chapter 1

Introduction

Power supply is essential for all electronic devices. No electronic circuit can function without some form of power. The need for power supply in modern electronic equipment is demanding. Drawing from the proliferation of microprocessor-based electronics and the shorter life cycles of the semiconductor market, alternating current/direct current (AC/DC) switching mode power supplies experienced strong growth in 2000. The U.S. consumption of merchant internal AC/DC switching mode power supplies was over U.S. $3.1 billion in 1998. The market was forecast to increase at a compound annual growth rate (CAGR) of 9.2%, reaching over U.S. $4.8 billion in 2003 [1]. However, the synchronized global economic downturn has resulted in the postponement of delivery dates and the cancellation of some shipments. In spite of the setback, the industry was recorded as being worth U.S. $4.2 billion in 2002 [2]. The market of AC/DC switching mode power supplies is currently forecast to bring in $4.9 billion by 2007.

Frost and Sullivan (F & S) predicts the entire power supply industry will grow at a CAGR of 6.5% through 2009, bringing in revenues of $15.6 billion. To date, the

largest product segment is the AC/DC switching mode power supplies. F & S estimates 64.4% of the total market in 2002 was held by AC/DC modules but this share is expected to erode steadily in the future. DC/DC revenues and shipments are predicted to eat into the market share of AC/DC devices because of the increased use of modular and distributed power architectures, which allow multiple DC/DC converters to be used within one AC/DC front-end supply.

By 2009, the revenue share of DC/DC modules will grow to 41.7%, up from 35.6% in 2002, while the revenue share of AC/DC switching mode power supply contracts will grow to 58.3%. No matter what the proportion of the revenue share between them, the need for switching mode power supplies is enormous in the 21st Century.

The technical requirements of these AC/DC switching mode power supplies and DC/DC converters are increasing to match the rapid growth of semiconductor technologies. For example, the power supply for mobile phones needs to have the advantages of light weight, high efficiency and multi-outputs. The efficiency of switching mode power supplies can be increased by using higher operating frequencies. The size of the passive components, such as output capacitors, transformers and inductors, is further reduced as the frequency of switching operation increases. With the higher efficiency, the power loss will be less during the power conversion, therefore the size of the heat sink to protect the switching elements can be smaller. The requirements of light weight and high efficiency can be achieved.

1.1 Essentials of High Frequency Magnetics

Magnetic components are irreplaceable elements of switching mode power supplies. As simple as a buck converter, shown in Figure 1.1, an inductor is one of the four necessary components of the circuit.

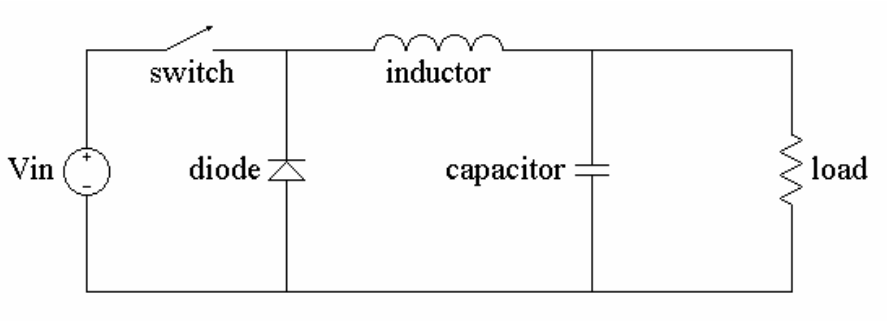

Figure 1.1 Buck converter.

The same situation occurs in the other two basic switching topologies. They are the boost converter and the buck-boost converter. A high frequency magnetic component is essential for switching mode power supplies.

With the requirement for multi outputs, a high frequency transformer must be used. Figure 1.2 shows a forward converter with multi outputs. By employing a high frequency transformer, multiple outputs of the switching mode power supply can be achieved.

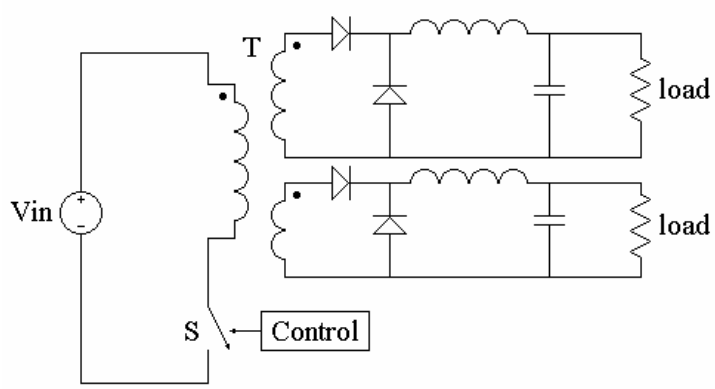

Figure 1.2 Forward converter with multi-outputs.

Therefore, high frequency magnetic components are necessary in switching mode power supplies. Especially, high frequency transformers are irreplaceable magnetic components if multiple outputs and electrical isolation are required.

1.2 Brief Outline the Existing Problems in High Frequency Magnetics

One of the main difficulties in the miniaturization of power conversion circuits, such as AC/DC switching mode power supplies and DC/DC converters, is the construction of inductors and transformers. Increased switching frequency can, in general, lead to decreased size of magnetic components. However, at a frequency in the MHz region, several problems arise. Core materials commonly used in the 20-500 kHz region have rapidly increasing hysteresis and eddy current loss at higher frequencies. Furthermore, eddy current loss in the windings can also become a severe problem.

The three electromagnetic phenomena, eddy current flowing in the copper wires, leakage inductance between the primary and secondary windings, skin effects and approximate effects, are obstacles for transformers operating at high frequencies. Eddy current is undesirable current inside the winding of transformers. It is the principal factor in introducing skin effects and approximate effects inside the copper windings, and strengthens the leakage inductance between the primary winding and the secondary winding of high frequency transformers. Therefore, eddy current is the chief obstacle of high frequency transformer design.

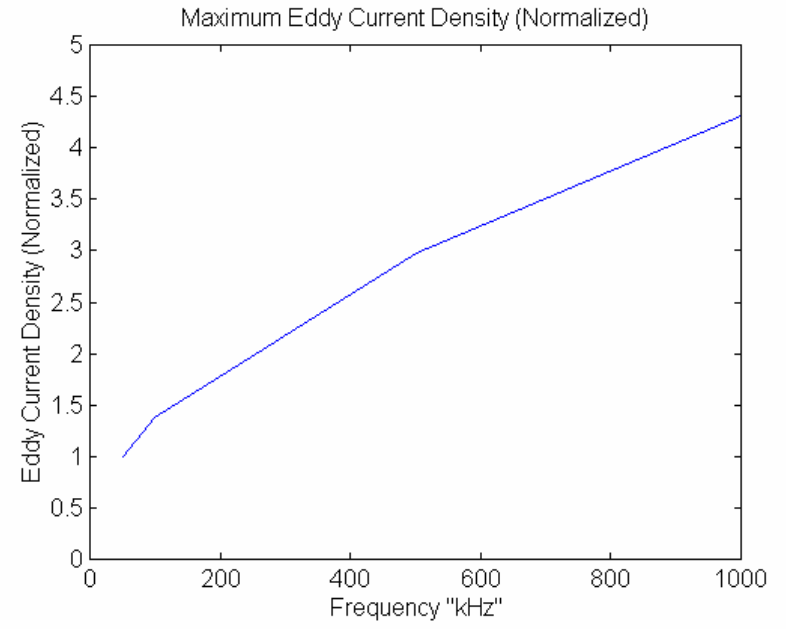

Figure 1.3 Maximum eddy current density (normalized) in the copper wiring of a traditional transformer operating at different frequencies [3].

Unbalanced magnetic flux distribution is the other defect of high frequency transformer design. Magnetic flux concentrated in a particular area will decrease the coupling efficiency and increase the chance of generating hot spots inside the transformer.

Therefore, eddy current flowing in transformers and the unbalanced distribution of magnetic flux are the major obstacles to the development of high frequency transformers at the end of 20th century.

In the 21st century, with the rapid growth of semiconductors, a great demand for high performance power supplies is expected. A new transformer for high frequency applications must be quickly developed to meet the huge demand in this century.

1.3 Chapter Preview

An overall review of fundamentals of high frequency power transformers is made in Chapter 2. The operating frequency of power transformers from 25 cycles per second increased to 50/60 Hz, and from this line frequency further increased to high frequencies of few hundreds of kHz. From materials to structures, the framework of power transformers can be seen in Chapter 2. The characteristic of the high frequency magnetic material – ferrite is introduced. The development trend of the ferrite material s in the last decade of the 20th century is outlined. The development of ferrite materials reflects that the winding structure is one of the critical factors to build up high frequency magnetic components.

The importance of winding structure of high frequency transformers is explained in depth in Chapter 3 with the fundamental electromagnetic phenomena, such as eddy current, skin effect, proximity effect and leakage inductance. Two winding structures used in high frequency transformers are introduced.

A new planar winding structure – Helical Winding Structure – is proposed in Chapter 4. With numerical simulation, the winding structure is found to have excellent performance at high frequency range. It has an evenly distributed magnetic flux around the winding and a low eddy current density in the conductors. The voltage ratio and power performance of the structure are also investigated. The experimental results support the structure working well in high frequency power transferring applications.

Conclusions are given in Chapter 5, and further direction of the research of helical winding structure is recommended.

1.4 References

1. Mark Gaboriault, Executive White Paper, U.S. Merchant Markets and Applications for AC/DC Switching Power Supplies and DC/DC Converters, 8th Ed., Venture Development Corporation, Nov 1999.

2. *"Power Supplies Market Outlook – Power Supplies Face Slow, Steady Recovery"*, Electronic Components, September 2003, pp.154.

3. Fu Wong, *High Frequency Switching Resonant Converters: Magnetics and Gate Drive Considerations*, Master Dissertation, Griffith University, May 1997.

Chapter 2

Fundamentals of High Frequency Power Transformer

Transformers are well known building blocks in electronics. On 29 August 1831, the first transformer was discovered. On the date, Michael Faraday carried out his famous ring transformer experiments. This famous experiment involved an iron ring and two coils, *A* and *B*. Coil *A* was made of three sections wound on the left-hand side of the ring. Coil *B* was made of two sections wound on the right-hand side. It is of interest to note that this arrangement constituted the first transformer in the world. The terminals of coil *B* were connected to a long wire passing above a magnetic needle. One section of coil *A* was connected to a battery. On making the connection, Faraday observed that the needle moved, oscillated, and then settled down on its original rest position. When he

disconnected the coil *A* from the battery, the needle moved again. Faraday repeated the experiment, but with three sections of coil A connected to the battery, and he observed that the effect on the needle was much stronger than before.

This idea was developed further in Joseph Henry's experiments in 1832, and was closely followed in 1836 by C. G. Page's work on what he termed a "dynamic multiplier". Page correlated the phenomena of self-induction and induction between two discrete conductors. From the prototype of the transformer, he evolved a design that featured a separate primary winding and a secondary winding [1, 2].

In 1856, C. F. Varley devised a device in which the advantages of a subdivided iron core to secure minimum eddy-current loss were combined with a simple construction. The core in Varley's construction was a bundle of iron wires. The primary and secondary windings were wound over the center one third of the core length. The ends of core wires were turned back over the windings to complete the magnetic circuit.

Close to 30 years later, Lucien Gaulard and John D. Gibbs introduced a system of single-phase 2000 V_{ac} distribution. The backbone of the system was a transformer with a core of soft iron wire with a primary of insulated wire coil that was surrounded by six equal coils. The secondary windings were brought out to separate terminals on the side, so that the six sections can be used if required. It was the ancestor of transformer with multiple outputs.

In 1885, George Westinghouse read the use of alternating current in Europe in conjunction with transformers displayed in England by L. Gaulard and J. D. Gibbs. The transformer configuration patented by Gaulard and Gibbs utilized multiple one-to-one turns-ratio transformers with primary windings connected in series across the high voltage primary circuit. The secondary circuit then supplied an individual low voltage secondary. Westinghouse bought the American rights from Gaulard-Gibbs patents and authorized the development of equipment for an experimental power plant at Great Barrington, Massachusetts. Under the direction of William Stanley, the Westinghouse transformers, which were designed in 1886, had the primary windings for the individual

units connected in parallel across the high voltage primary circuit rather than in series. With his tests being successful, Westinghouse marketed the first commercial alternating current system at the end of 1886.

In the 1910's and 1920's, the electrical technology was advanced enough for transformer technology. The knowledge about coil properties, metallurgy, insulating materials, etc. was commonly known. The materials may not have been as sophisticated as what they are today, but the principles were the same and the products worked very well [2, 3].

Nikola Tesla was influential in standardizing the frequency of power distribution systems to 60 cycles in the USA. A frequency of 25 cycles had been common in some areas of the United States and Canada in the late 1920's to the early 1930's. It was used because power apparatus, such as synchronous converters and alternating-current commutator motors, works better at this lower frequency. However, at 25 cycles the flicker of lamps can be seen and is objectionable. The advantage of the higher frequency is that transformers require less iron and copper making them less expensive and lighter in weight. It is the earliest experimental result to demonstrate the size related with the operating frequency of a transformer.

Some of older transformers were for use with 25/40 cycle currents. Others were rated at 50/133 cycles. Fortunately, a 25/40-cycle transformer can be used safely with today's 60-cycle house current. About 1965, the term for line frequency was changed from cycles to hertz (Hz), and the line frequency around the world was standardized at 50/60 Hz.

For the line frequency of 50/60 Hz, transformers have been well developed for the power applications in the last century. The principle consideration for power transformers operating at line frequency is the losses in the magnetic core. Core materials and core structures have been deeply investigated. The hysteresis losses and the eddy current losses in the magnetic core can be minimized by high-saturation flux density materials, such as low-silicon iron and silicon steel, with laminated transformer

core structure. Although the transformer is not ideal, it is good enough to complete the task of power conversion at line frequency of 50/60 Hz.

2.1 Birth of High Frequency Power Transformer

Whereas the invention of the semiconductor integrated circuit brought sudden and dramatic improvements in the size, cost and performance of electronic equipment, especially computers and portable telecommunication instruments, it also induced more requirements for the power supply system. Early minicomputer power supplies consisted of 50/60 Hz line frequency power transformer for high to low voltage transformation, followed by rectifiers and linear dissipative regulators. The line frequency power transformers were always big and heavy. In addition, the inefficiency of the linear regulators required large heat sinks for cooling, therefore adding more weight and size to the power supply. As long as electronic equipment itself was large, large size power supplies were not a critical problem. However, the size of the equipment itself became smaller through advances in semiconductor processing, bulky and inefficient power supplies were therefore unacceptable.

Fortunately, during the 1960s, the U. S. Navy and some aerospace organizations developed the switching mode power supply technologies which reduce the size and weight of power supply systems. Theoretically, the techniques of switching mode power supply had been developed for many years, but the practical application of these techniques did not move very quickly. It is because of the shortage of high frequency power switch components and magnetic materials. The dream of high frequency switching mode power supplies became true in the 1950s, when power transistors and the silicon controlled rectifier (SCR) were available [4, 5]. These new semiconductor switches enabled the development of multi-kHz switching power converters which use smaller power transformers and filter components compared with their 50/60 Hz counterparts. At the same time, pulse width modulation techniques were found to control these switching power converters and regulate their outputs. With these developments, the stage was set to advance the state of the art in commercial power electronics technology.

At first, low voltage DC-DC converters replaced the linear regulators on the secondary side of the line frequency transformers. These converters achieved regulation by varying the duty cycle of the power switch rather than by dropping excess voltage across a "variable resistance" transistor as in the linear regulator. This approach improved power system efficiency, but the bulky line frequency step down transformer still remained. Very soon thereafter high voltage (500-1000 V_{ceo}) power switching transistors became available and enabled the development of the high frequency (20-50 kHz) "direct-off-line" switching power supplies [6]. Off-line switchers, as they have come to be known, rectify the utility line directly, without any step down transformers, and filter the rectified input with large electrolytic capacitors. This unregulated DC voltage is chopped into a high frequency square wave so that a much smaller power transformer can be used to change the voltage level. The regulating function can be accomplished through the control of the duty cycle of the power switches. Thus, both the large step down transformers and inefficient linear regulators were eliminated.

The operating frequency of power transformers suddenly jumped up from line frequency of 50/60 Hz to few tens kilohertz, even up to few hundreds kilohertz in a decade. The name of "high frequency power transformer" has been introduced by the researchers to make the difference to the traditional power transformer of line frequency of 50/60 Hz. In the last decade of the twentieth century, the term of the "decade of power electronics" was introduced by a famous power electronic researcher, B. K. Bose. He pointed out that the device evolution along with converter, control and system evolution has been so spectacular in the decade, and the operating frequency of high frequency power transformers has been driven to Megahertz level. It is much far away from the line frequency [7, 8].

The term of high frequency power transformers is referred to the line frequency, 50/60 Hz. Actually the transformers employed in switching mode power supply applications should be considered as low frequency electromagnetic devices. It follows the low frequency approximations – for all problems in which the excitation frequency times a characteristic dimension is small compared with the speed of light, the

"displacement current" in Maxwell's equations can be neglected without introducing perceptible errors. The upper limit to low frequency analysis is generally about 10-50 MHz in practical applications [9]. The high frequency power transformers discussing in the thesis are operated within this frequency range.

It is often said that solid-state electronics brought in the first electronics revolution, whereas solid-state power electronics brought in the second electronics revolution. It is interesting to note that power electronics essentially blends the technologies brought in by the mechanical age, electrical age and electronic age. It is truly an interdisciplinary technology. In the 21st century, power electronics is one of the two most dominating areas in the highly automated industrial environment, according to B. K. Bose's prognosis for the 21st century's Energy, Environment and Advance in Power Electronics. High frequency power transformer is the backbone of the modern power electronics. The investigation of high frequency power transformers for switching mode power supply application is very important for 21st century power electronic area.

2.2 Basic Theory of Transformer

The theory of transformers is based on Faraday's law: the induced *emf* equals the negative rate of time variation of the magnetic flux through the contour. The input current flowing through the primary winding generates a time varying magnetic flux, and this time varying flux will induce an output voltage coming out from the secondary winding of the transformer. So transformers are inductors that are coupled through a shared magnetic circuit, that is, two or more windings that link some common flux, shown as Figure 2.1.

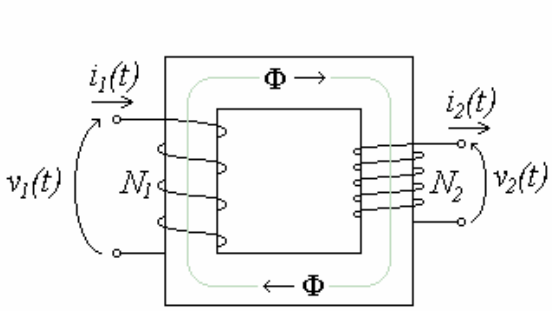

Figure 2.1 Schematic diagram of a transformer.

Theoretically, a transformer is an alternating-current device that transforms voltages, currents, and impedances. Faraday's law of electromagnetic induction is the principle of operation of transformers. For the closed path in the magnetic circuit, shown in Figure 2.1, traced by magnetic flux, the magnetic circuit can be expressed as:

$$N_1 i_1 - N_2 i_2 = \Phi \Re, \tag{2.1}$$

where Φ is the magnetic flux, $\Re$ is the reluctance for the magnetic path, N_1, N_2 and i_1, i_2, are the numbers of turns and the current in the primary and secondary windings, respectively. According to Lenz's law, the induced *mmf* in the secondary winding, $N_2 i_2$, opposes the flow of the magnetic flux Φ created by the *mmf* in the primary winding, $N_1 i_1$. The reluctance is defined as,

$$\Re = \frac{l}{\mu A_c} \tag{2.2}$$

where l is the length of the magnetic path, μ is the permeability of the core material, and A_c is the cross section area of the path. Then Eqn. (2.1) can be written as:

$$N_1 i_1 - N_2 i_2 = \Phi \frac{l}{\mu A_c} \tag{2.3}$$

If $\mu \to \infty$, then

$$\frac{i_1}{i_2} = \frac{N_2}{N_1} \tag{2.4}$$

and this transformer is defined as an ideal transformer [10]. According to Faraday's law,

$$v_1 = N_1 \frac{d\Phi}{dt} \tag{2.5}$$

$$v_2 = N_2 \frac{d\Phi}{dt} \tag{2.6}$$

then the ratio of the voltages across the primary and secondary windings of an idea transformer is equal to the turns ratio, i.e.

$$\frac{v_1}{v_2} = \frac{N_1}{N_2} \tag{2.7}$$

The coefficient of coupling,

$$K = \frac{L_{12}}{\sqrt{L_{S1}L_{S2}}}, \tag{2.8}$$

where L_{12} is the mutual inductance, L_{S1} is the primary self-inductance and L_{S2} is the secondary self-inductance. The coupling coefficient is equal to 1, if $L_{12} = \sqrt{L_{S1}L_{S2}}$ (no leakage inductance). The model of an ideal transformer is shown in Figure 2.2.

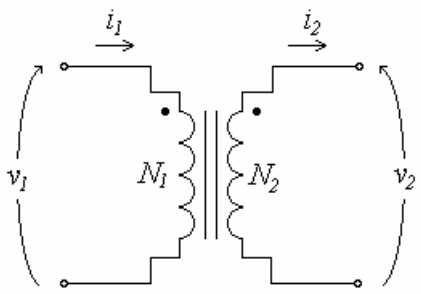

Figure 2.2 Model of ideal transformers.

According to this ideal transformer model, a practical model for a transformer, shown in Figure 2.3, can be made. In a practical transformer, there are some additional elements, such as primary leakage inductance, L_1, secondary leakage inductance, L_2, equivalent magnetizing inductance of primary, L_m, primary winding resistance, R_1, secondary winding resistance, R_2, equivalent resistance corresponding to core losses, R_c.

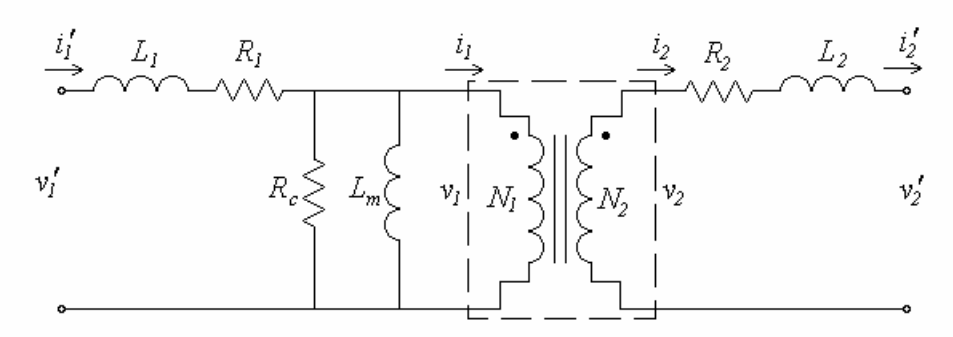

Figure 2.3 Model of practical transformers.

The voltages of the practical transformer can be expressed as:

$$v_1' = L_{S1}\frac{di_1'}{dt} - L_{12}\frac{di_2'}{dt} \tag{2.9}$$

$$v_2' = L_{12}\frac{di_1'}{dt} - L_{S2}\frac{di_2'}{dt} \tag{2.10}$$

where L_1, L_2, and L_{12} are the self-inductance of the primary winding, the self-inductance of the secondary winding, and the mutual inductance between the primary and secondary windings, respectively. The coefficient of coupling, K, is less than 1, as $L_{12} < \sqrt{L_{S1}L_{S2}}$, because the leakage inductance exists in the windings.

For high frequency applications, the equivalent circuit of a transformer becomes more complex. Figure 2.4 shows the equivalent circuit of a broadband transformer over a nominal frequency range of 20 Hz to 20 kHz [11].

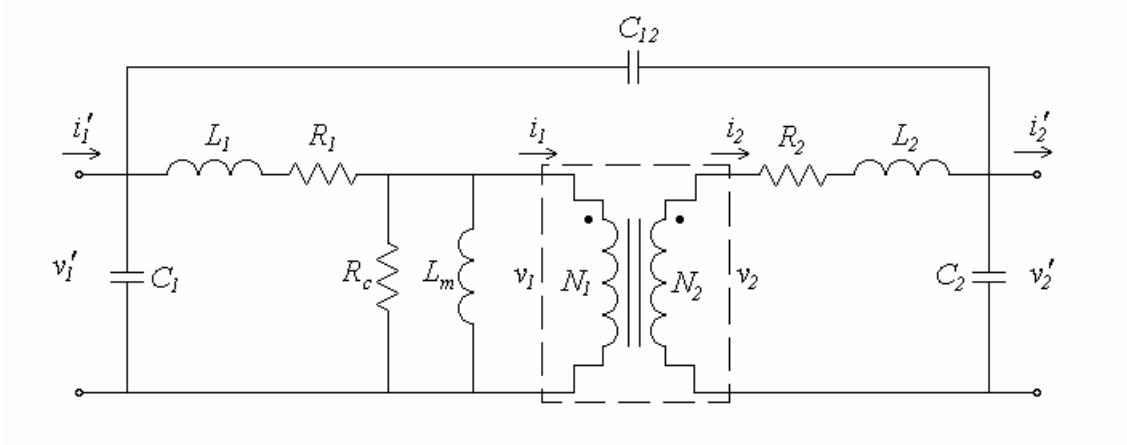

Figure 2.4 Equivalent circuit of a broadband transformer.

In a broadband transformer model, there are three more parasitic elements, primary shunt and distributed capacitor, C_1, secondary shunt and distributed capacitor, C_2, and primary to secondary interwinding capacitance, C_{12}.

Besides the broadband transformer model, a network transformer model for high frequency transformers has been developed [12]. It is also known as the distributed parameter model for a high frequency transformer. This model is useful in determining the voltage distribution on the windings. This model will not be discussed further in the thesis, however, it is evidence to prove the change of the model from the low frequency

conventional transformer to the high frequency transformer. As mentioned in Section 2.1 the term of high frequency power transformers of power supply applications is referred to the traditional line frequency power transformers, but they should be classified as low frequency electromagnetic devices, according to the low frequency approximations.

2.3 Numerical Analysis of High Frequency Transformer

Electromagnetic fields carry energy in all electromagnetic devices and systems. Therefore, the accurate analysis and computation of electromagnetic fields is the essential basis to investigate the characteristics of these devices and systems.

2.3.1 Basic Field Equations

For introducing the field equations, it is convenient to consider an elementary model configuration for eddy currents. This model consists of:

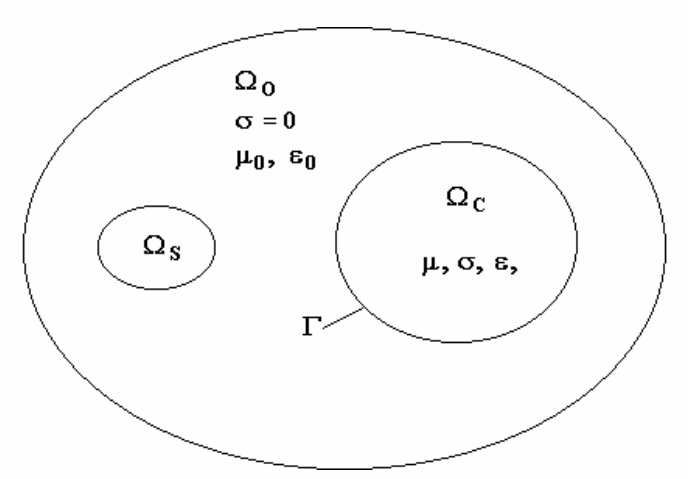

Figure 2.5 Eddy currents configuration model.

where Ω_S : a region containing exciting sources;

Ω_C : a conductive volume bounded by boundary Γ ; and

Ω_O : an outer space region full of air.

This model can represent a number of industrial application problems included high frequency power transformers in electrical engineering.

It is well known that the displacement current term in the Maxwell equations can be neglected if the dimension of the regions Ω_S and Ω_C are small compared with the wavelength of the prescribed fields. Such problems are so-called quasi-static electromagnetic problems [13].

In this situation, the Maxwell equations can be expressed by:

$$\nabla \times \vec{H} = \vec{J}_e + \vec{J}_0 \tag{2.11}$$

$$\nabla \times \vec{E} = -\frac{\partial \vec{B}}{\partial t} \tag{2.12}$$

$$\nabla \cdot \vec{B} = 0 \tag{2.13}$$

$$\nabla \cdot \vec{D} = \rho \tag{2.14}$$

where $\vec{H}$ is magnetic field strength (A/m),

$\vec{B}$ magnetic flux density (T),

$\vec{E}$ electric field strength (V/m),

$\vec{D}$ electric displacement (C/m^2),

$\vec{J}_e$ eddy current density (A/m^2),

$\vec{J}_0$ external current density (A/m^2) and

ρ free charge density (C/m^3).

These variables are related by the material constitutive equations:

$$\vec{B} = \mu \vec{H} \tag{2.15}$$

$$\vec{D} = \varepsilon \vec{E} \tag{2.16}$$

and when no motion is involved:

$$\vec{J}_e = \sigma \vec{E} \tag{2.17}$$

where μ is permeability (H/m),

σ conductivity (S/m) and

ε permittivity (F/m).

At the interface between two different media the field vectors must satisfy the following continuity conditions:

$$\vec{H}_1 \times \vec{n} = \vec{H}_2 \times \vec{n} + \vec{K} \tag{2.18}$$

$$\vec{E}_1 \times \vec{n} = \vec{E}_2 \times \vec{n} \tag{2.19}$$

$$\vec{B}_1 \cdot \vec{n} = \vec{B}_2 \cdot \vec{n} \tag{2.20}$$

$$\vec{D}_1 \cdot \vec{n} = \vec{D}_2 \cdot \vec{n} + S \tag{2.21}$$

where $\vec{n}$ is the normal unit vector, $\vec{K}$ is the surface current density perpendicular to $\left(\vec{H} \times \vec{n}\right)$, S is surface charge density.

For the time harmonic eddy current problems, Eqn. (2.21) can be rewritten as [14]:

$$\left(\varepsilon_1 - \frac{\sigma_1}{j\omega}\right)\dot{\vec{E}}_1 \cdot \vec{n} = \left(\varepsilon_2 - \frac{\sigma_2}{j\omega}\right)\dot{\vec{E}}_2 \cdot \vec{n} \tag{2.22}$$

where $\dot{\vec{E}}$ is the complex phaser of electric field strength.

2.3.2 Magnetic Vector Potential and Electrical Scalar Potential

In the 2-D eddy current problems, it is significantly beneficial to use magnetic vector potential $\vec{A}$ as a solution variable, because $\vec{A}$ has only one component in many 2-D application problems. Therefore in this section, a magnetic vector potential will be introduced, and then some properties of magnetic vector potential are to be observed.

Since Eqn. (2.13), magnetic vector potential $\vec{A}$ can be introduced by:

$$\vec{B} = \nabla \times \vec{A} \tag{2.23}$$

and then inserting Eqn. (2.23) into Eqn. (2.12), it follows that,

$$\vec{E} = -(\frac{\partial \vec{A}}{\partial t} + \nabla \phi) \tag{2.24}$$

thus

$$\vec{J}_e = -\sigma(\frac{\partial \vec{A}}{\partial t} + \nabla\phi) \tag{2.25}$$

where ϕ is electrical scalar potential.

In inserting Eqns. (2.23) and (2.25) into Eqn. (2.11), the following can be obtained:

$$\nabla \times \frac{1}{\mu}\nabla\vec{A} + \sigma(\frac{\partial \vec{A}}{\partial t} + \nabla\phi) = \vec{J}_0 \tag{2.26}$$

The other equation can be derived from the current continuity condition: $\nabla \cdot \vec{J} = 0$. From Eqn. (2.25) it follows that

$$\nabla \cdot \sigma\frac{\partial \vec{A}}{\partial t} + \nabla \cdot \sigma\nabla\phi = 0 \tag{2.27}$$

These are the differential equations which vector potential $\vec{A}$ and scalar potential ϕ must obey in eddy current problems. However these two equations are not independent because Eqn. (2.27) is a consequence of taking the divergence of Eqn. (2.26).

On the other side, the magnetic vector potential $\vec{A}$ itself has no specific physical meaning. It is only an auxiliary variable, with which the analysis and computation of many field problems can be simplified. However, it is well known that the flux across a certain area can be expressed by the contour integral of the vector potential $\vec{A}$ along the closed boundary of this area [15].

From Eqns. (2.23 – 2.25), it can be seen that eddy current density cannot be calculated by the magnetic vector potential alone. This implies that the vector potential at a point does not directly correspond to the interlinkage flux across the area between this point and the reference point, where the vector potential $\vec{A}$ = 0. Therefore, $\nabla\phi$ is a

correction term to modify the interlinkage flux of the conductive media which is denoted by the vector potential.

From Eqns. (2.23 – 2.24), $\vec{A}$ and $\nabla\phi$ are not completely defined, i.e. the solution of the fields by using $\vec{A}$ and $\nabla\phi$ is not unique. It is because the gradient of an arbitrary scalar function can be added to $\vec{A}$ and the time derivative of the same function can be subtracted from ϕ without affecting the physical quantities, $\vec{E}$ and $\vec{B}$. The uniqueness of the solution can be assured by specifying the divergence of $\vec{A}$ and sufficient boundary conditions [16]. There are two types of gauge conditions used, they are:

Coulomb Gauge:

$$\nabla \cdot \vec{A} = 0 \tag{2.28}$$

and

Lorentz Gauge (Low frequency form):

$$\nabla \cdot \vec{A} = -\mu\sigma\phi \tag{2.29}$$

When using the Lorentz Gauge, the following two equations can be derived from Eqns. (2.26 – 2.27) and (2.29):

$$\nabla \times \frac{1}{\mu}\nabla\vec{A} = -\sigma\frac{\partial\vec{A}}{\partial t} + \sigma\nabla(\frac{1}{\mu\sigma}\nabla\cdot\vec{A}) \tag{2.30}$$

$$\nabla \cdot \sigma\nabla\phi - \mu\sigma^2\frac{\partial\phi}{\partial t} = 0 \tag{2.31}$$

where σ is assumed piecewise constant. This reflects the significant character that the equations containing $\vec{A}$ and $\nabla\phi$ is decoupled.

In the 2-D problems, the magnetic vector potential $\vec{A}$ has only one component, A_Z, as the exciting current flows parallel to the z-axis for the common case of infinitely long models. Thus, the vector potential $\vec{A} = A_z(x, y)\vec{e}_z$. It means that the Coulomb Gauge, Eqn (2.28) is automatically imposed. Therefore, the solution to the 2-D field problems with the vector potential $\vec{A}$ is unique, provided that the appropriate boundary conditions are prescribed.

The governing equation for the 2-D eddy current problems can be directly obtained from Eqn. (2.26), i.e.:

$$\nabla \cdot \frac{1}{\mu} \nabla A_z - \sigma \frac{\partial A_z}{\partial t} - \sigma(\nabla \phi \cdot \vec{e}_z) = -J_0 \tag{2.32}$$

where $\nabla \phi \cdot \vec{e}_z = \frac{\partial \phi}{\partial t}$.

2.3.3 Physical Meaning of $\nabla \phi$

From Eqns. (2.11) and (2.25), it follows that

$$\vec{J} = \vec{J}_e + \vec{J}_0 = -\sigma(\frac{\partial \vec{A}}{\partial t} + \nabla \phi) + \vec{J}_0 \tag{2.33}$$

where $\vec{J}$ is total current density.

In the 2-D case, where $\vec{J} = J\vec{e}_Z$. Thus, the total measurable current I can be obtained by:

$$I = \int_{\Omega} \vec{J} \cdot d\vec{\Omega} = \int_{\Omega} -\sigma(\frac{\partial \vec{A}}{\partial t} + \nabla \phi) \cdot d\vec{\Omega} + \int_{\Omega} \vec{J}_0 d\vec{\Omega} \tag{2.34}$$

According to the definition of I and $\vec{J}_0$,

$$\int_{\Omega} \vec{J}_0 d\vec{\Omega} = I \tag{2.35}$$

then

$$\int_{\Omega} \sigma(\frac{\partial \vec{A}}{\partial t} + \nabla \phi) \cdot d\vec{\Omega} = 0 \tag{2.36}$$

Thus, it follows that

$$\nabla \phi = -\frac{1}{\Omega} \int_{\Omega} \frac{\partial \vec{A}}{\partial t} d\vec{\Omega} \tag{2.37}$$

where Ω is the area of the cross section of the conducting domain. Therefore, in the 2-D electromagnetic field problems, $\nabla \phi$ is the mean value of $\frac{\partial \vec{A}}{\partial t}$ in the domain.

2.3.4 Basic Theory of the Boundary Element Method for Electromagnetics

The Boundary Element Method (BEM) has been developed on the basis of the integral equation method. The name of The Boundary Element Method was firstly proposed by Brebbia [17]. Concretely, the BEM is a numerical procedure for solving a boundary value problem. It consists of the following steps:

(1) Derivation of a BEM formulation

Starting from the governing differential equations describing the field problem, a boundary integral equation is deduced by application of the Weighted Residual Method. The so-called BEM formulation, corresponding to the field problem, is such a boundary integral equation.

(2) Discretization

All of the boundaries re discretized into a series of elements over which the function and its normal derivative are assumed to very according to interpolation functions, i.e. shape functions. The geometry of these elements may be modelled using straight lines, quadratic arcs, etc., for 2-D or triangular cells, plane parellelipipedal cells and so on for 3-D problems.

The discretized BEM equation is applied to a number of particular nodes, or the boundary nodes. Therefore, the number of the total discretizes equations is equal to the number of the boundary nodes.

(3) Integration

For nonsingular integrals, the integral over each element is carried out by using the Gaussian Quadrature Formulae. Various special methods have been used for singular integrals.

(4) Solution of the Equation System

By using the prescribed boundary conditions, a system of linear algebraic equations is obtained. The solution of the equation system, which can be affected by using direct or iterative methods, produces the remaining function data on the boundary.

(5) Calculation of the variables at interior points

By using the obtained boundary values on the boundary of the problem, the variables within the region can be calculated by applying the discretized BEM formulation to the corresponding interior points.

2.3.5 BEM Formulation for 2-D Electromagnetics

From Eqn. (2.29), a general governing equation for 2-D eddy current problems was derived by using $\vec{A}$ and ϕ. It has also been noted that $\nabla\phi$ can be neglected, if the line of the vector potential $\vec{A}=0$ can be selected to coincide with the central line of the eddy current loop. Therefore, without losing generality, the following differential equation will be derived,

$$\nabla\cdot\frac{1}{\mu}\nabla\vec{A}-\sigma\frac{\partial\vec{A}}{\partial t}=-\vec{J}_0 \tag{2.38}$$

Considering only the linear steady harmonic solution, i.e.

$$\vec{J}_0(x,y,t) = \mathrm{Re}\left\{\dot{J}_0(x,y)e^{j\omega t}\right\} \tag{2.39}$$

and

$$\vec{A}_0(x,y,t) = \mathrm{Re}\left\{\dot{A}_0(x,y)e^{j\omega t}\right\} \tag{2.40}$$

it follows that

$$\nabla^2 \dot{A} - j\omega\mu\sigma\dot{A} = -\mu\dot{J}_0 \tag{2.41}$$

where ω is angular frequency, $\omega = 2\pi f$, $\dot{A}$ and $\dot{J}_0$ are the complex phasor corresponding to $\vec{A}$ and $\vec{J}_0$ respectively.

If the Green function $G(r)$ satisfying the equation

$$\nabla^2 G(r) - j\omega\mu\sigma G(r) = \delta(r) \tag{2.42}$$

where $G(r) = \dfrac{e^{-kr}}{4\pi r}$,

$k^2 = j\omega\mu\sigma$, and

r is the distance between the field point at (x,y,z) and the source point at (x',y',z').

Applying Green's second theorem,

$$\int_V (G\nabla^2\vec{A} - \vec{A}\nabla^2 G)dV = \oint_S (G\frac{\partial\vec{A}}{\partial n} - \vec{A}\frac{\partial G}{\partial n})dS \tag{2.43}$$

and using Eqns. (2.41) and (2.42), the following expression is obtained:

$$\vec{A} = \int_V -\mu G\vec{J}_0 dV + \oint_S (\vec{A}\frac{\partial G}{\partial n} - G\frac{\partial\vec{A}}{\partial n})dS \tag{2.44}$$

where S is the boundary of the volume V and

n the outward normal to the boundary.

In the 2-D eddy current problems, the solution of Eqn. (2.42) is the Green function

$$G(r) = \frac{K_0(kr)}{2\pi} \tag{2.45}$$

where K_0 is the modified Bessel function of zero order and of the second kind, and the corresponding integral equation is

$$\vec{A} = \int_S -\mu G \vec{J}_0 dS + \oint_l (\vec{A}\frac{\partial G}{\partial n} - G\frac{\partial \vec{A}}{\partial n})dl \tag{2.46}$$

2.3.6 Magnetic Field inside the Region

According to Eqn. (2.23), the magnetic flux density $\vec{B}$ inside the region can be calculated by the following equations:

$$\dot{B}_{x,i}(x,y) = (\frac{\partial \dot{A}}{\partial y})_i \tag{2.47}$$

$$\dot{B}_{y,i}(x,y) = (\frac{\partial \dot{A}}{\partial x})_y \tag{2.48}$$

where (*x, y*) is the coordinate of the field point.

2.4 Analysis of Magnetic Materials for Power Transformers

Magnetic phenomena have been known and exploited for many centuries. The earliest experiences with magnetism involved magnetite, the only material that occurs naturally in a magnetic state. This mineral was also known as lodestone. According to its property of aligning itself in certain directions if allowed to rotate freely, it can be able to indicate the positions of north and south, and to some extent also latitude. The other well-known property of lodestone is that two pieces of it can attract or even repel each other.

After the production of iron from ores had become possible, it was realized that magnetite could also attract iron. There are many magnetic materials known today, and it is therefore useful first of all to give a very empirical rule for what might be called a magnetic material.

One of the most important applications of magnetic materials can be described in very general terms as the enhancement of the magnetic effects produced by a current-carrying coil. If a material is useful for such applications, it is necessary that it should be easily magnetized. Materials having this property are called soft magnetic materials. The term *soft* refers to their magnetic, not their mechanical property. However, the conditions in which the material is magnetized can vary widely, and a material that has useful soft properties in some applications, may be quite useless in others. A good soft magnetic material should have a large saturation magnetization, and the magnetization should be large even in relatively small applied field – in other words, it should have a large permeability. [18 - 20]

Soft magnetic materials exhibit magnetic properties only when they are subject to a magnetizing force such as the magnetic field created when current is passed through the wire surrounding a soft magnetic core. Soft ferromagnetic materials are generally associated with electrical circuits where they are used to amplify the flux generated by the electric currents. These materials can be used in a.c. as well as D.C. electrical circuits.

Soft magnetic materials play a key role in power distribution, make possible the conversion between electrical and mechanical energy, underlie microwave communication, and provide both the transducers and the active storage material for data storage in information systems.

The fundamental requirements of magnetic material for power transformers are the highest relative permeability, the largest saturation flux density, the lowest core loss, and the lowest remanent flux density. Magnetic materials using as the cores of power transformers keep changing as the operating frequency increased. At the line frequency of 50/60 Hz, iron, low-silicon iron and silicon steel are the major materials for the cores of the power transformers. They have high-saturation flux densities, thus they can handle high power transformation at low operating frequency. When the operating frequency of power transformer increased, the eddy currents inside the magnetic cores become a critical problem for the transformer designers. Although the laminated core materials have been used, the power losses generated by the eddy currents still heat up

the core significantly, and this hot spot generated inside magnetic core can destroy the whole power transformer.

Table 2.1 Properties of soft magnetic materials. [21, 22]

Material	Initial Perm. μ_i	B_{max} (kGausses)	Resistivity (Ω-cm)	Operating Frequency
Iron	250	22	10×10^{-6}	50-1000Hz
Low-Silicon Iron	400	20	50×10^{-6}	50-1000Hz
Silicon Steel	1500	20	50×10^{-6}	50-1000Hz
Nickel Iron Alloy	2000	16	40×10^{-6}	50-1000Hz
78 Permalloy	12000-100000	8-10	55×10^{-6}	1kHz-75kHz
Amorphous Alloy	3000-20000	5-16	140×10^{-6}	to 250kHz
Iron powder	5-80	10	10^4	100kHz-100MHz
Ferrite-MnZn	750-15000	3-5	10 - 100	10kHz-2MHz
Ferrite-NiZn	10-1500	3-5	10^6	200kHz-100MHz

As the operating frequency increased, more and more magnetic materials have been introduced for high frequency power transformer applications. Table 2.1 shows the major properties of magnetic materials common used in nowadays.

2.4.1 Introduction of Ferrite

Ferrites are ceramic materials, dark gray or black in appearance and very hard and brittle. The magnetic properties arise from interactions between metallic ions occupying particular positions relative to the oxygen ions in the crystal structure of the oxide. In magnetite, in the first synthetic ferrites and indeed in the majority of present-day magnetically soft ferrites the crystal structure is cubic, it has the form of the mineral spinal. The general formula of the spinel ferrite is $MeFe_2O_4$ where Me usually represents one or, in mixed ferrites, more than one of the divalent transition metals Mn, Fe, Co, Ni, Cu and Zn, or Mg and Cd. Other combinations, of equivalent valency, are

possible and it is possible to replace some or all of the trivalent iron ions with other trivalent metal ions.

In the early practical ferrites Me represented Cu + Zn, Mn + Zn, or Ni + Zn. The first of these compounds was soon abandoned and the other two, referred to as manganese zinc ferrites and nickel zinc ferrites (often abbreviated to MnZn ferrites and NiZn ferrites) were developed for a wide range of applications where high permeability and low loss were the main requirements. These two compounds are still by far the most important ferrites for high-permeability, low-loss applications and constitute the vast majority of present-day ferrite production. By varying the ratio of Zn to Mn or Ni, or by other means, both types of ferrites may be made in a variety of grades, each having properties that suit it to a particular class of application. The range of permeabilities available extends from about 15 for nickel ferrites to several thousand for some manganese zinc ferrites grades.

Magnetite, or ferrous ferrites is an example of a naturally occurring ferrites. It has been known since ancient times and its weak permanent magnetism found application in lodestone of the early navigators. Hilpert in 1909 attempted to improve the magnetic properties of magnetite and in 1928 Forestier prepared ferrites by precipitation and heat treatment. Magnetic oxides were also studied by Japanese scientists between 1932 and 1935. In 1936 Snock was studying magnetic oxides in Holland, by 1945 he had laid the foundations of physics and technology of ferrites and a new industry came into being [23, 24].

The first practical soft ferrite application was in inductors used in LC filters in frequency division multiplex equipment. The combination of high resistivity and good magnetic properties made these ferrites an excellent core material for these filters operating over the 50-450 kHz frequency range. The large-scale introduction of TV in the 1950's was a major opportunity for the fledgling ferrite industry. In TV sets, ferrite cores were the material of choice for the high voltage transformer and the picture tube deflection system. For four decades ferrite components have been used in an ever-widening range of applications and in steadily increasing quantities [22].

2.4.2 Magnetic Properties of Ferrite

From the point of view of power transformer design, the essential properties of ferrites in general are specified by their hysteresis characteristics, shown in Figure 2.6.

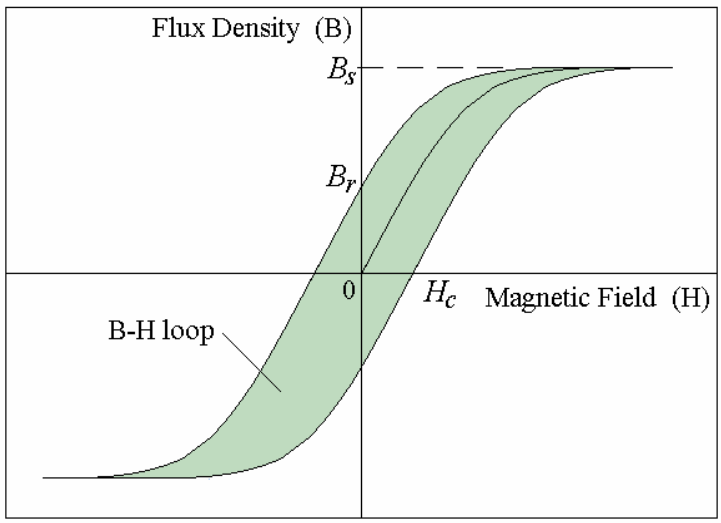

Figure 2.6 Typical BH curve.

The principal properties of ferrites which determine their technical performance are permeability and its variation in response to external field, to frequency and to temperature. Permeability is defined as the ratio between the magnetic field applied to the ferrite material and the resulting magnetic flux density. It is called the absolute permeability.

$$\frac{B}{H} = \mu_{absolute} = \mu_0 \mu_r \tag{2.49}$$

The absolute permeability can be expressed as the product of the magnetic constant of free space and the relative permeability, μ_r. The magnetic constant is also called as the permeability of free space, μ_0, it has the numerical valve of $4\pi \times 10^{-7}$ and has the dimensions of henries/meter (H/m). Since there are several version of μ_r depending on conditions the index '*r*' is generally removed and replaced by the applicable symbol, e.g. μ_i, μ_e and μ_a.

There are some magnetic properties of ferrite, such as saturation flux density, resistivity, coercivity and specific power loss. The detail explanation for these terms can be found in the Appendix B at the back of this document. The general magnetic properties of ferrite are enumerated as follow [22, 23]:

- Permeability of several tens.
- A very high resistivity, generally, in excess of 10^8 Ω-m.
- Saturation magnetization is appreciable, but significantly smaller than that of ferromagnetic materials.
- Low coercive force.
- Curie temperature varies from 100 °C to several hundred °C.
- Dielectric constant of the order of 10-12 at high frequencies (microwaves) with extremely low dielectric loss.

2.4.3 Development Trends

New ferrite materials have been frequently introduced by the manufacturers for power magnetics in switching mode power applications. The power handling capability also increases with these new materials. Table 2.2 lists the core losses for ferrite materials from some manufacturers at various frequencies and peak flux densities at 100 °C in the beginning of 21st Century.

Table 2.2 Core losses for various ferrite materials in Year 2003 [25 – 29].

Frequency	Material	Core loss, W/m^3 for various peak flux density, mT								
		200	100	80	60	40	20	10	8	6
100 kHz	Ferroxcube 3C96	370	45	22						
	Ferroxcube 3F3	500	72	40	20					
	Ferroxcube 3F4		200	100	40					
	Magnetics K	700	95	42	20	5				
	Magnetics F	700	110	65	30	9				
	TDK PC40	400	70	42	20					
	Siemens-EPCOS N87	370	50		10		1			
	Siemens-EPCOS N92	400	55		9					
	Siemens-EPCOS N97	300	41		8		1			
	Siemens-EPCOS N49	720	82		15		1			
	MMG F47	600	72		12		2			
200 kHz	Ferroxcube 3C96		170	95	42					
	Ferroxcube 3F3		210	120	60	22				
	Ferroxcube 3F4		430	230	100	30				

	Magnetics K									
	Magnetics F	2000	380	200	95	30				
	TDK PC40	1100	200	100	40					
	TDK PC50	3000	340	160	80	22	3			
	Siemens-EPCOS N87	1200	180		35		4			
	Siemens-EPCOS N92	1100	200		35		3			
	Siemens-EPCOS N97	900	140		40		4			
	Siemens-EPCOS N49	2000	200		30		2.5			
	MMG F47		200		40		5			
500 kHz	Ferroxcube 3C96		1400	800	380	135				
	Ferroxcube 3F3@400kHz		800	480	220	90	18			
	Ferroxcube 3F4		1000	520	250	70				
	Ferroxcube 3F45		900	450	200	62				
	Magnetics K		900	410	180	42	5			
	Magnetics F		1500	900	500	180	35	8		
	TDK PC40		1100	670	320					
	TDK PC50		1500	620	230	55	5			
	Siemens-EPCOS N87		1100		280		35			
	Siemens-EPCOS N92		1100		300		35	10		
	Siemens-EPCOS N97		950		300		35	8		
	Siemens-EPCOS N49		740		100		12	2		
	MMG F47		1050		300		50			
700 kHz	Ferroxcube 3F4			2000	1000	350	53			
	Ferroxcube 3F45			1050	500	180	30			
	Ferroxcube 3F5			1050	500	180	28			
	Magnetics K			2050	950	250	30	4		
	Magnetics F				1850	750	180	40	22	12
	TDK PC50		7500	3500	1800	500	60	8		
	Siemens-EPCOS N92		5500		1500		200	50		
	Siemens-EPCOS N97				1000		200	45		
	Siemens-EPCOS N49		2500		500		60	14		
	MMG F47						350			
1 MHz	Ferroxcube 3F4					2000	400	85	52	27
	Ferroxcube 3F45					1100	250	55	32	18
	Ferroxcube 3F5					710	150	32	20	
	Magnetics K					4200	500	70	30	12
3 MHz	Ferroxcube 3F4						1200	290	180	100
	Ferroxcube 3F5					1750	400	100	60	35
	Ferroxcube 4F1						650	150	100	55
	Magnetics K						3200	450	210	90
5 MHz	Ferroxcube 4F1						1200	300	180	100
10 MHz	Ferroxcube 4F1							850	450	220

Table 2.2 can be compared with Table 2.3, which was made by Abraham Pressman in Year 1991. From these two tables, some points for the development trends of ferrite materials can be found. The first important point found is that the operating

frequency range shifted up from 20 kHz – 500 kHz to 100 kHz – 10 MHz. However, at the frequency above 3 MHz, there is only one material from Ferroxcube can achieve the task. The practical frequency range should be concluded from 100 kHz to 3 MHz only. If the number of ferrite materials grouped by frequency is taken as consideration, the large number of ferrite materials is 13 (22% of the total number of ferrite materials in the list) in the frequency range of 500 kHz in Year 2003. But it was 9 (15% of the total number of ferrite materials in the list) in the same frequency range in Year 1991.

According to this statistic analysis, the operating frequency of the most popular switching mode power system is changing from 100 kHz – 200 kHz in Year 1991 up to 500 kHz in Year 2003. It can further verify this point by Figure 2.7 – Development trends of ferrite materials from Philips / Ferroxcube.

Table 2.3 Core losses for various core materials at various frequencies and peak flux density at 100 °C [30].

Frequency, kHz	Material	Core loss, W/m^3 for various peak flux density, mT					
		160	140	120	100	80	60
20	Ferroxcube 3C8	85	60	40	25	15	
	Ferroxcube 3C85	82	25	18	13	10	
	Ferroxcube 3F3	28	20	12	9	5	
	Magnetics R	20	12	7	5	3	
	Magnetics P	40	18	13	8	5	
	TDK H7C1	60	40	30	20	10	
	TDK H7C4	45	29	18	10		
	Siemens N27	50			24		
50	Ferroxcube 3C8	270	190	130	80	47	22
	Ferroxcube 3C85	80	65	40	30	18	9
	Ferroxcube 3F3	70	50	30	22	12	5
	Magnetics R	75	55	28	20	11	5
	Magnetics P	147	85	57	40	20	9
	TDK H7C1	160	90	60	45	25	20
	TDK H7C4	100	65	40	28	20	
	Siemens N27	144			96		
100	Ferroxcube 3C8	850	600	400	250	140	65
	Ferroxcube 3C85	260	160	100	80	48	30
	Ferroxcube 3F3	180	120	70	55	30	14
	Magnetics R	250	150	85	70	35	16
	Magnetics P	340	181	136	96	57	23
	TDK H7C1	500	300	200	140	75	35
	TDK H7C4	300	180	100	70	50	
	Siemens N27	480			200		
	Siemens N47				190		

200	Ferroxcube 3C8				700	400	190
	Ferroxcube 3C85	700	500	350	300	180	75
	Ferroxcube 3F3	600	360	250	180	85	40
	Magnetics R	650	450	280	200	100	45
	Magnetics P	850	567	340	227	136	68
	TDK H7C1	1400	900	500	400	200	100
	TDK H7C4	800	500	300	200	100	45
	Siemens N27	960			480		
	Siemens N47				480		
500	Ferroxcube 3C85				1800	950	500
	Ferroxcube 3F3		1800	1200	900	500	280
	Magnetics R		2200	1300	1100	700	400
	Magnetics P		4500	3200	1800	1100	570
	TDK H7C1						100
	TDK H7C4		2800	1800	1200	980	320

From the following figure, it can be found that there is no big change from 1996 to 1998. The major materials for high frequency power transfer applications have been developed. In the last decade of 20^{th} century, they were 4F1, 3F4 and 3F3 for the operating frequency from 500 kHz to 10 MHz, and the other group of materials, such as 3C80, 3C85 and 3C90, were the materials for 100 kHz to 200 kHz. Four years later, 2002, more materials have been introduced. Five new materials of 3C90 series have been developed for the operating frequency range from 200 kHz to 400 kHz, and one new derivative for each group of materials of 3F3 and 3F4 is listed in the new product catalogue.

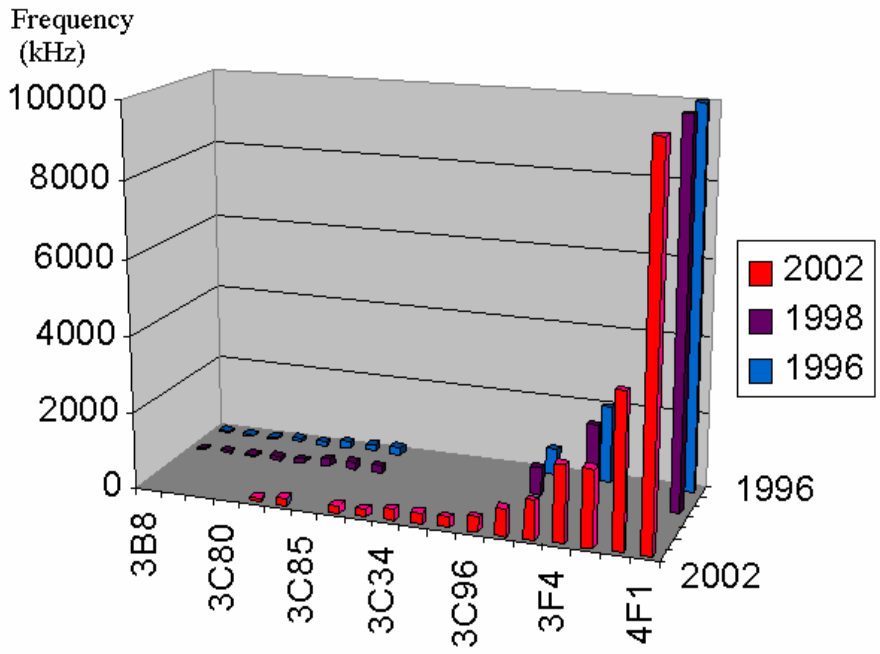

Figure 2.7 Development trends of Philips ferrite materials [25, 31, 32].

The similar development approach can be seen from the other major manufacturer in Japan, TDK. PC30 and PC40 were two ferrite materials of power transformers of high frequency application ten years ago. Five more materials, named PC33, PC44, PC45, PC46 and PC47, are announced for similar operating frequency range, < 300 kHz. There is a product only for the other frequency level of 700 kHz, it is PC50.

According to the development trends of ferrite materials, it looks like a mirror to reflect the image of the development of high frequency transformers in the real world. The operating frequency of the transformers in switching mode power supply applications keeps increasing. However, the rate of increasing is very slow.

The operating frequency for the majority switching power applications is still under 200 kHz at the end of the 20th century. It is very hard to further increase to megahertz levels. The magnetic materials are ready developed, and the switching technique and the electronic components are well prepared for frequencies of megahertz [33, 34], however, the copper loss in the windings is the principle obstacle of the

development of high frequency magnetics. The characteristic of windings of high frequency magnetics will be deeply investigated in the next chapter.

2.5 Winding Structure in High Frequency Transformers

Transformers consist of magnetic core and coils. The magnetic cores, the magnetic materials for the flux to go through, have been briefly discussed in the section 2.4. The second element of transformers is the coil. The coil of transformers is actually a copper winding around the magnetic materials to generate the magnetic flux by the input power source and reproduce electric energy to the loading of the transformer. At line frequency, a single copper wire with low resistance can perfectly complete this task. The dc resistance of the copper wires is the main point to be considered. The arrangement of conductors in the winding of transformer is a very important factor to determine the dc resistance of the copper winding of transformers. The cross-sections of two ideal arrangements of conductors, such as square arrangement and hexagonal arrangement, are shown in Figure 2.8. The basic principle of the ideal arrangement of conductors is fully using the winding space in the transformer to have the maximum cross-section area of conductors. Therefore, the DC resistance of copper windings is the minimum and the power loss is decreased to the lowest level also.

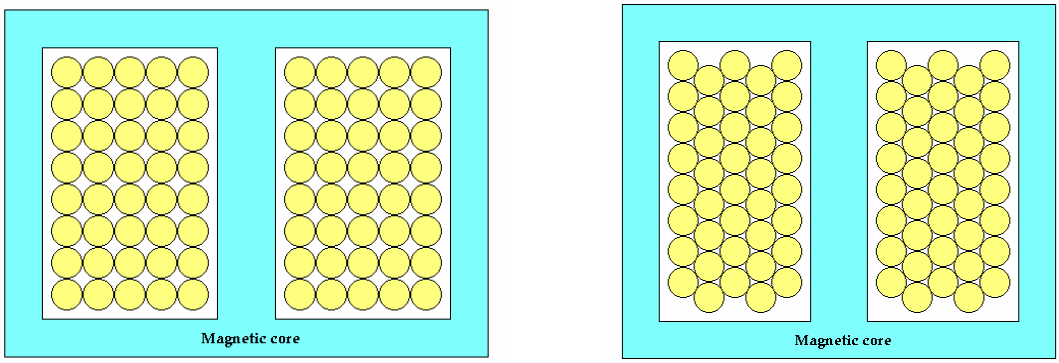

(a) Square **(b) Hexagonal**

Figure 2.8 Cross-sections of ideal arrangements of conductors in a winding.

When the operating frequency increased to few tens kilohertz, the skin depth of the conductor reduces the effective cross section area of the wire and increases the ac

resistance of the conductor. The ac resistance of the copper wire creates a heavy power loss in the windings of high frequency transformers. Furthermore, proximity effects between conductors in the transformer winding structures become significant when the operating frequency increased to few hundreds kilohertz level. More and more electromagnetic problems were discovered in the winding of high frequency power transformers. Therefore, the structure of transformer winding becomes a significant topic for high frequency power transformer design.

The phenomenon of skin depth of the copper wire significantly increased the ac resistance of the wire, and the power loss of i^2R_{ac}, when the operating frequency of power transformers increased from line frequency to tens of kilohertz. This power loss can be reduced by using litz wires to replace the single copper wire. The term "Litz wire" is derived from the German word "litzendraht" meaning woven wire. It is constructed of individually insulated copper wires either twisted or braided into a uniform pattern. Litz construction is designed to minimize the power losses exhibited in solid conductors due to the skin effect. Skin Effect is the tendency of high frequency current to be concentrated at the surface of the conductor. Litz constructions counteract this effect by increasing the amount of surface area without significantly increasing the size of the conductor. In general, constructions composed of many strands of finer wires are best for the higher frequency applications [35].

The usage of litz wires in high frequency power transformers significantly reduces the power loss of i^2R_{ac}. However, there is another electromagnetic phenomena appeared in the transformer windings. It is the proximity effect. Proximity effect is an eddy current effect in a conductor due to the alternating magnetic field of other conductors in the vicinity. There is a tendency for current to flow in loops or concentrated distributions due to the presence of magnetic fields generated by nearby conductors. In transformers and inductors, proximity effect losses are generally more significant than skin effect losses.

The power losses created by proximity effect in the windings of high frequency power transformers can be reduced by special winding arrangements, called sandwich

winding structure [23]. The principle of this arrangement is to separate the primary and secondary windings into few small parts and make them interweaving each other, shown in Figure 2.9.

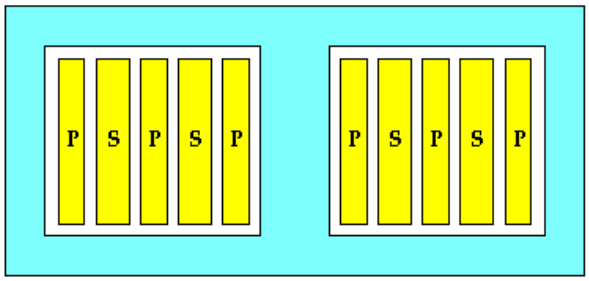

Figure 2.9 Sandwich winding structure of transformers.

As mentioned in the previous Section 2.3, magnetic cores are used to intensify the magnetic field generated by the current flowing through the primary winding. At line frequency, the high permeability magnetic cores concentrate the flux with very little leakage. However, when the operating frequency of transformers increased to hundreds of kilohertz, the magnetic flux dose not follow this path totally, leakage flux is coming out from the transformer core. It decreases the coefficient of coupling, and significantly increases the eddy current inside the copper windings. The following figure shows the leakage flux distribution of a high frequency power transformer operating at 1 MHz.

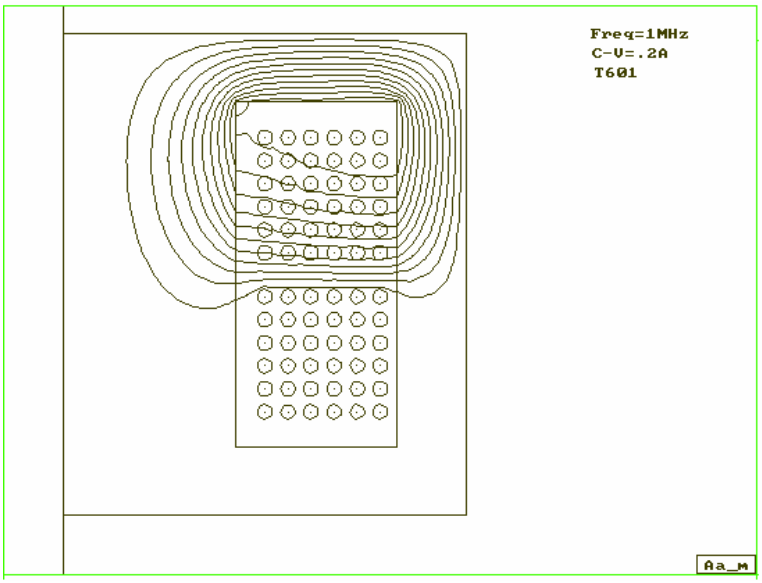

Figure 2.10 Leakage flux distribution of a high frequency power transformer.

The electromagnetic phenomena, such as eddy current, leakage inductance, skin effect and proximity effect, inside the winding structure of high frequency power transformers is a critical point for the transformer designs.

2.5.1 Fundamental Transformer Winding Properties

At low frequency, the most important thing to be considered in the transformer windings is the DC resistance of copper wires. Transformer designers attempt to fully use the winding window area of transformer to minimize the DC resistance of wires for primary and secondary windings, therefore the copper losses can be reduced and the efficient of the whole transformer can be increased. Figure 2.11 shows the winding window area, A_w, of typical transformer core types.

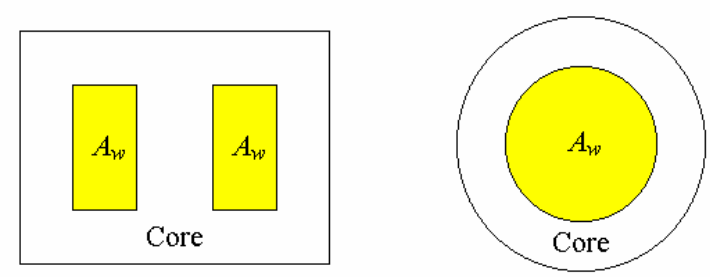

Figure 2.11 Winding windows area of transformer core types.

To simplify the calculation, the rectangular shell-type core is used for the following explanation. With the ideal arrangements of conductors, the total number of conductors to be fitted into the winding window can be calculated. If the overall conductor diameter, d_0, is much smaller than the dimensions of the available winding space, then the number of wires, n, can be fitted in the winding area, A_w, is given for the square arrangement of conductor by:

$$n = \frac{A_w}{d_0^2} \tag{2.50}$$

If the winding copper (space) factor, F_w, is defined as

$$F_w = \frac{\text{the total cross - sectional area of copper in winding}}{\text{actual cross - sectional area of the winding space}},$$

then, for the perfect square arrangement with fully winding window fitted, the factor is

$$F_w = \frac{\pi}{4}\left(\frac{d}{d_0}\right)^2 \tag{2.51}$$

where d is the bare diameter of the conductor. If the overall diameter of the conductor is close to the bare diameter of the conductor ($d_0 = d$), then the winding copper factor is equal to 0.785.

(a) The square arrangement. **(b) The hexagonal arrangement.**

Figure 2.12 The ideal arrangement of conductors in transformer windings.

For the other arrangement, the hexagonal arrangement of conductors, the copper winding factor is given by

$$F_w = \frac{\pi}{2\sqrt{3}}\left(\frac{d}{d_0}\right)^2 \tag{2.52}$$

for a large number of copper wires. If $d_0 = d$, $F_w = 0.907$.

In a practical winding, the conductor pattern will not correspond to both ideal arrangements. However, in a carefully wound coil, without interlayer insulation, the hexagonal arrangement will occur over large regions of the winding. Although successive layers approximate to helices of opposite lay, in practice the conductor will tend to lie in the groove formed by the previous layer. The majority of the turn is in the hexagonal arrangement before it is forced to cross over into the next groove. In the region of the crossover the square configuration will occur.

From the above definition of winding copper factor, its value for a practical winding is given by

$$F_w = \frac{N\pi d^2}{4} \cdot \frac{1}{A_w}. \tag{2.53}$$

Another useful factor is the overall copper factor, F_o, defined by

$$F_o = \frac{\text{total cross - sectional area of copper in winding}}{\text{actual window area in the core}}$$

$$F_o = \frac{N\pi d^2}{4} \cdot \frac{1}{A_o} \tag{2.54}$$

where A_o is the overall winding window area, shown in Figure 2.13.

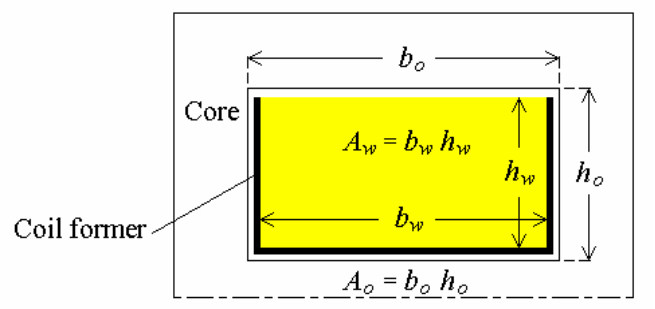

Figure 2.13 Effective window area.

2.5.2 DC Winding Resistance

The resistance of a conductor with a total length, l, and a cross-section area, A, is defined as

$$R = \frac{\rho_c l}{A} \tag{2.55}$$

where ρ_c is the resistivity of the material of the conductor. For copper, the most common winding material, at a temperature of 20 °C the normal value of resistivity is 1.694×10^{-8} Ω-m. The temperature coefficient of the resistivity is 0.00393 per °C.

In the copper winding of a transformer, if d is the diameter of bare conductor, l_w is the mean length of a turn and N is the number of turns on the winding, then Eqn. (2.55) becomes

$$R_{DC} = \frac{4\rho_c N l_w}{\pi d^2} = N l_w R_c \tag{2.56}$$

where R_c is the resistance per unit length of the conductor,

$$R_c = \frac{4\rho_c}{\pi d^2}. \tag{2.57}$$

Refer to Eqn. (2.50), $d^2 = \frac{A_w}{N}$, and if the total number of turns is kept as a constant for a particular transformer design, then the resistance per unit length of the conductor can be expressed as

$$R_c = \frac{4N\rho_c}{\pi A_w} = \frac{4N\rho_c}{\pi} \cdot \frac{1}{A_w} \tag{2.58}$$

The resistance per unit length of the conductor is inversely proportion to the winding window area, that is the bigger winding window area the smaller resistance per length of the conductor if the total number of turns is the same.

2.5.3 Power Loss due to DC Resistance

Copper loss in power transformers at low frequencies is mainly related to the DC resistance. The power loss is determined as

$$P_c = I^2 R_{DC} \tag{2.59}$$

where I is the current flowing through the winding. To reduce the DC resistance, as mentioned in the previous section, bigger winding window area is needed.

At the line frequency, the power loss in the transformer winding is proportionally related on this DC resistance. However, it is not the only power loss when the operating frequency increased.

2.5.4 High Frequency Characteristic of Transformer Windings

When the operating frequency increases, the total number of turns decrease significantly. Therefore the total length of the copper winding is also decreased dramatically. The power loss due to the DC resistance almost becomes zero suddenly. It is very good for the power transformer design, however, with the disappearing of the

DC resistance, the ac resistance increases enormously. The power loss due to ac resistance is larger than the one generated from DC counterpart.

At high frequencies, the major loss within windings is due to eddy currents produced by the skin and proximity effects. These effects can cause the winding losses to be significantly greater than the I^2R_{DC} loss calculated using the DC resistance of the copper winding.

2.5.4.1 Eddy Current

According to Faraday's law, a voltage is induced in a conductor loop if it is subjected to a time varying magnetic flux. As a result a current flows in the conductor if there exists a closed path. In fact, this is the basic principle of eddy current also.

The same phenomenon occurs when, instead of a conductor loop, a massive conducting body is subjected to a time varying magnetic field. The body may consist of nonmagnetic or magnetic material. Voltages are again induced in this body, which give rise to currents circulating in appropriate paths. These currents are now distributed and are referred to as eddy currents, shown in Figure 2.13. In a conductor, the induced magnetic field may be due to its own current and the current of another adjacent conductor. Both of the currents are time varying [36].

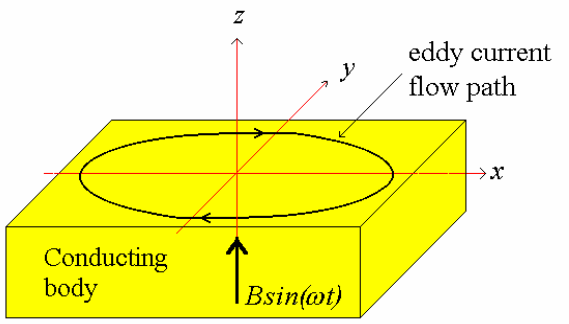

Figure 2.14 Eddy current induced in a conducting body.

Eddy currents in transformers are detrimental. The circulating currents dissipate energy through ohmic losses. According to Lenz's law, the magnetic fields generated by

the circulating currents oppose the original time varying field. In fact, the eddy currents lead to a non-uniform current distribution in conductors, which produces higher ohmic losses.

Eqn. (2.11), the second expression of Maxwell's equations, with Eqn. (2.15), can be rewritten as

$$\nabla \times \left(\frac{1}{\mu} \nabla \times \vec{A} \right) = \vec{J} \tag{2.60}$$

and $\vec{J} = \vec{J}_0 + \vec{J}_e$, and $\vec{J}_e$ is the frequency-dependent eddy current defined as

$$\vec{J}_e = -\sigma \frac{\partial \vec{A}}{\partial t} \tag{2.61}$$

Taking into consideration the quasi-static field ($j\omega \approx \frac{\partial}{\partial t}$), it arrives at the following expression for the eddy current:

$$J_e = -\sigma j \omega A \tag{2.62}$$

where σ is the conductivity and ω is the angular frequency. The amplitude of the eddy current is proportional to the operating frequency.

2.5.4.2 Skin Effect

A single straight isolated conductor carrying an alternating current, shown in Figure 2.15(a), will be surrounded by a concentric magnetic field, *H(t)*. This field will induce opposing eddy currents within the conductor itself as shown in the center diagram. These currents trend to oppose the main current in the vicinity of the axis of the conductor and to enhance it at the surface. Thus the current distribution tends to become non-uniform across the section, the current being least at the center and greatest at the surface.

As the frequency increases, the induced *emf*'s increase and the non-uniformity becomes more pronounced until the current is virtually confined to a thin skin at the surface, and the inner region plays no part in the conduction.

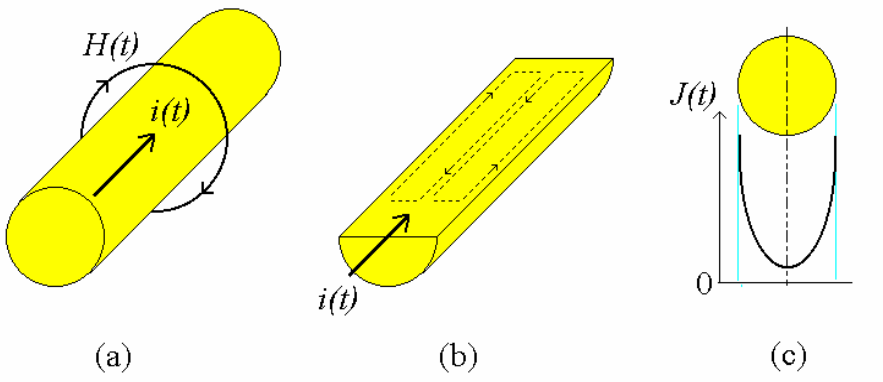

Figure 2.15 Skin effect inside a single conducting wire.

The ac resistance of a straight conductor of circular cross-section is given by

$$R_{ac} = R_{DC} + R_{se} = R_{DC}(1 + F_{se}) \tag{2.63}$$

where R_{se} is the increase in resistance due to skin effect and F_{se} is the skin effect factor.

The skin effect factor is a function of $\frac{d}{\delta}$ where δ is the skin depth. This is a property of a conducting material and is strictly the depth beneath an infinite plane surface at which an incident plane *em* wave is attenuated to $\frac{1}{\varepsilon}$ or 37% of its surface value due to the effect of eddy current

$$\delta = \sqrt{\frac{\rho}{\pi \mu f}} \text{ or } \delta = \sqrt{\frac{2}{\omega \mu \sigma}} \tag{2.64}$$

where μ is the permeability, σ is the conductivity, and ρ is the resistivity of the conductor.

When the current in a round conductor is confined by skin effect to a depth beneath the surface that is much less than the diameter, this depth, measured as the distance over which the current falls to $\frac{1}{\varepsilon}$ of its surface value, tends to the value of the skin depth. Skin depth of some common used conducting materials in terms of frequency are given in Table 2.4.

Table 2.4 Skin depth of various materials.

Material	Conductivity,σ,(S/m)	f = 60Hz	1MHz	1GHz
Silver	6.17×10^7	8.27mm	0.064mm	0.0020mm
Copper	5.80×10^7	8.53mm	0.066mm	0.0021mm
Gold	4.10×10^7	10.14mm	0.079mm	0.0025mm
Aluminium	3.54×10^7	10.92mm	0.084mm	0.0027mm

Skin effect may be virtually eliminated by using conductors consisting of thin insulated strands so composed that individual strands weave cyclically from the center of the conductor to the outside and back as they run along the length of the conductor. Such a stranding and transposition makes the current density uniform. However, since skin effect is not usually the most important form of eddy current losses in winding conductors, it is not usual to use this special stranding. To combat the proximity effect loss described in the next section bunched conductor is often used. This consists of a number of thin insulated strands simply twisted into the form of a rope. If the strands formed perfect helical paths, keeping at a constant distance from the axis, the skin effect would be the same as for a solid conductor having the same copper cross section, assuming that all the strands were connected together at each end of the conductor. In practice, however, such bunched conductors are usually made up of groups of strands, then the appreciable transposition of the strands occurs. Careful measurements have shown that most bunched conductors behave as though the strands are transposed almost perfectly and the skin effect can be ignored.

In isolation, a perfectly transposed bunched conductor will be subject to a further eddy current loss due to its own field traversing the strands, each of which carries the same current. This may be called internal proximity effect [23]. It may be comparable to, and at high frequencies may be larger than, the skin effect in an equivalent conductor consisting of perfectly non-transposed strands. However when a perfectly transposed bunched conductor is in winding, the field due to the bunch, as such, largely disappears due to the proximity of the other turns, the winding behaves as though it consists only of strands, all carrying equal current. Under these conditions only the normal proximity effect described in the next section is important.

2.5.4.3 Proximity Effect

This is the eddy current in a conductor due to the alternating magnetic field of other conductors in the vicinity. Figure 2.16 shows the proximity effect between two adjacent rectangular wires carrying currents in opposite directions. Magnetic fields of current in one wire induce voltage in loop of adjacent wire. The resultant eddy currents flow along the full length of the wire on its top and bottom surfaces. Inside the top wire, eddy currents at the bottom surface of the wire are in the same direction as the main current flow and reinforces it. The same situation exists inside the bottom wire. The consequence is that current in each wire is confined to thin skins in the surfaces facing each other.

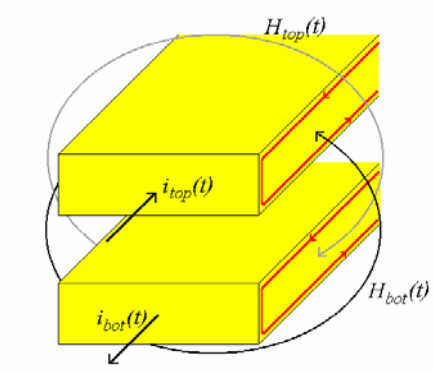

Figure 2.16 Proximity effect in two adjacent rectangular wires.

In practice, this may usually be interpreted as the eddy current effect in the conductors of winding due to the field of the winding as a whole. The field will, in general, depend on the geometry of the core, if any. It must be remembered that any additional windings or conductors in the same field will have eddy currents induced in them whether or not they are carrying a main current. The resultant energy loss will simply add to the corresponding loss in the current carrying winding and will be apparent as an additional resistance in that winding.

The magnetic field generated by a current carrying conductor, the white one of the conductors in Figure 2.17(a), will normally cut the next conductors, the highlighted

conductor in the figure, perpendicular to the conductor axis. The resultant eddy current distribution is shown in Figure 2.17(b).

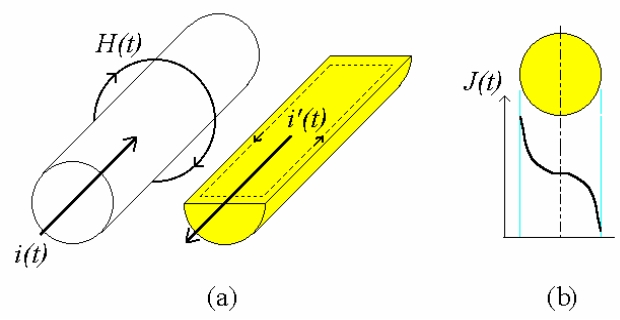

Figure 2.17 Proximity effect in two round wires.

When the skin effect factor is less than unity the effect of the magnetic fields of the eddy currents themselves may be ignored and the calculations of the eddy current loss are quite simple, the following derivation of proximity effect in a thin tape illustrates the principles.

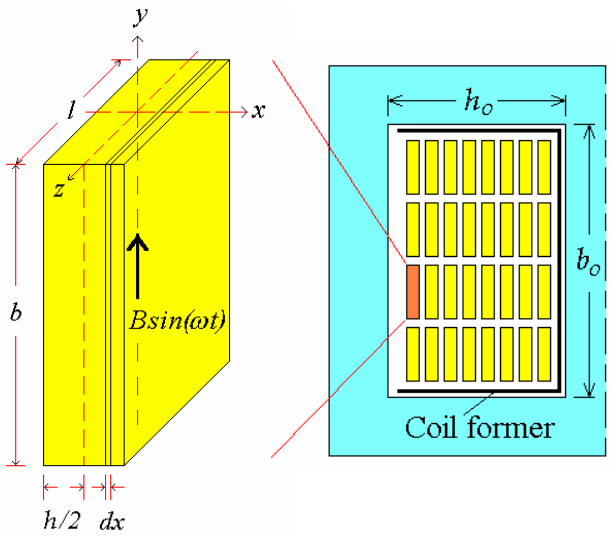

Figure 2.18 Calculation of eddy current in a thin tape with relationship of notations of transformer windings.

Figure 2.18 shows the cross-section of a tape having width b and thickness h. An alternating magnetic flux density, $\vec{B}\sin\omega t$, is everywhere parallel to the plane of the tape. The *emf* induced in a loop consisting of the two elementary laminae is given by

$$E = \frac{2l\omega\vec{B}x}{\sqrt{2}} \tag{2.65}$$

where l is the length of the tape being considered.

An eddy current will flow along the laminate parallel to the length of the tape, in one direction on one side of the axis and in the opposite direction on the other side. Neglecting the short paths connecting the laminae at the ends of the tape, the resistance of the elementary eddy current circuit is given by

$$R = \frac{2\rho l}{b} \cdot \frac{1}{dx} \tag{2.66}$$

Therefore the power loss due to the proximity effect is

$$dP_{pe} = \frac{E^2}{R} = \frac{x^2\omega^2\vec{B}^2 lbdx}{\rho} \tag{2.67}$$

$$P_{pe} = \frac{\omega^2\vec{B}^2 lb}{\rho}\int_0^{h/2} x^2 dx = \frac{\omega^2\vec{B}^2 lbh^3}{24\rho} \tag{2.68}$$

2.5.4.4 Leakage Inductance

Not all the magnetic flux created by primary winding of transformer follows the magnetic circuit and links the other windings. The flux linkage between primary and secondary windings or parts of the same winding is never complete. Some flux leaks from the core and returns through the air, thus some flux is not linked by the other, and causing imperfect coupling. In addition to the mutual flux, which does link both of the windings, there is leakage flux. This effect is modeled by series leakage inductances, which are shown as L_1 and L_2 in Figure 2.3. The voltage ratio of the transformer is no longer related by the turn ratio, as modeled in an ideal transformer. It is necessary to subtract the voltage drop across the leakage inductances from the terminal voltages to get the ideal transformer winding voltages.

If the primary winding is energized by a current flowing in the direction shown then, if the secondary winding is loaded, the secondary current will flow in the reverse

direction. The instantaneous difference between the primary and secondary ampere-turns will equal the instantaneous magnetizing ampere turns and determine the instantaneous mutual flux. In practice, these flux combines with the main magnetic flux within the core, and so lose their identities. The resultant flux pattern not only depends on the geometry of the winding and core but also varies with time over the operating cycle.

If the secondary winding is short-circuited, the main flux which links both windings will be negligible because the primary and secondary ampere turns almost cancel each other. These two bunches of flux contributed by each winding are in the same direction in the winding space and mutually repel. The residual *emf* due to this flux will appear as inductance in series with the primary terminals and is named the leakage inductance referred to the primary. The symbol L_g will be used to denote leakage inductance. Its magnitude may be calculated by equating its energy, $\frac{1}{2}L_g I^2$, to the magnetic energy of the leakage flux.

Figure 2.19 shows an elementary layer of winding, of thickness *dx*, situated at a distance *x* from the inner surface of the winding. The field strength along the flux path which includes this layer depends on the number of ampere turns linked by the path, i.e.

$$\oint Hds = N_1 I_1 \frac{x}{h_1} \tag{2.69}$$

where s is the distance along the flux path

N_1 is the number of primary turns

and I_1 is the primary current.

Since the reluctance of the path within the magnetic core is negligible compared with that of the path in the winding, *H* may be taken as the field strength in the winding layer *dx*. It is assumed to be constant along the layer and this is supported by experimental results. The uniformity arises mainly from the flux direction is substantially parallel to the interface between the windings, if the primary and secondary are wounded side-by-side, shown in Figure 2.19. Thus

$$H = \frac{N_1 I_1}{b} \cdot \frac{x}{h_1} \tag{2.70}$$

where b is the winding breadth.

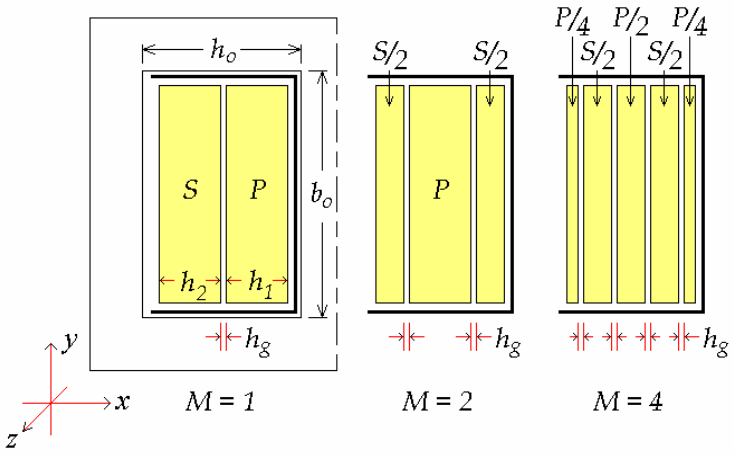

Figure 2.19 Winding arrangements for calculation of leakage inductance.

The magnetomotive force will vary linearly from zero when $x = 0$ to N_1I_1 when $x = h_1$. It will be constant across the interwinding space because the ampere turns embraced by the line integral in this region are constant. As the secondary winding space is traversed the magnitude of the magnetomotive force will fall linearly to zero since $N_1I_1 = N_2I_2$.

The volume of the elementary layer is $l_w \cdot b \cdot dx$, therefore the energy stored in the field is

$$\frac{\mu_0}{2} \int_0^h H^2 dx \cdot l_w \cdot b \tag{2.71}$$

The mean length, l_w, is usually taken as a constant for the windings as a whole, i.e. it is based on $\frac{h_w}{2}$. The energy in the total winding space is then

$$\frac{\mu_0}{2} \cdot l_w \cdot b \cdot \left\{ \int_0^{h_1} \left(\frac{N_1 I_1 x}{b \cdot h_1} \right)^2 dx + \left(\frac{N_1 I_1}{b} \right)^2 h_g + \int_0^{h_2} \left(\frac{N_2 I_2 x}{b \cdot h_2} \right)^2 dx \right\} = \frac{1}{2} L_g I_1^2 \tag{2.72}$$

by definition. Since $|N_1 I_1| = |N_2 I_2|$, the equation reduces to

$$\frac{1}{2}L_g I_1^2 = \frac{\mu_0 l_w}{2b}\cdot\left(\frac{h_1+h_2}{3}+h_g\right)\cdot N_1^2 I_1^2 \tag{2.73}$$

$$\therefore \qquad L_g = \mu_0 N_1^2 \frac{l_w}{b}\cdot\left(\frac{h_1+h_2}{3}+h_g\right) \tag{2.74}$$

This equation gives the value of the leakage inductance referred to the primary. The value referred to the secondary may be obtained by the simply substituting N_2 for N_1.

Figure 2.19 shows commonly used winding arrangements for high frequency transformer, the leakage inductance can be derived as

$$L_g = \mu_0 N_1^2 l_w \cdot \frac{1}{M^2}\cdot\frac{1}{b}\cdot\left(\frac{\sum h}{3}+\sum h_g\right) \tag{2.75}$$

where M is the number of section interfaces.

It often happens that $\sum h_g$ is negligible compared with $\sum h$, and if the winding is fully fitted with the winding window area, then Eqn. (2.75) can be rewritten as

$$L_g = \mu_0 N_1^2 l_w \cdot \frac{1}{M^2}\cdot\frac{h_w}{b_w} \ . \tag{2.76}$$

Therefore, the leakage inductance is proportional to the height of the winding and inversely proportional to the breadth of the winding. The leakage inductance is also inversely proportional to the square of the number of section interfaces of the winding.

Leakage inductance is a very important factor for transformer design, it interferes with the basic operation of a transformer. The leakage inductance can cause over voltage in power switch at turn-off action, and requiring a snubber circuit to protect the power switch. The leakage inductance will be discussed in the next two sections with the simulation results.

2.6 High Frequency Power Transformers in 1990s

In the last decade of the 20th Century, electronic equipment becomes steadily smaller. The power density requirement of power supplies becomes higher and higher [30, 37 – 39]. The need of high frequency power transformers is enormous. Some new structures of high frequency power transformers have been developed. Two of them are commonly accepted by switching mode power supply designers. They are planar transformers and coaxial winding transformers.

2.6.1 Planar Transformers

As the operating frequency increased, the number of turns of primary winding and secondary winding are dramatically decreased. The total number of windings decrease from few thousand turns at line frequency down to few ten turns at hundreds kilohertz of frequencies. It is also found that the eddy current losses are less for thin copper foils than circular copper wires. Therefore planar transformer gets an increasing importance for power supplies. Planar transformers are characterized by a high power density and a high efficiency at high frequency operation [40 – 43].

Planar transformers first became known at the beginning of the 1980s. Their worldwide acceptance has only recently begun, due to technological advances that has enabled drastic cost reductions, making them a viable and competitive product.

Planar transformers normally use flat copper foil or printed-circuit boards instead of round copper wire. Used together with appropriately flat ferrite cores, they result in an especially compact transformer with a very low profile. Planar transformers are primarily planar technology products but they can be fabricated by the microfabrication techniques and make them to be possible as “Integrated Magnetics”.

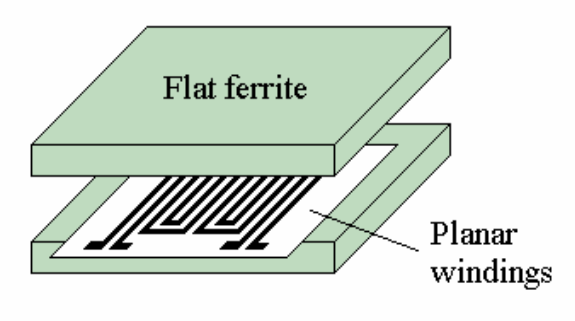

Figure 2.20 Planar transformer.

Planar transformers consist of a set of planar flat cores and a planar winding, shown in Figure 2.20. The windings are etched in each layer of multi-layer printed circuit board and built a coil. For the transformers with extreme high currents handling, the stacking technology can be used to increase the cross-section area of each track.

Planar transformer has advantages of low profile, high power density and good heat transfer properties. Planar transformers can be implanted with integrated circuits to form hybrid power IC. The manufacturing cost is also relatively low by using microfabrication techniques. This type of transformers can provide an excellent solution for the power supply's problems of portable telecommunication devices and handheld electronic equipment.

2.6.2 Planar E Core Transformers

There are many transformers called planar transformers. The planar transformers consist of two pieces of flat magnetic cores and a planar winding structure can be classified as true planar transformers. Some planar E core transformers, shown in Figure 2.21 (a), and low profile RM core transformers are called as planar transformers commonly [44]. However, they are using a set of E cores or RM cores with relatively short legs and combine with flat copper foil or printed circuit boards as windings. The most important thing is that they are still using the traditional concept as the normal E core transformers are working with. Figure 2.21 (b) shows the low profile RM core structure.

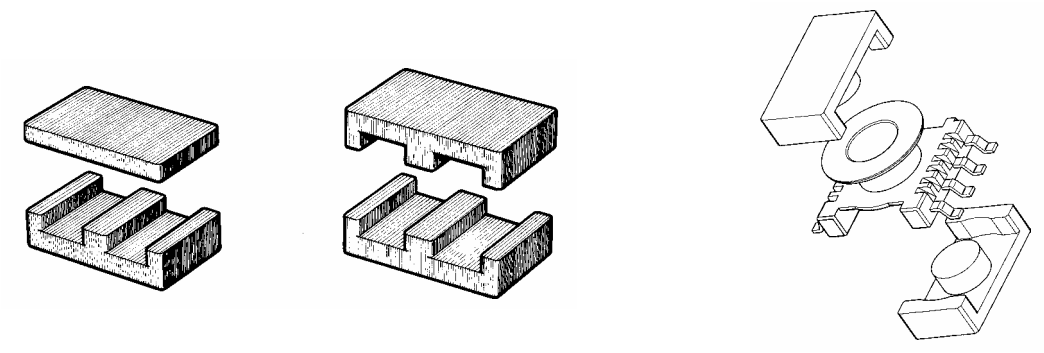

(a) **(b)**

Figure 2.21 (a) Planar E cores, and (b) Low profile RM core structure.

2.6.3 Coaxial Winding Transformers

Coaxial winding transformers have recently been found to have excellent performances at high frequencies. Very low leakage inductance, low eddy current losses and high power density are the advantages of the transformer [45 – 47]. Coaxial windings structure transformers can be used in high frequency switching mode power supply perfectly. According to its flexible combination of number of toroids, the power range of the type of transformers can be easily adjusted to desired level. It is a perfect power transformer for UPSs and chargers for electric vehicles.

Figure 2.22 shows the basic structure and the cross section of a coaxial winding transformer. The coaxial winding transformer consists of ferrite ring cores, copper tubes and a central wire. The copper tubes which connected together at the far end work as the single turn primary winding and the central wire goes through the tube as the secondary winding. The turn ratio of the transformer is 1:1. The ferrite ring cores are around the copper tubes to provide the magnetic path for the transformer.

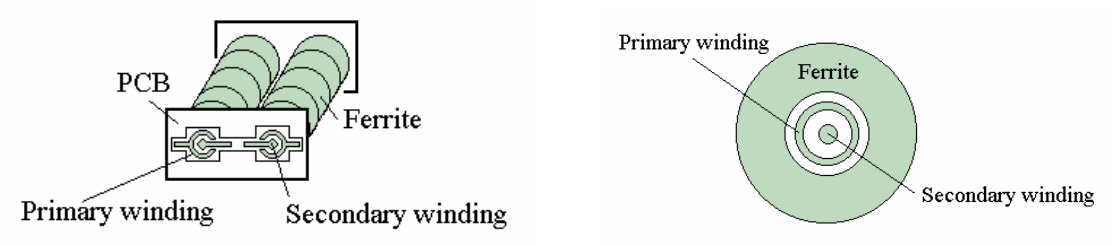

(a) (b)

Figure 2.22 (a) Basic structure and (b) Cross section of coaxial winding transformer.

2.7 Obstacles in High Frequency Power Transformers

The operating frequency of power transformers increased from 25 cycles per second to line frequency of 50/60 Hz in the first half of the 20 Century, it kept increasing in the last two decades from tens of kHz to few MHz, or even more [33]. The structures and winding configurations have been changed to overcome the problems generated by the eddy currents. The laminated core materials and new soft magnetic materials have been investigated and used to minimize the eddy current losses in the magnetic cores. Litz wires techniques and new structures of transformer windings have been developed and put into practice to reduce the copper losses in high frequency power transformers.

High frequency magnetic materials, such as ferrites and power cores, have improved to suit the requirement of high frequency operations. Still, transformers and inductors have many obstacles for high frequency applications. Parasitic elements, such as leakage inductance, eddy current, skin and proximity effects, make it very difficulty to design high-frequency magnetics. For this reason, it seems likely that commercial switching frequencies will be limited to about 1 MHz in the first five years of 21st century. A survey of operating frequencies in use today would show that most supplies switch at 100 kHz or less. Much work still needs to be done to exploit the improved capability of component and design technology and move this average frequency substantially higher.

2.8 References

1. Mohamed E. El-Hawary. *Principles of Electric Machines with Power Electronic Applications, 2nd ed*. John Wiley & Sons, Inc., 2002.

2. The Expanded Columbia Electronic Encyclopedia, Columbia University Press, 2000.

3. A.C. Franklin and D.P. Franklin, *The J&P Transformer Book*, 11th ed., Butterworth-Heinemann Ltd., 1983.

4. Marty Brown, *Practical Switching Power Supply Design*, Academic Press, Inc. 1990.

5. Marty Brown, *Power Supply Cookbook*, Butterworth-Heinemann, 1994.

6. B. J. Baliga, "Trends in Power Semiconductor Devices", *IEEE Trans. on Elect. Dev.*, vol. 43, 1996, p.1717.

7. B. K. Bose, "Energy, Environment, and Advances in Power Electronics", IEEE Trans. on Power Electronics, vol. 15, No. 4, July 2000.

8. B. K. Bose, *Modern Power Electronics*, IEEE Press, Inc. 1992.

9. Michael P.Perry, *Low Frequency Electromagnetic Design*, Marcel Dekker Inc., New York, 1985.

10. D.K. Cheng, *Field and Wave Electromagnetics*, 2nd ed., Addison-Wesley Publishing Company, Inc., 1989.

11. D.G. Fink and D. Christiansen, *Electronics Engineers' Handbook*, 3rd ed., McGraw Book Co., 1989.

12. Jun W. Lu, Y. Kagawa and D.V. Thiel, "Numerical Solutions of Wave Propagation in Dispersive and Lossy Transmission Lines", International Journal of Applied Computational Electromagnetics, vol. 9, pp.57-66, July, 1994.

13. C. W. Trowbridge, An introduction to computer aided electromagnetic analysis, Vector Field Ltd., 1990.

14. K. Preis, Ein Beitrag zur Berechnung ebener Wirbelstromverteilungen, Archiv für Elektrotechnik, vol.65, 1982, 309-314.

15. W. R. Smythe, *Static and dynamic electricity*, 3rd ed. McGraw-Hill Book Company, 1968.

16. J. A. Stratton, *Electromagnetic theory*, New York, McGraw-Hill, 1941.

17. C. A Brebbia, *The Boundary Element Method for engineers*, London: Pentech Press, 1978.

18. J.P.Jakubovics, *Magnetism and Magnetic Materials*, 2nd ed. The university Press, Cambridge 1994.

19. David Jiles, *Introduction to Magnetism and Magnetic Materials*, Chapman and Hall, 1991.

20. Richard M. Bozorth, *Ferromagnetism*, D. Van Nostrand Company, Inc. 1951.

21. *A Critical Comparison of Ferrites with Other Magnetic Materials*, Magnetics Technology Center, 1990.

22. *Soft Ferrites: A User's Guide*, Magnetic Materials Producers Association, 1998.

23. E.C. Snelling, *Soft Ferrites: Properties and Applications*, Iliffe Books Ltd. 1969.

24. P.S. Neelakanta, *Electromagnetic Materials – Monolithic and Composite Versions and their Applications*, CRC Press, Inc. 1995.

25. *Soft Ferrites and Accessories*, 2002 e-version, Ferroxcube / Philips Magnetics.

26. *Magnetics Ferrites 2003*, Magnetics, 2003.

27. *MMG-Neosid Magnetic Components*, MMG-Neosid, 1997.

28. *Siemens Ferrites and Accessories Data Book 1990/91*, Siemens, 1990.

29. *Ferrite Cores*, e-version, TDK Electronics Co., Ltd. 2002.

30. Abraham I. Pressman, *Switching Power Supply Design*, McGraw-Hill, Inc., 1991.

31. *Soft Ferrites – Data Handbook MA01*, Philips, 1996.

32. *Soft Ferrites – Data Handbook MA01*, Philips, 1998.

33. Wojciech A. TabisZ, Pawel M. Gradzki and Fred C. Y. Lee, "Zero-Voltage-Switched Quasi-Resonant Buck and Flyback Converters – Experimental Results at 10 MHz", *IEEE Trans. on Power Electronics*, vol. 4, No. 2, April, 1989.

34. Kwang-Hwa Liu and Fred C. Y. Lee, "Zero-Voltage Switching Technique in DC/DC Converters", *IEEE Trans. on Power Electronics*, vol. 5, No. 3, April 1990.

35. Charles R. Sullivan, "Optimal Choice for Number of Strands in a Litz-Wire Transformer Winding", *IEEE Trans. on Power Electronics*, vol. 14, no. 2, March 1999, pp. 283-291.

36. E. E. Kriezis and J. A. Tegopoulos, “Eddy Cureents: Theory and Applications”, *Proceedings of the IEEE*, vol. 80, No. 10, October, 1992.

37. Ralph E. Locher, “Introduction to Power Supply”, National Semiconductor Application Note AN-556.

38. J.G. Kassakian, M.F. Schlecht and G.C. Verghese, *Principles of Power Electronics*, Addison-Wesley Publishing Company, Inc., 1991.

39. F.C. Lee, W.A.Tabisz and M.M. Jovanovic, “Recent Developments in High-Frequency Quasi-Resonant and Multi-Resonant Converter Technologies”, *Proc. EPE Aachen*, 1989.

40. Jun W. Lu, Francis P. Dawson and Sotoshi Yamada. “Analysis of High Frequency Planar Sandwich Transformers for Switching Converters”, IEEE Trans. on Magnetics, vol. 31, No. 6, Nov. 1995, pp.4235-4237.

41. M. Mino, T. Yachi and etc., “Planar Microtransformer with Monolithically-Integrated Rectifier Diodes for Micro-Switching Converters”, *IEEE Trans. on Magnetics*, vol. 32, No. 2. Mar., 1996, pp.291-296.

42. K. Yamaguchi, S. Ohnuma and etc., “Characteristics of a Thin Film Microtransformer with Circular Spiral Coils”, *IEEE Trans. On Magnetics*, vol. 29, No. 5, Sep. 1993, pp.2232-2237.

43. Kiyohito Yamasawa, Kenji Maruyama, Isao Hirohama and Paul P. Biringer, “High-Frequency Operation of a Planar-Type Microtransformer and Its Application to Multilayered Switching Regulators”, *IEEE Trans. on Magnetics*, vol. 26, No. 3, May, 1990, pp. 1204-1209.

44. *Planar E Core*, Application Note, Philips Magnetic Product, 1997.

45. J. W. Lu, F.P. Dawson and S. Yamada, "Application and Analysis of Adjustable Profile High Frequency Switchmode Transformer Having a U-Shape Winding Structure", *Proceeding of IEEE 3M-INTERMAG Conference 1998.*

46. K.W. Klontz, D.M. Divan and D.W. Novotny, "An Actively Cooled 120-kW Coaxial Winding Transformer for Fast Charging Electric Vehicles", *IEEE Trans. on Industry Applications*, vol.31, No. 6, Nov., 1995, pp.1257-1263.

47. R. Williams, D. Grant and J. Gowar, "Use of Multielement Transformers in Quasiresonant Converters", *IEE Proceedings-B*, vol. 140, No. 6, Nov, 1993.

Chapter 3

High Frequency Power Transformer Windings[1]

The manufacturers of ferrite supply their magnetic products as sets of ferrite parts and possibly ancillary parts from which the magnetic material user may construct a wound component to meet specific requirements. The winding, with all its possible variety in design and execution, is usually the concern of the user. For this reason, the magnetic component differs from other electrical components. Whereas a resistor or a capacitor leaves the manufacturer as a finished and tested component, the quality of a

[1] The work reported in this chapter resulted in the following publications:
1. Jun Lu and Fu Wong, "Faraday Shielding in Coaxial Winding Transformer," International Journal Of Applied Electromagnetics and Mechanics, Vol. 11, No. 4. July 2001. pp. 261-267.
2. Jun Lu and Fu Wong, "Effectiveness of Shielded High Frequency Coaxial Transformer for Switching Power Supplies," 2002 International Symposium & Technical Exhibition on Electromagnetic Compatibility.
3. Jun Lu and Fu Wong, "High Frequency Coaxial Transformer with Faraday Shield," IEEE Intermag 2000.

wound magnetic component depends on both the core manufacturer and the user, the designer of magnetic component.

Winding structure of high frequency transformers is the major factor to determine the performance of the transformer. The magnetic flux distribution and the eddy current flowing through the windings are two important things to be considered for high frequency transformer design.

3.1 Magnetic Flux Distribution in Transformer Windings

Leakage inductance and eddy current are two dangerous phenomena in high frequency transformer windings. They cannot be seen directly and are hard to be detected by some testing equipment. Fortunately they are governed by Maxwell's equations. In the last two decades of 20^{th} century, with the powerful computing machines and useful numerical analysis software packages, the images of the distributions of eddy currents and magnetic flux can be computed and appeared as visible pictures. With these numerical simulations, high frequency transformer winding structures can be further investigated.

Figure 3.1 shows the magnetic flux distribution inside a pot core transformer. The primary winding has been highlighted in Figure 3.1(a), it is located at the lower section of two groups of windings. The primary winding and the secondary winding are totally separated. At the operating frequency of 1 kHz, the magnetic flux mostly goes through the core structure and couples both windings. The phenomena of leakage flux happen, but not much compared with the main flux distribution. However, there is a big different when the operating frequency increases to 10 kHz. The majority of flux goes out from the magnetic core into the gap between the primary and secondary windings. In the last two pictures, the operating frequencies of 100 kHz and 1 MHz, all the flux goes out from the core, and none of all can couple between primary and secondary. According to these numerical simulations, the transformer can be defined not working well the operating frequency of 10 kHz or above.

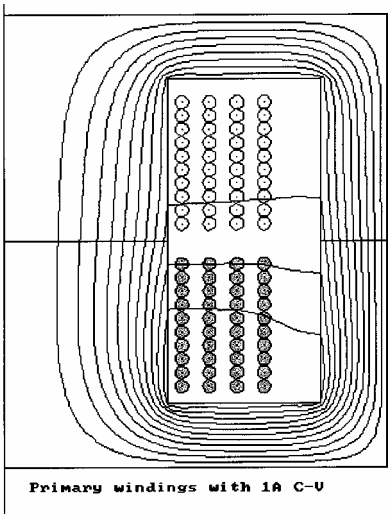

(a) Frequency = 1 kHz

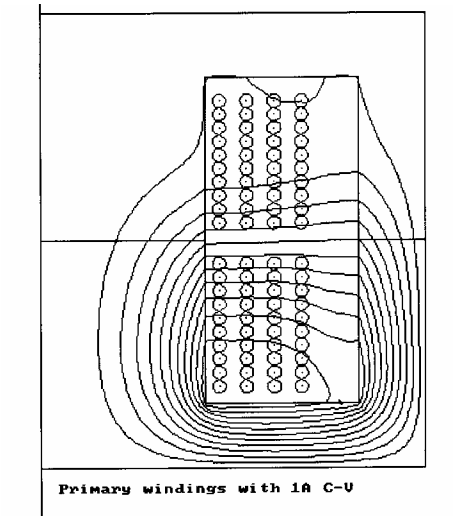

(b) Frequency = 10 kHz

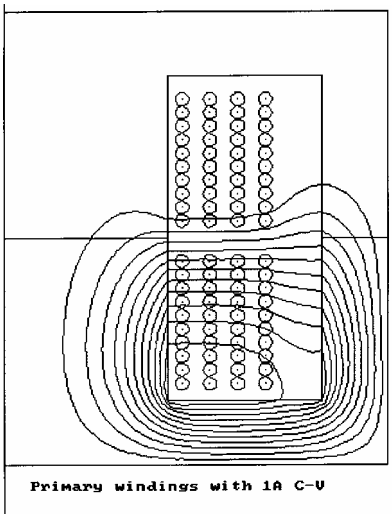

(c) Frequency = 100 kHz

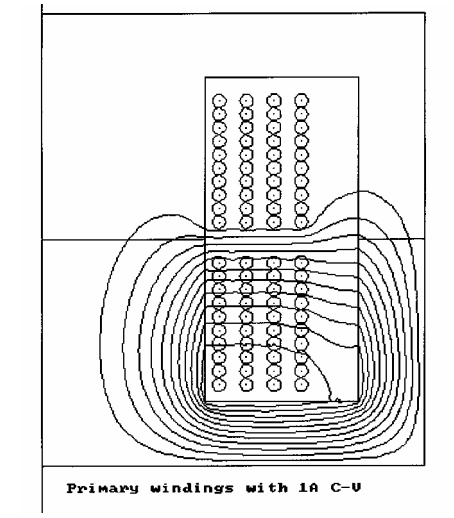

(d) Frequency = 1 MHz

Figure 3.1 Magnetic flux distribution at different operating frequencies.

The same situation can be seen from Figure 3.2. It is a transformer with single layer, primary winding is located on the top section of three copper wires, and the secondary is arranged at the bottom half section. The leakage flux appears when the

operating frequency up to 10 kHz, and it becomes destructive when the frequency increases to 100 kHz.

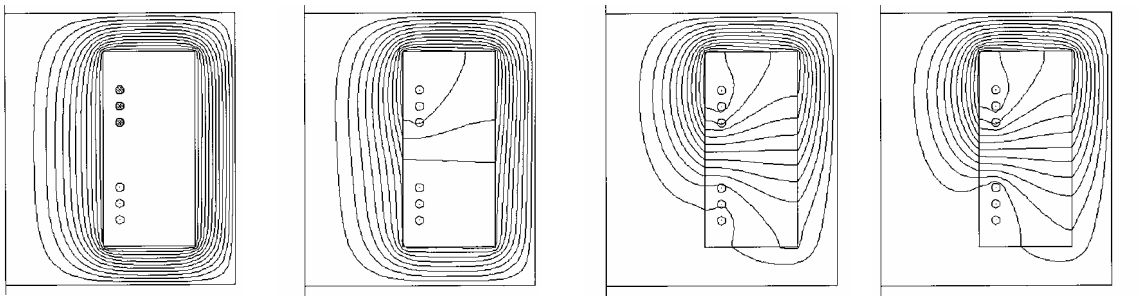

(a) f = 1 kHz **(b) f = 10 kHz** **(c) f = 100 kHz** **(d) f = 1 MHz**

Figure 3.2 Magnetic flux distribution of a transformer with single layer.

It is better to design a transformer with the windings fully using the winding window. In this case, the magnetic flux distribution of a high frequency pot core transformer is shown in Figure 3.3 with different operating frequencies. In Figure 3.3, the primary winding of the transformer is located at the top section of the winding windows. It is a 36 turns in six layers winding structure. The excitation current of 0.2 A is flowing through the primary.

The leakage flux coming out from the magnetic core goes through the space between the primary and the secondary of the transformer. This leakage flux generates eddy currents flowing inside the primary winding and the top section of the secondary winding. With this induced eddy current, the leakage flux is repelled. Therefore, no flux can penetrate the secondary winding as the operating frequency further increasing. The phenomenon of leakage flux inside a high frequency operated transformer can be explained by the eddy current flowing in the windings. Figure 3.4 shows the eddy current distribution of the windings of the transformer shown in Figure 3.3 (d) with the operating frequency of 1 MHz.

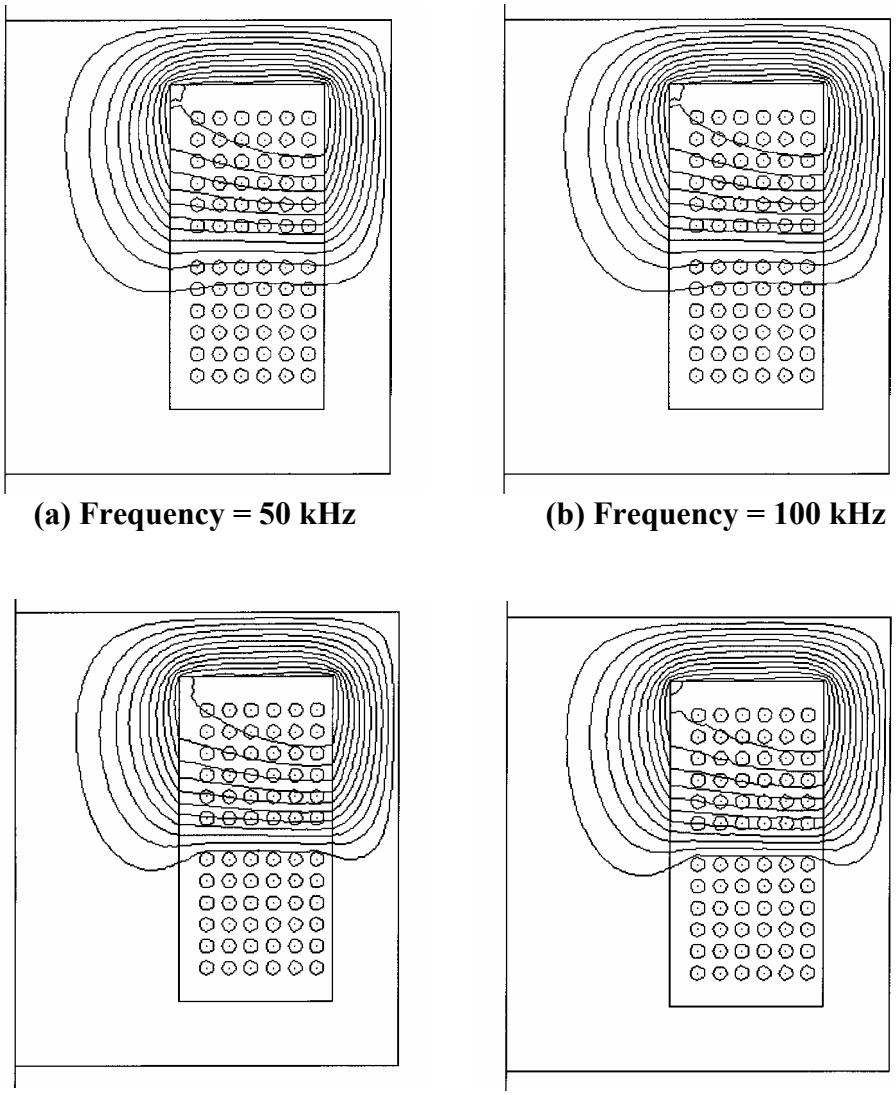

(a) Frequency = 50 kHz **(b) Frequency = 100 kHz**

(c) Frequency = 500 kHz **(d) Frequency = 1 MHz**

Figure 3.3 Magnetic flux distribution of pot core transformer with fully used the winding window.

3.2 Eddy Current in Transformer Windings

The maximum eddy current concentrates on the left top corner of the secondary winding with the value of 116,900 kA/m^2. It is a tremendous current density and generates huge power loss theoretically. The bottom section of the primary winding also experiences the eddy current density of 109,000 kA/m^2. It is an evident to prove the tradition winding structure cannot work with high frequency operations.

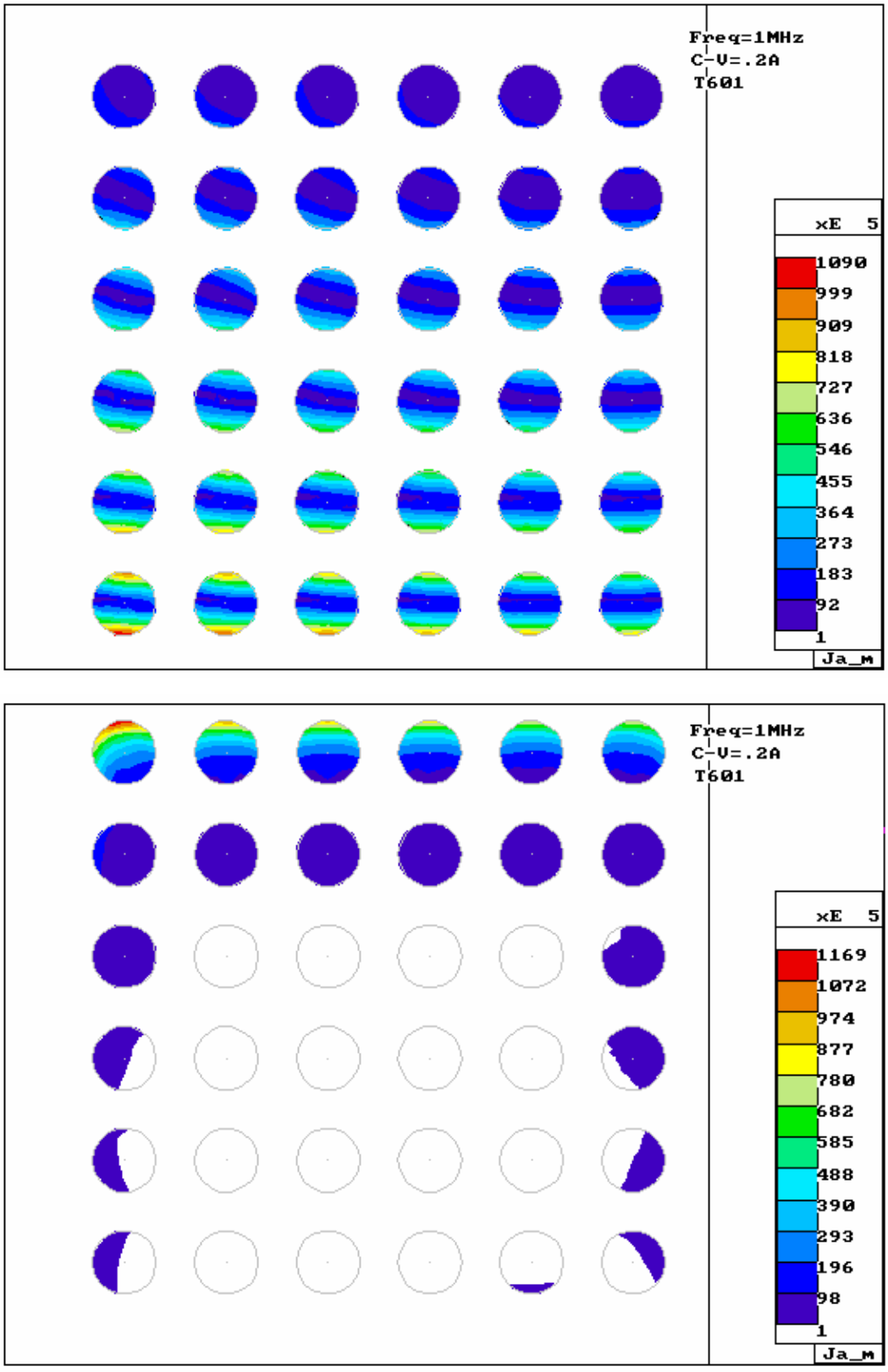

Figure 3.4 Eddy current distribution of the windings of transformer, shown in Figure 3.3 (d).

3.3 Leakage Inductance in Transformer Windings

From the Eqn. (2.76) of the previous section, the leakage inductance is found as

$$L_g \propto \frac{1}{M^2} \cdot \frac{h_w}{b_w} \tag{3.1}$$

where M is the number of section interfaces. If the number of section interfaces increases, the leakage inductance decreases. The relationship between them is that the leakage inductance is inversely proportional to the square of the number of section interfaces of the winding. According to the relationship, the special winding structure with interweaving has been developed [3]. The leakage inductance is greatly reduced, as shown in Figure 3.5.

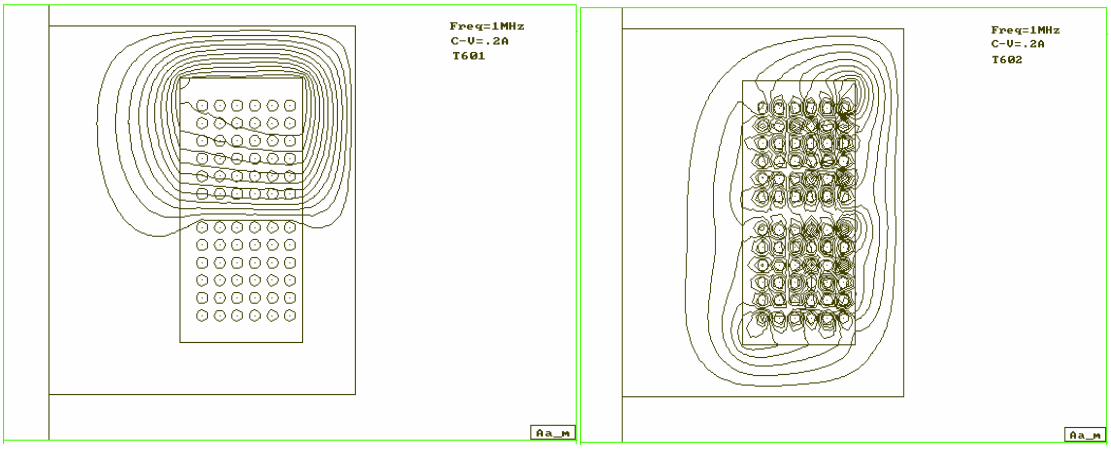

(a) **(b)**

Figure 3.5 Magnetic flux distribution
(a) pot core transformer with separated windings, and
(b) pot core transformer with interweaving windings.

Figure 3.5 (a) shows the magnetic flux distribution inside a pot core transformer with separated primary winding and secondary winding. The primary winding is located on the top section. The flux is against by the eddy current generated in the secondary winding. It is around the primary winding only. The main flux comes out from the core and becomes leakage flux.

Figure 3.5 (b) shows the magnetic flux inside the transformer with interweaving winding structure. It is a winding structure with the most number of section interfaces. Each wires of primary winding is separated by secondary wires, as shown in Figure 3.6. The leakage flux of this winding structure is much less than the leakage flux of the separated winding structure. Some main magnetic flux can go through the core to couple the windings. The comparison of the leakage inductance of these transformers is listed in Table 3.1.

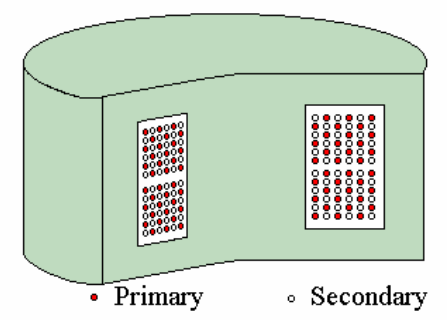

Figure 3.6 Interweaving winding structure.

Table 3.1 Leakage inductance of two winding structures at the frequency of 1MHz [3].

Model of Transformer		Leakage inductance
Separated windings	Primary	22.087μH
	Secondary	22.097μH
Interweaving windings	Primary	**0.362μH**
	Secondary	**0.389μH**

The leakage inductance of the interweaving winding structure is very small compared with the separated winding structure, however, it is still existing in the windings and not good for traditional transformer design. Figure 3.7 shows the difference of the magnetic flux distributions at different operating frequencies.

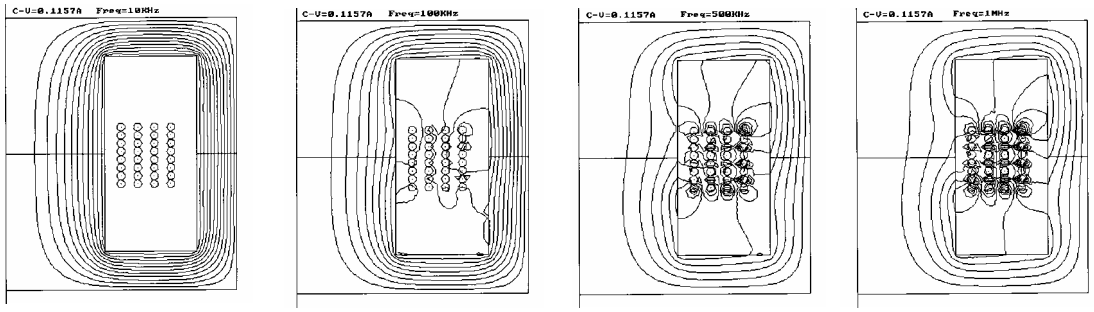

(a) f = 10 kHz **(b) f = 100 kHz** **(c) f = 500 kHz** **(d) f = 1 MHz**

Figure 3.7 Magnetic flux distributions of a transformer with interweaving winding structure operating at different frequencies.

The interweaving winding structure can increase the operating frequency of the transformer. It can be seen from the above figure and Figure 3.5. At the frequency of 10 kHz, the transformer with interweaving winding structure has almost no leakage inductance, refer to the numerical simulation shown in Figure 3.7 (a). However, the transformer with separated winding structure at the same frequency has all the main flux coming out from the magnetic core, Figure 3.1 (b). At the frequency of 100 kHz, the interweaving structure can have some main flux going through the core, even the frequency up to 1 MHz. But the separated winding structure cannot do the same job at 100 kHz already.

The interweaving winding structure can further reduce the leakage inductance inside high frequency power transformers, however, it is very hard to produce as mentioned in the fifth section of last chapter. It is not easy to wound circular copper wires in a perfect square arrangement by hand or by machine. Therefore new structure of windings, or new structure of whole transformers are urgently needed for power electronics recently.

3.4 New Winding Structures for High Frequency Transformers

In the last two decades of the 20th century, new structures of high frequency power transformers have been developed to meet the requirement of high frequency switching mode power supply applications. Two major transformer structures have been introduced by researchers, they are planar transformers [7, 8] and coaxial winding transformers [2, 9, 10]. According to these two structures of transformer, there are two new winding structures – planar winding structure and coaxial winding structure employed in high frequency power transfer applications.

3.4.1 Planar Winding Structure

Planar winding structure is the winding from a planar transformer which consists of a set of planar ferrite and the planar winding structure. Planar windings are commonly fabricated by printed circuit board (PCB) with track pattern etching on its copper foil. The PCB can be single-sided, double-sided or multi-layers boards. A typical planar transformer with planar winding is shown in the following figure.

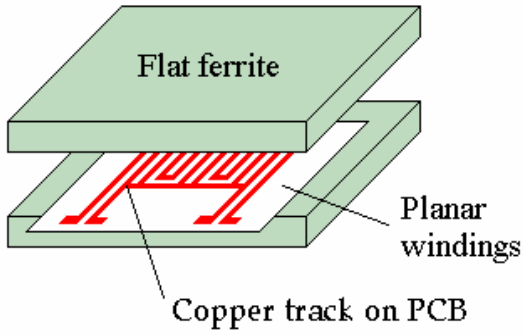

Figure 3.8 Typical planar transformer.

3.4.2 Type of Planar Windings

Three basic types of planar windings are shown in Figure 3.9. Hoop type is the simplest. Spiral type gives the largest inductance, but it is difficult to take the lead from the center of the coil. Meander type gives smaller loss at high frequency [1].

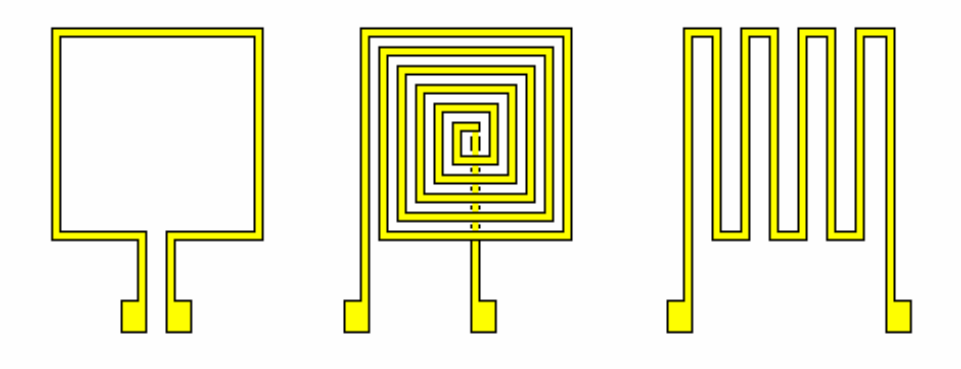

(a) (b) (c)

Figure 3.9 Basic type of planar winding structures, (a) hoop type, (b) spiral type, and (c) meander type.

3.4.2.1 Hoop Planar Winding

Figure 3.10 shows the top view and the cross section area of hoop type planar winding. Two pieces of flat ferrite sandwich the hoop winding. The simple hoop planar winding for high frequency transformer applications have two windings located on the top side and bottom side of the PCB. They are basically identical.

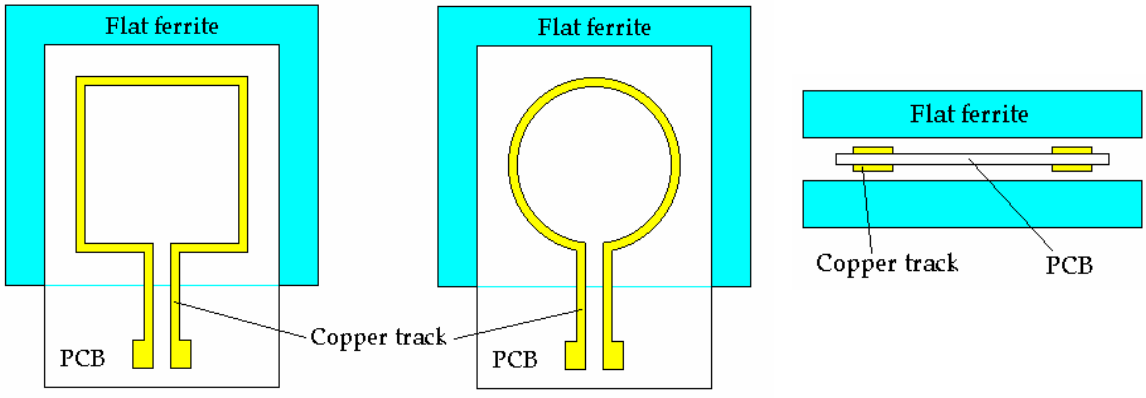

(a) (b) (c)

Figure 3.10 Hoop planar winding and its cross section of transformer.

One of the windings can be worked as primary winding of a transformer, and the other winding is performed as secondary winding to produce output power. Hoop type

windings can be the rectangular sharp or circular sharp. It is a very simple structure and it is the pioneer of planar transformer windings. However, its inductance and input impedance are very small, it is not common used in power transfer applications.

The hoop planar winding can be modified and fabricated by single-sided PCB to reduce the air gap between two pieces of flat ferrite. But, the length of the two windings is different. Therefore, the inductance and impedance of the two windings are not equal.

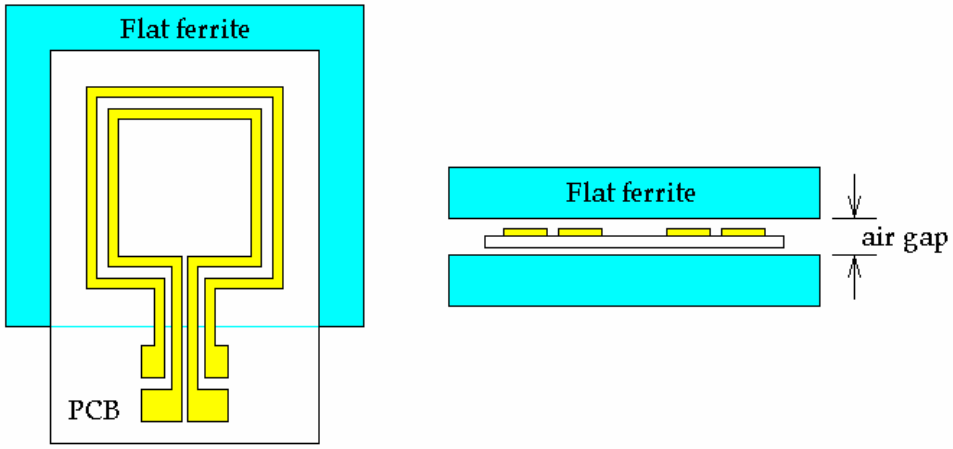

Figure 3.11 Hoop windings formed by single-sided PCB.

3.4.2.2 Spiral Planar Winding

Based on hoop planar windings, spiral planar windings have been developed [4, 5]. A hoop type of planar winding consists of two single turn windings as primary and secondary windings. The inductance and the impedance for each winding are very small. Spiral planar windings have more turns in each winding, therefore, the structure becomes more flexible by changing of wiring arrangements. The primary winding and secondary winding of winding structure can occupy one side of the PCB, shown in Figure 3.9 (b), or interleave between the two sides of the board, shown in the figure below.

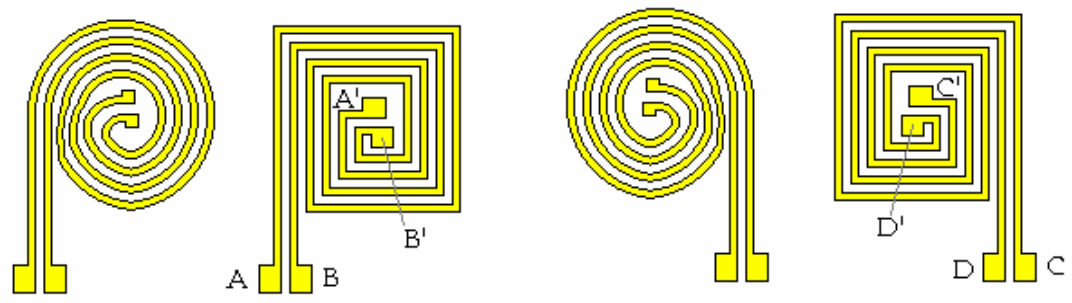

(a) Top side track pattern **(b) Bottom side track pattern**

Figure 3.12 Spiral planar winding structures.

A primary winding can be started from the connection pad, A, to the other pad, A', as the end terminal for a single-sided arrangement, or extended from the pad, A', to the pad, C', on the other side of the PCB by using a "via" of PCB fabrication skill. Then the final terminal is ended at the pad, C, for a double-sided configuration. The similar situation of the secondary winding starts at B to B' for single-sided planar winding, or extended from B' to D' and further to D as the end point.

The spiral planar windings have large inductance for both primary and secondary windings, and large input impedance of the whole transformer. This winding structure can be used with or without flat ferrite pieces. Without flat ferrite pieces, it is called "coreless planar transformers" [6, 11].

3.4.2.3 Meander Planar Winding

The basic structure of meander winding can be seen in Figure 3.9 (c). The direction of the copper track keeps changing from clockwise to anti-clockwise. It is totally different from the hoop type and spiral type winding structures, their directions keep at clockwise or anti-clockwise for the same track all the time.

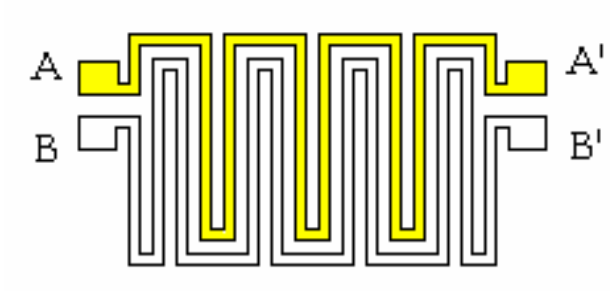

(a)

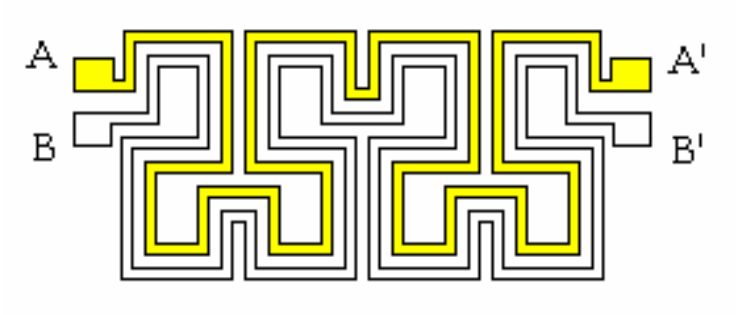

(b)

Figure 3.13 Meander planar windings.

Figure 3.13 shows two styles of meander planar windings of high frequency transformer applications. Both of them can be fabricated by single-sided or double-sided PCBs. A modified meander winding, called S-line Meander Planar Winding is shown in Figure 3.13 (b).

The voltage ratio of these two meander type windings are very similar with the same winding area. Figure 3.14 shows the voltage ratio of them.

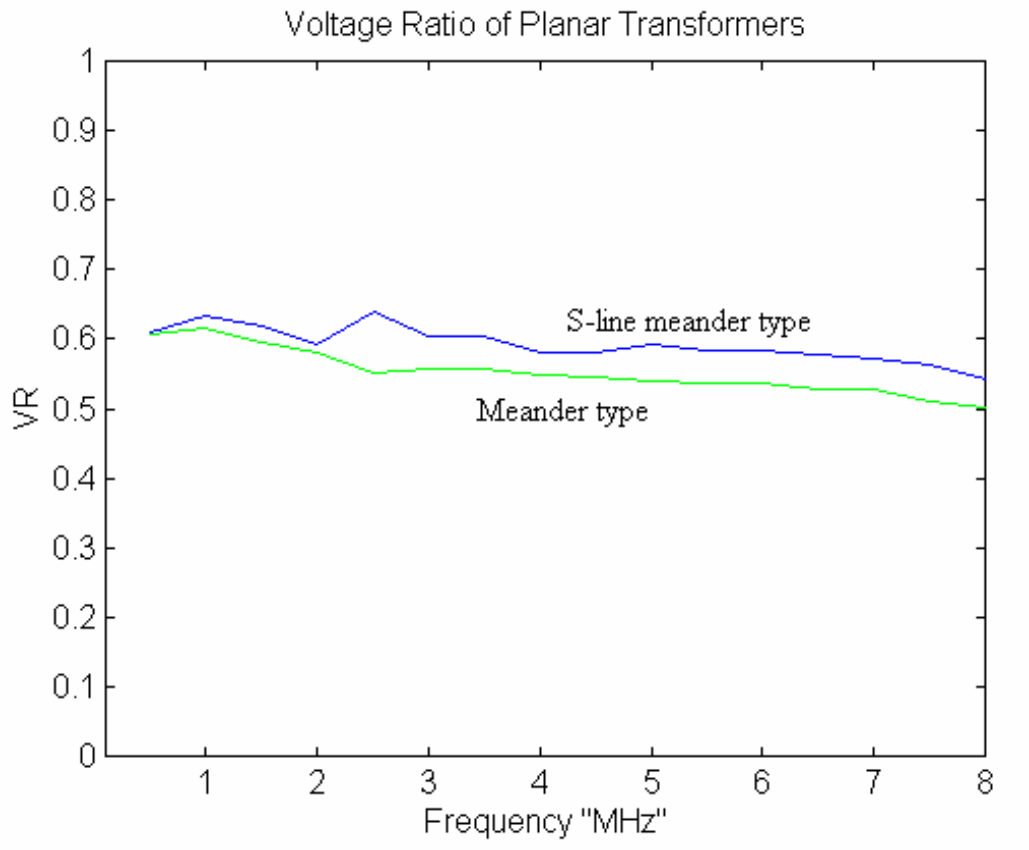

Figure 3.14 Voltage ratio of the two meander types of windings.

Each type of the planar winding structures has its own advantages and disadvantages. The detail analysis will be discussed in the next chapter with numerical simulations and experimental results.

3.4.3 Coaxial Winding Structures

Coaxial windings are the winding structures of coaxial winding transformers, shown in Figure 3.15. Coaxial winding transformers have recently been reported to have excellent performances at high frequencies. Very low leakage inductance, low eddy current losses and high power density are the advantages of the transformer [2, 9, 10]. Coaxial windings structure transformers can be used in high frequency switching mode power supply perfectly. According to its flexible combination of number of magnetic ring cores, the power handling range of the type of transformers can be easily adjusted to desired level.

Figure 3.15 shows the basic structure and the cross section of a coaxial winding transformer. The coaxial winding transformer consists of ferrite ring cores, a copper tube and a central copper rod. The turn ratio of the transformer is 1:1. The ferrite ring cores are around the copper tubes to provide the magnetic path for the transformer. The coaxial windings have a copper tubes working as the single turn primary winding and the central rod going through the tube as the secondary winding normally.

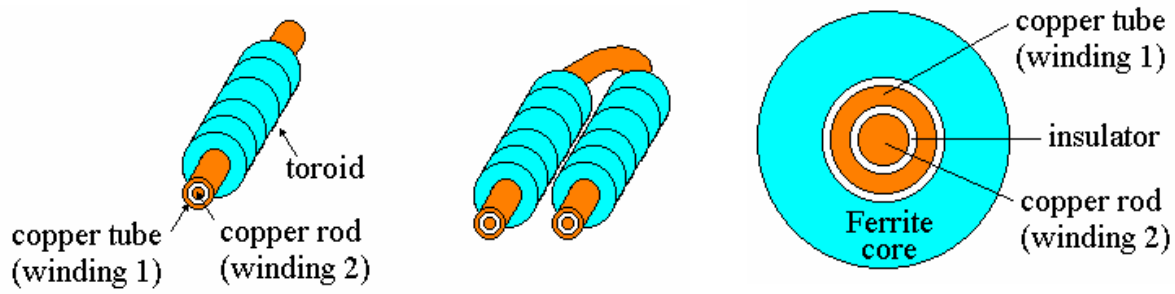

Figure 3.15 (a) Basic structure, (b) U-Shape, and (c) Cross section of coaxial winding transformer.

According the basic structure of coaxial winding, the U-shape coaxial winding structure has been developed, shown in Figure 3.15 (b). The U-shape structure has the advantages of half of the total length of the basic structure and single side termination of transformer [2]. The end termination of the coaxial winding structure is completed by a piece of PCB, and the overall structure of coaxial winding transformer is shown in

Figure 3.16 (a). Furthermore the U-shape was replaced by another piece of PCB, and the fundamental structure of coaxial winding transformer is finalized as shown in Figure 3.16 (b).

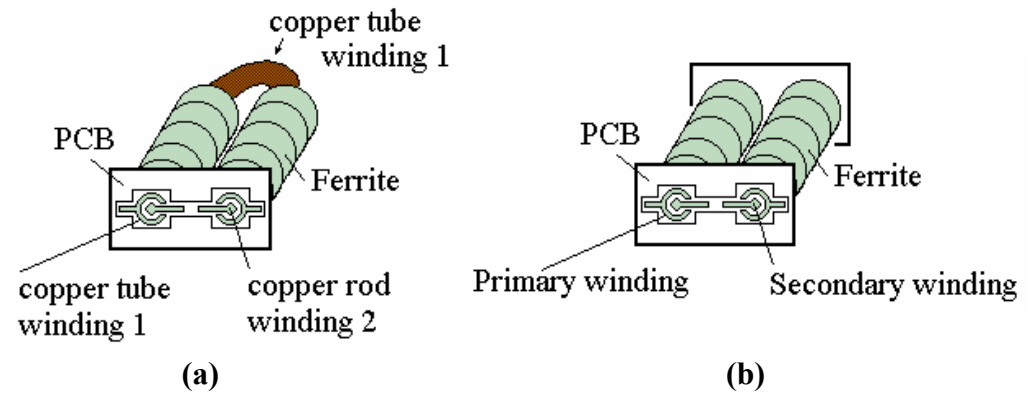

Figure 3.16 Fundamental structure of coaxial winding transformers.

Coaxial winding structure has been further modified to some derivatives. Figure 3.17 shows cross sections of them.

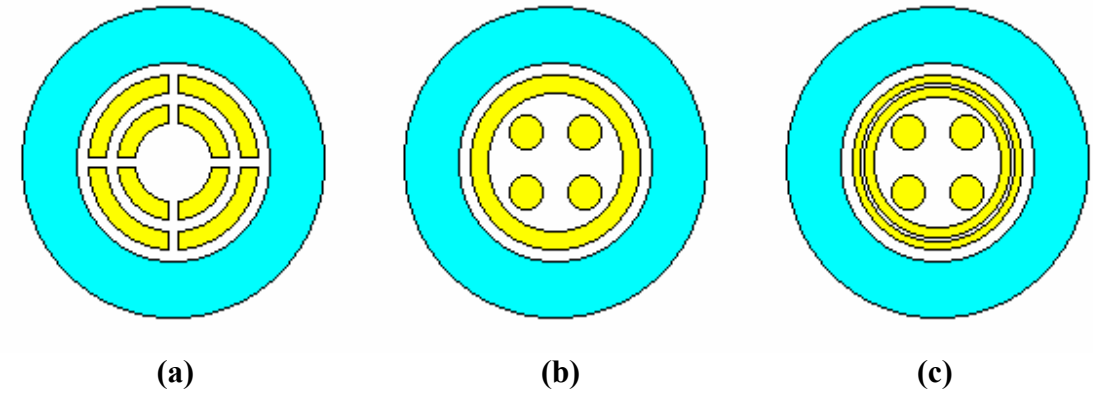

Figure 3.17 Cross sections of derivatives of coaxial winding structures.

The first modified structure is shown in Figure 3.17 (a), there are two changes of the structure compared with the basic type of the coaxial winding. The copper tube of winding 1 was separated in two parts as half circle or even in four pieces as quarter circle in shape. The other change is the copper rod was replaced by another copper tube and separated as the winding 1.

The second derivative can be seen in Figure 3.17 (b), four copper wires were used as winding 2, instead of the copper rod or the separated copper tube. The number of wires can be adjusted to match with special requirements of power transfer applications. By using a single copper wire with few times passing through the copper tube, the winding 2 becomes few tuns to one turn of the windings, as shown in Figure 3.18. The turn ratio is not fixed to 1 : 1 ratio.

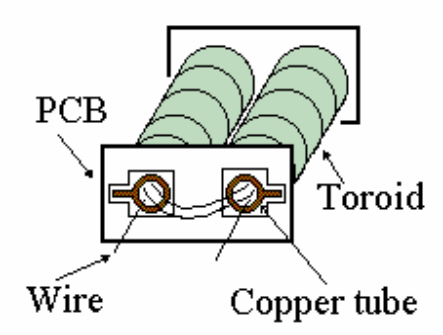

Figure 3.18 Arrangement of the copper wires of coaxial winding.

There is another modified winding by inserting one more shield copper tube between winding 1 and winding 2. It is a Faraday shield. With suitable arrangement of this Faraday shield, the interwinding capacitance, C_{12}, in Figure 2.4 of Chapter 2, can be minimized [12 – 14].

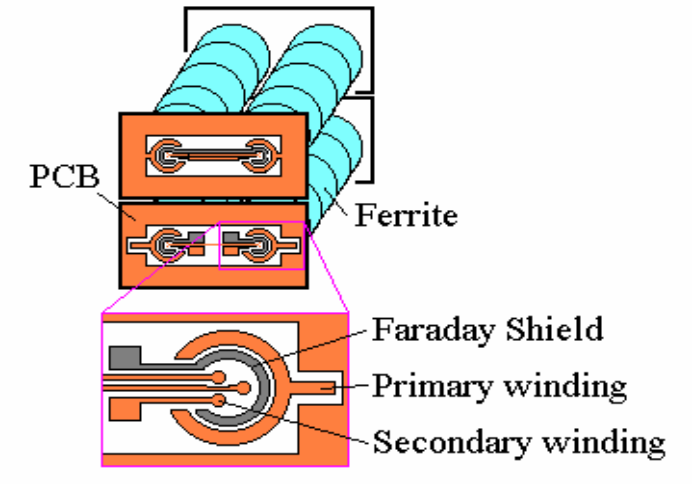

Figure 3.19 Coaxial winding structure with Faraday shield.

3.5 Coaxial Winding Structure with Faraday Shield

Actual transformers, not being ideal, have capacitance between the primary and secondary windings, which allows noise coupling through the transformer. This coupling can be eliminated by providing an electrostatic (Faraday) shield which is formed by a grounded conductor between the two windings. If it is properly designed, this shield does not affect the magnetic coupling, but it eliminates the capacitive coupling when the provided shield is grounded. In addition, the shield coil may contribute the eddy-current loss in the high frequency range, the location and the thickness of shield should be considered in the design.

In most applications, a Faraday shield will be required where the high-frequency, high voltage switching waveforms can capacitively couple to the ground plane or secondary output [12].

As Faraday shield inserted between the primary and secondary windings, it can significantly reduce the capacitive coupling between the windings. The equivalent circuit of a transformer with a shield is shown in Figure 3.20. The coupling capacitance, C_{12}, theoretically could be decreased to zero by means of a grounded shield. The insertion loss of a HF transformer can be minimized by using this faraday shield, because the insertion loss is basically determinant by the parasitic capacitances of the winding and the capacitive coupling between the windings

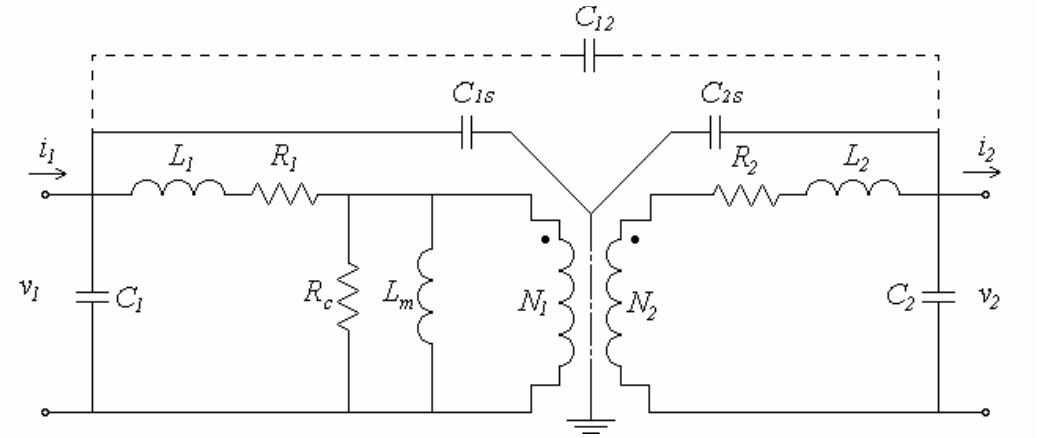

Figure 3.20 Equivalent circuit of high frequency transformer with Faraday shield.

3.5.1 Eddy-Current Distribution in Coaxial Windings

The coaxial winding structure has many advantages over conventional transformer winding structures. It has low eddy-current losses in the windings compared with any other conventional transformer [3]. Figure 3.21 shows the eddy-current distribution in both windings and the shield coil, where the excitation source is applied to the primary winding. The secondary winding is short-circuited and the shielding coil located between primary and secondary windings is open-circuited. From the numerical simulation results, the eddy-current in the shield coil can be seen to be relatively small compared with the eddy-current in the secondary windings, but it contributes some power losses in the transformer.

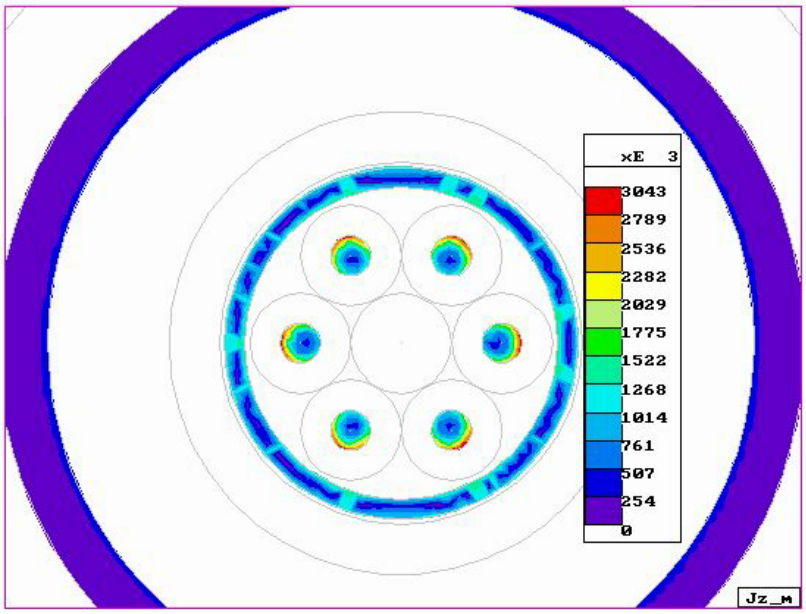

Figure 3.21 Eddy-current distribution in the HF coaxial transformer with Faraday shield at the excitation frequency of 1 MHz.

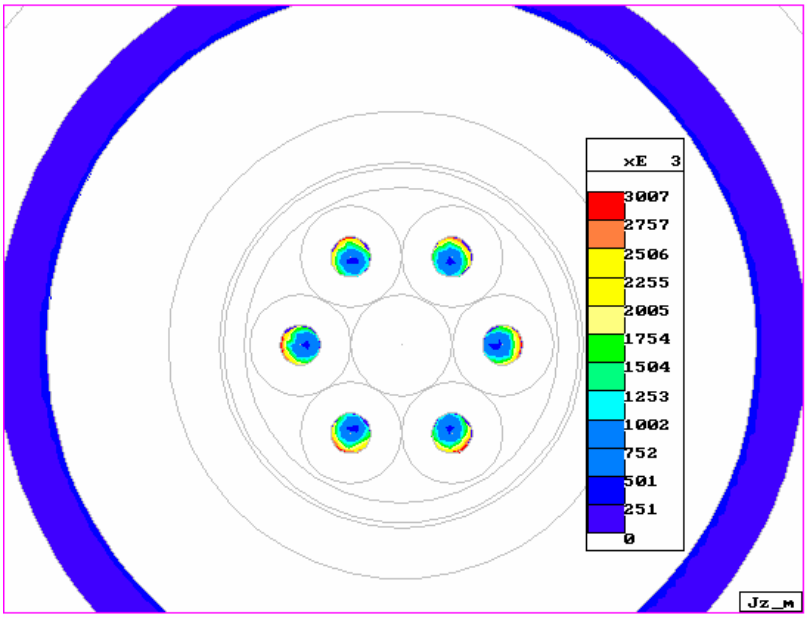

Figure 3.22 Eddy current distribution of the HF transformer without Faraday shield at operating frequency of 1MHz.

3.5.2 Comparison of the HF Transformers with and without Shield

From the above two figures, Figure 3.21 and Figure 3.22, the eddy current distributions are almost similar. From the following two figures, Figure 3.23 and Figure 3.24, the magnetic flux distributions of these two transformer windings are nearly identical. It is a solid evident to prove the Faraday shield will not effect the magnetic flux and eddy current distribution, but it can minimized the inter-winding capacitance.

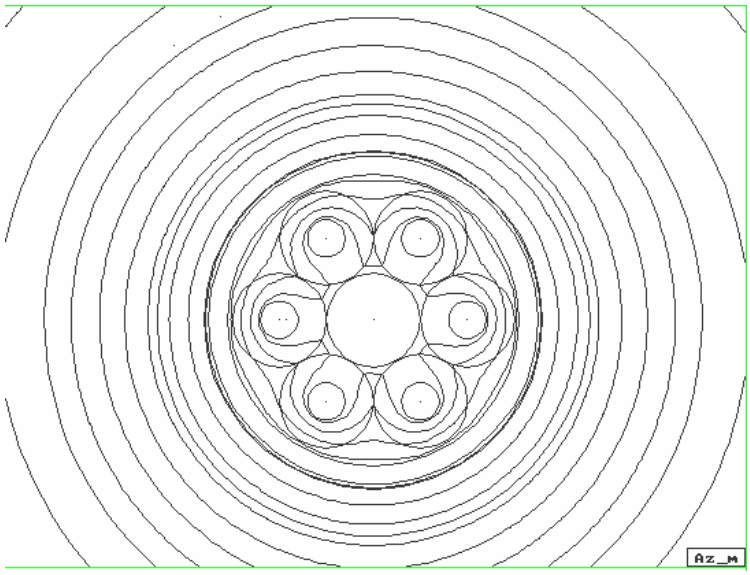

Figure 3.23 Magnetic flux distribution of the transformer with Faraday shield.

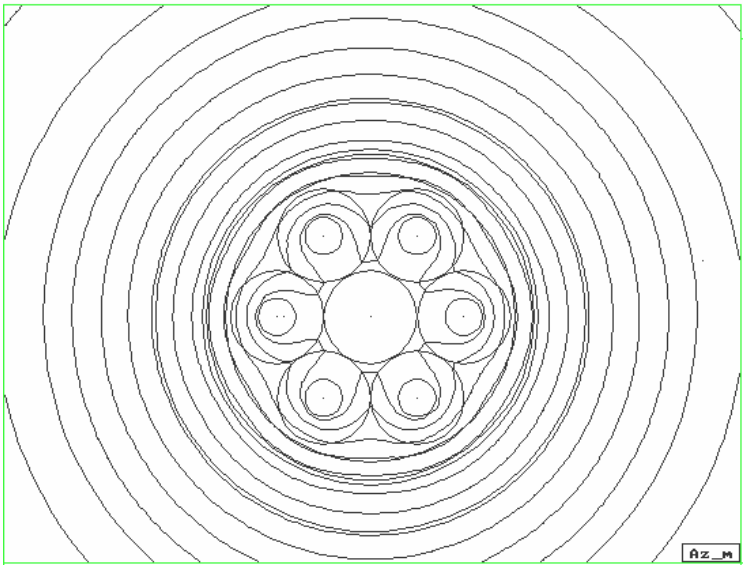

Figure 3.24 Magnetic flux distribution of the transformer without Faraday shield.

The magnetic flux circulated locally around the each wire of secondary winding has been calculated by numerical method as shown in the above figures.

3.5.3 Experimental Results with Load

The coaxial winding transformer has been tested with load by using single switch forward switching resonate converter configuration. Two switching frequencies, 736.44 kHz and 1.144 MHz, have been used to investigate the characteristic of the transformer. The measured waveforms of 1.144 MHz are shown in the Figure 3.25.

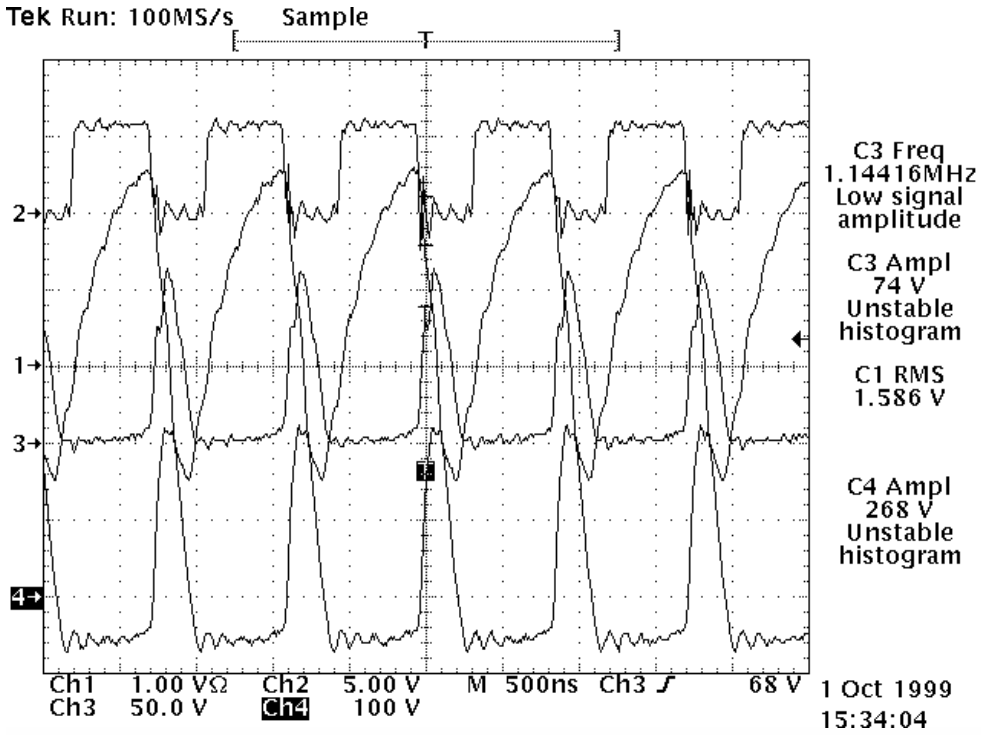

Figure 3.25 Switching waveforms of the coaxial transformer at 1.144 MHz.

The waveform (Channel 2) at the top of Figure 3.25 is measured between the gate and the source of the switching MOSFET. Channel 3 is the waveform of V_{DS} of the MOSFET. The output from the secondary winding of the testing transformer is monitored by channel 4. The current flowing through the primary winding indicated by channel 1. The peak to peak voltage ratio is 3.62 for the operating frequency at 1.144MHz. It is agree with the physical structure of the coaxial transformer, the turn

ratio of the transformer 1:3, and the length of the tracks on the printed circuit board at the ends of the transformer.

3.5.4 Eddy Current Distribution at 10 MHz

The coaxial transformer winding has been simulated at the operating frequency of 10 MHz. The eddy current distribution is shown in Figure 3.26.

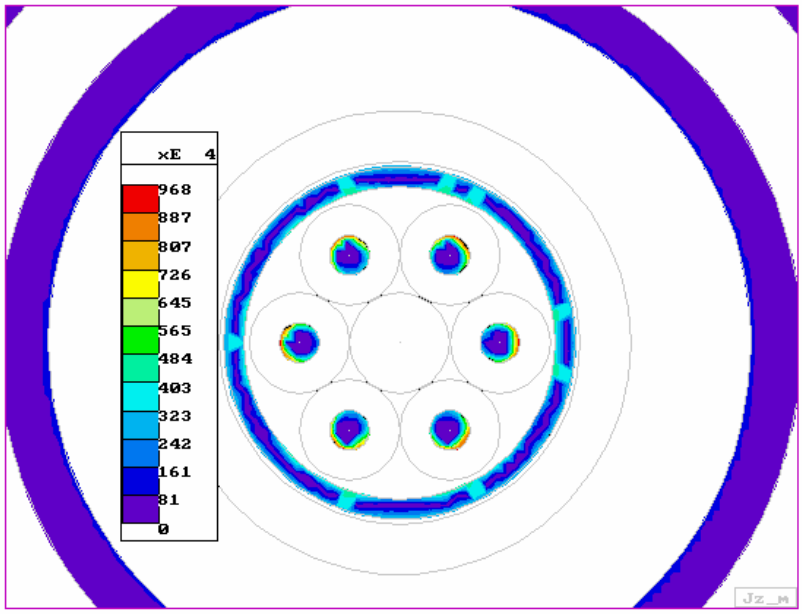

Figure 3.26 Eddy current distribution of the transformer at the operating frequency of 10 MHz.

The highest current density is only located on the surface of the secondary windings. Comparing with Figure 3.21, the maximum eddy current densities in the windings of the HF transformer increased only three times higher, when the excitation frequency increased from 1MHz to 10MHz. While the eddy current density in the Faraday shield was kept in the same level at these frequency range. Therefore, the coaxial winding structure can be used at very high frequency and high power applications.

Coaxial winding structures have been found that they are very outstanding

performance at very high operating frequencies. However, the manufacturing technique of the winding structure is very complicated and the height of the transformer does not match with the needs of the low profile of modern miniature electronic devices. It can be employed in heavy power applications, such as electric vehicle industry area. However, for the low to medium power applications, the planar transformer is still the best choice of the high frequency magnetics. In the next Chapter, a planar transformer with an excellent high frequency characteristic will be introduced.

3.6 References

1. K. Kawabe, H. Koyama and K. Shirae, "Planar Inductor", *IEEE Trans. on Magnetics*, vol. MAG-20, No.5, September, 1984, pp. 1804-1806.

2. J. Lu, F. P. Dawson and S. Yamada, "Application and analysis of adjustable profile high frequency switchmode transformer having a U-shaped winding structure", IEEE Trans. on Magnetics, Vol. 34.

3. Fu Wong, *High Frequency Switching Resonant Converters: Magnetics and Gate Drive Considerations*, Master Dissertation, Griffith University, May 1997.

4. K. Yamaguchi, S. Ohnuma T. Imagawa, J. Toriu, H. Matsuki, and K. Murakami, "Characteristics of a Thin Film Microtransformer with Circular Spiral Coils", *IEEE Trans. On Magnetics*, vol. 29, No. 5, Sep. 1993, pp.2232-2237.

5. Jun W. Lu, Francis P. Dawson and Sotoshi Yamada, "Analysis of High Frequency Planar Sandwich Transformers for Switching Converters", *IEEE Trans. on Magnetics*, vol. 31, No. 6. Nov., 1995, pp.4235-4237.

6. S.C. Tang , S.Y.(Ron) Hui and Henry Shu-hung Chung, "Coreless Planar Printed-Circuit-Board (PCB) Transformers – A Fundamental Concept for Signal and Energy Transfer", *IEEE Trans. on Power Electronics*, vol. 15, No. 5, September 2000. pp 931-940.

7. O.Oshiro, H. Tsujimoto and K. Shirae, “Structures and characteristics of planar transformers”, *J. Magn. Soc. Japan*, vol. 12, pp. 385-388, 1988.

8. M. Mino, T. Yachi, A. Tago, K. Yanagisawa and K. Sakakaibara, “A new planar mcirotransformer for use in microswitching converters”, *IEEE Trans. Magnetics*, vol.28, pp.1969-1073, July 1992.

9. R. Williams, D.A. Grant and J. Gowar, “Use of multielement transformers in quasiresonant convertors”, *IEE Proceedings-B*, vol. 140, no. 6, November 1993, pp. 357-361.

10. Keith W. Klontz, Deepakraj M. Divan and Donald W. Novotny, “An Actively Cooled 120-kW Coaxial Winding Transformer for Fast Charging Eletric Vehicles”, *IEEE Trans. on Industry Applications*, vol. 31, no. 6, November, 1995, pp. 1257-1263.

11. S. Y. (Ron) Hui, Henry Shu-hung Chung, and S. C. Tang, “Coreless Printed Circuit Board (PCB) Transformers for Power MOSFET/IGBT Gate Drive Circuits”, *IEEE Trans. on Power Electronics*, vol. 14, no.3, May 1999, pp. 422-430.

12. Jun Lu and Fu Wong, “Faraday Shielding in Coaxial Winding Transformer”, *International Journal Of Applied Electromagnetics and Mechanics*, Vol. 11, No. 4. July 2001. pp. 261-267.

13. Jun Lu and Fu Wong, “Effectiveness of Shielded High Frequency Coaxial Transformer for Switching Power Supplies”, 2002 International Symposium & Technical Exhibition on Electromagnetic Compatibility.

14. Jun Lu and Fu Wong, “High Frequency Coaxial Transformer with Faraday Shield”, IEEE Intermag 2000.

Chapter 4

Planar Transformer with Helical Winding Structure[1]

1 The work reported in this chapter resulted in the following publications:

1. Fu Wong, Jun Lu and David Thiel, "Design Consideration of High Frequency Planar Transformer," IEEE Transactions on Magnetics. (accepted)
2. Fu Wong, Jun Lu and David Thiel, "Characteristics of High Frequency Planar Transformer with Helical Winding Structure," Series of Japan Society of Applied Electromagnetism and Mechanics (JSAEM), vol. 14, 2003. pp. 213-217.
3. Fu Wong and Jun Lu, "High Frequency Planar Transformer with Helical Winding Structure," IEEE Trans. on Magnetic, September 2000. pp.3524-3526.

The 21st century saw the rapid development of semiconductor and the electronic world is dominated by integrated circuits. Personal computers, mobile phones, portable CD players, DVD players and TVs, all of them are microminiaturised by integrated semiconductors. All these things have become part of our daily life. It is a truly integrated age. High frequency magnetic components are important elements of the electronic circuits and are changing to be more integrated with electronic devices.

Planar magnetic components are one major group of integrated magnetics [1]. Their importance was confirmed in the last decade of the 20th century [2-8]. They have highly been used in the modern integrated power electronic devices. Some planar transformer structures have been introduced in the previous chapter, with very good performance in high frequency operations. However, there are still disadvantages.

4.1 Introduction of Planar Transformer

A planar transformer is different from the traditional transformers, such as core-type transformers and shell-type transformers discussed in Chapter 2. A planar transformer consists of a planar winding structure and a set of planar magnetic material pieces. The planar winding structure is commonly constructed on printed circuit boards fabricated with the photographic reproduction technique. The reproduction technique can guarantee the pattern of the winding to be identical with the original design. It is very important to maintain the high frequency characteristics of the planar winding structure. Another method to produce relatively small planar winding structures is by the fabrication of an integrated circuit to form micro-transformers and integrated magnetics. However, this will not be considered in this thesis. The planar winding structure discussed in the document was made of printed circuit boards with double sided copper layers.

While the transformer works without magnetic materials, performance is improved using a set of flat ferrite pieces. Various winding and magnetic core structures have been developed for high frequency transformer applications recent years [2-3, 6, 19-21]. Among them, the planar air core transformers and the planar magnetic core transformers are targeted by high frequency switched mode power supply designers. Both of them have their advantages and disadvantages for high frequency applications.

4.1.1 Advantage of Planar Transformers

The main advantages of planar transformers are the low profile and the good high frequency properties, which lead to a high power density. The traditional transformer has a relatively large dimension in height which is an obstacle for miniaturizing the design of the electronic device. A planar transformer can overcome this problem with its low height, and matches with the other electronic components sitting on the printed circuit board easily. Compared with the round wires used in the conventional transformers, very thin tracks are employed in the planar winding structure. They can significantly reduce the skin effect in the winding of the transformers. The most important point is that the arrangement of planar windings can be precisely duplicated simply by photographic reproduction technique. The high frequency performance of planar magnetics can be guaranteed. Planar transformers can be easily adopted by integrated circuits with their fabrication techniques.

The advantages of planar transformers can be summarized:

- low leakage inductance
- low eddy current losses
- high frequency capability
- high efficiency
- high power density
- lower height
- exactly repeatable
- solid mechanical construction
- high process capability

- good thermal performance

There are many advantages of planar transformers, however, there are also some disadvantages of existing ones.

4.1.2 Disadvantage of Existing Planar Transformers

The drawback of the existing planar transformer structures is mainly based on the unbalance of magnetic flux distribution inside the winding structure [2]. Therefore, the eddy currents concentrate on the area of high leakage flux. The uneven eddy current losses will selectively heat up some sections of the high frequency transformer, and these hot spots may damage the transformer.

The planar magnetic core transformers using meander type or spiral type winding structures have severe problems resulting from the proximity effect, therefore the unbalance magnetic flux distribution phenomena is of concern. The high frequency characteristic of the winding structures can be significantly degraded. In the next section, the disadvantage of existing planar winding structures is demonstrated by numerical simulation. From these simulation results, these non-visible electromagnetic phenomena can be seen and better winding structures are developed.

4.2 Numerical Simulation of Existing Planar Winding Structures

To understand the current and field structure at high frequencies, numerical simulation is a very useful tool. The tool can visualize fields and currents inside the winding structures. According to these simulation results, the details of the structures can be further investigated. In the following section, the magnetic flux and eddy current distributions are calculated by a software package, Oersted, with Boundary Element Method [9]. The magnetic flux around planar windings and the eddy current flowing in each track can be totally discovered.

4.2.1 Magnetic Flux and Eddy Current Distribution of Meander Windings

Magnetic flux distribution of planar meander type winding structure has been calculated by the simulation package and the flux distribution is shown in Figure 4.2. The simulation is based on the winding structure shown in Figure 4.1. The operating frequency is 1 MHz and the excitation current is 0.2 A. The magnetic flux is highly concentrated on the outer tracks of the windings. But there is very little of flux around the middle area of the planar winding structures. The uneven distribution of magnetic flux of meander type winding structure can be clearly demonstrated.

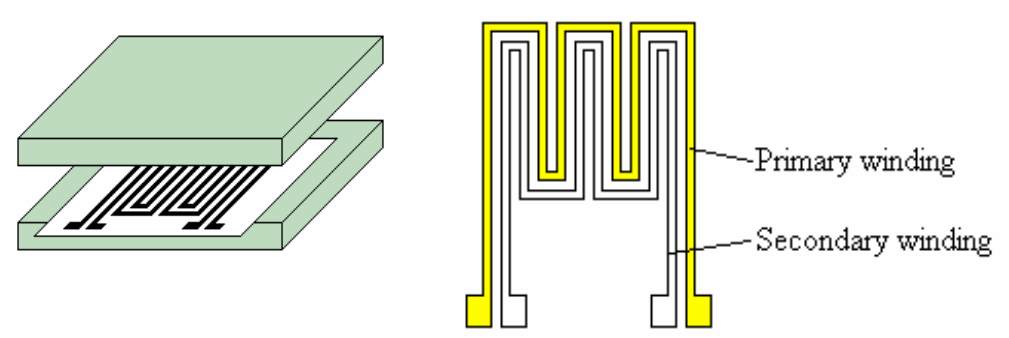

Figure 4.1 The structure of meander type planar transformer.

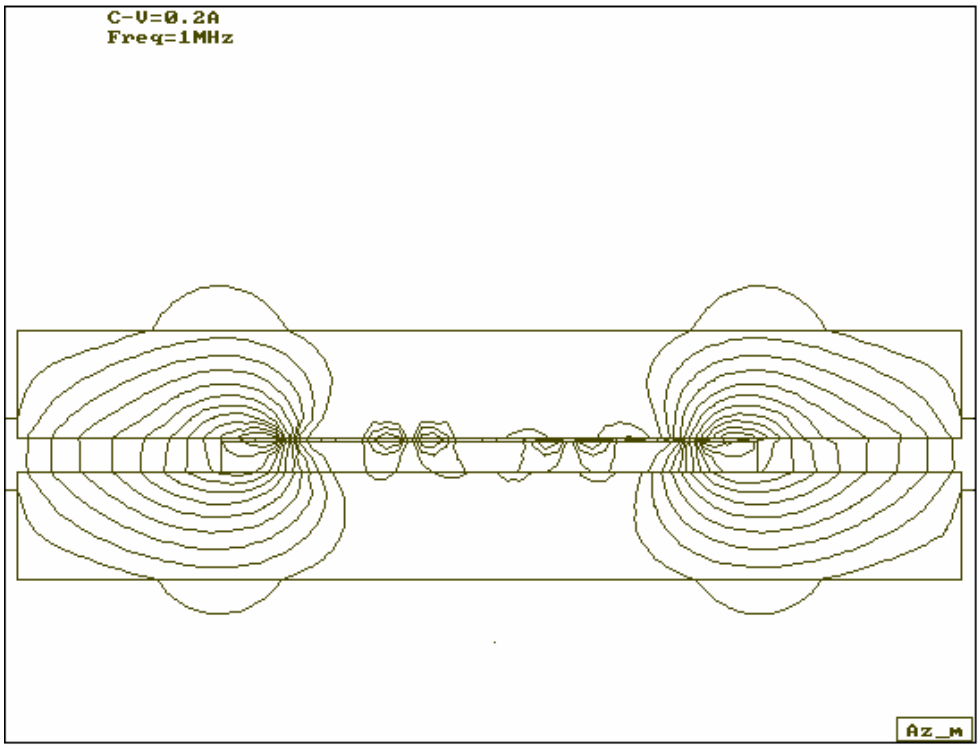

Figure 4.2 Magnetic flux distribution of meander type planar transformer.

Figure 4.3 shows the eddy current distribution of the transformer. From these figures, the unbalanced flux distribution can be seen, the eddy current and the leakage flux highly concentrate at the most outer pair of tracks. The magnetic flux generated by the most outer tracks has been repelled by the tracks sitting next to them, due to the eddy current flowing inside these tracks. The eddy current distribution inside the winding structure is found very uneven on each track. Based on the excitation current of 0.2 A flowing through the primary winding, the maximum eddy current density is calculated of 1670×10^4 A/m^2, it is located at the opposite sides of the most outer pair of tracks. This highly concentrated eddy current is the major problem when the operating frequency is getting higher. It will heat up the tracks, melt the copper tracks, and destroy the whole structure of the transformer.

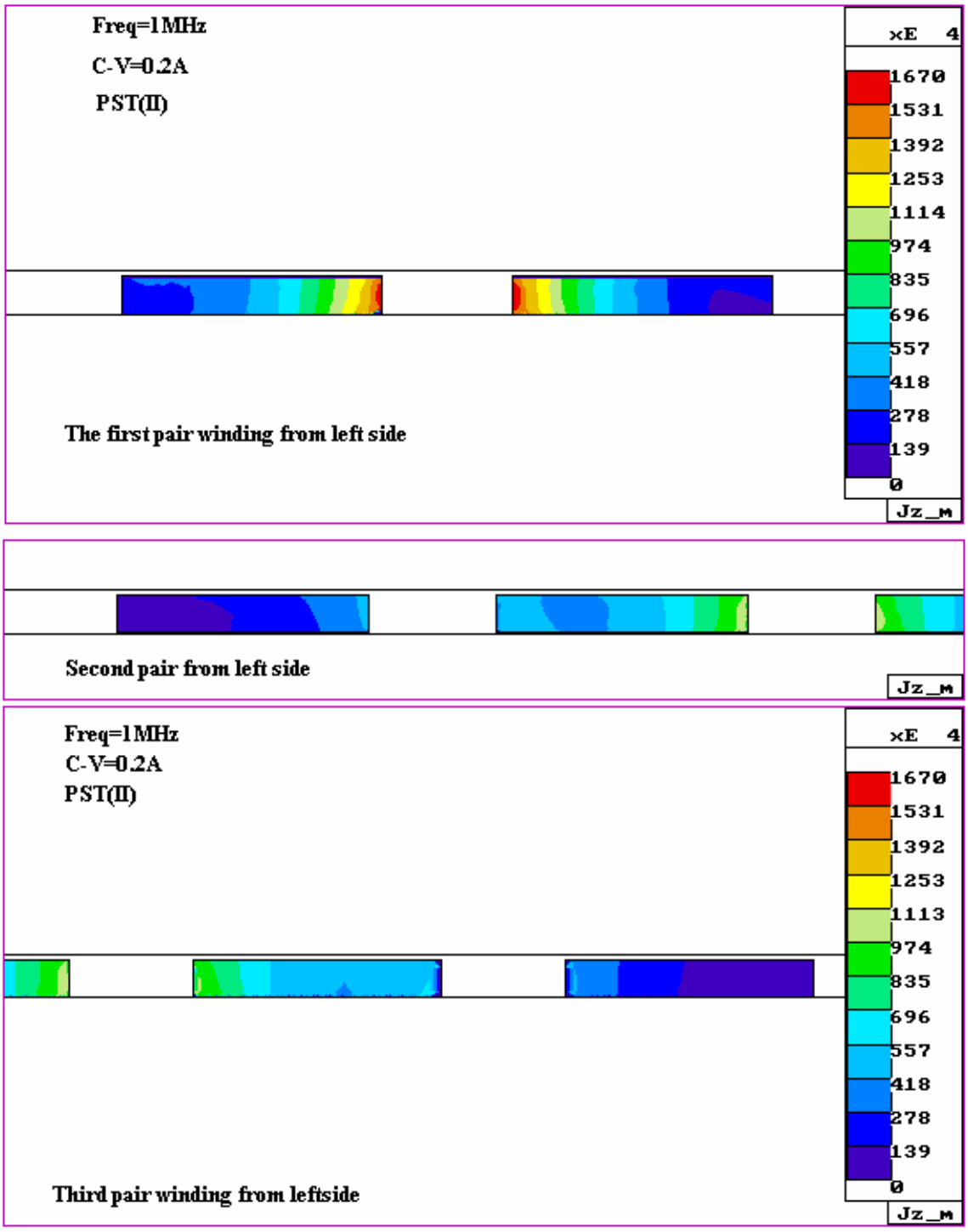

Figure 4.3 Eddy current distribution of meander type planar transformer.

4.2.2 Magnetic Flux and Eddy Current Distribution of Spiral Windings

The second existing type of planar transformer windings is spiral type winding structure. The magnetic flux distribution is simulated and shown in Figure 4.4. The top planar winding is working as primary coil with 0.2 A excitation current at the frequency of 1 MHz. The overall structure of the transformer is shown in Figure 4.5. There are two pieces of planar windings, the top one is primary coil with three turns. The bottom winding is secondary winding also with 3 turns on it.

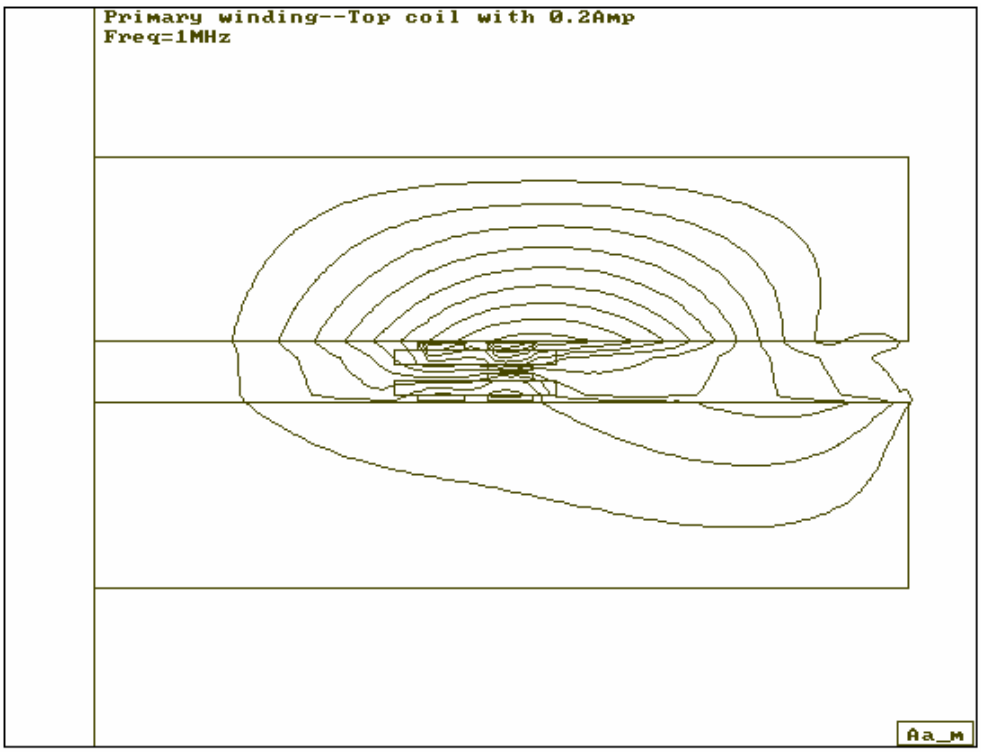

Figure 4.4 Magnetic flux distribution of spiral type planar transformer.

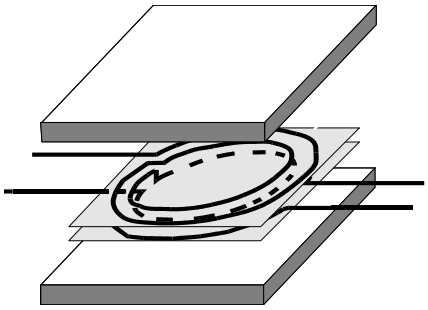

Figure 4.5 The structure of spiral planar winding transformer.

The magnetic flux is going around the primary winding and the top piece of ferrite mostly. The leakage flux is existing between the primary and the secondary windings.

Figure 4.6 shows the eddy current distribution of the transformer, the eddy current is distributed in the windings with extremely uneven condition. It is because the magnetic flux in the winding is unbalanced as well. The maximum eddy current density is recorded as high as 1380×10^4 A/m^2.

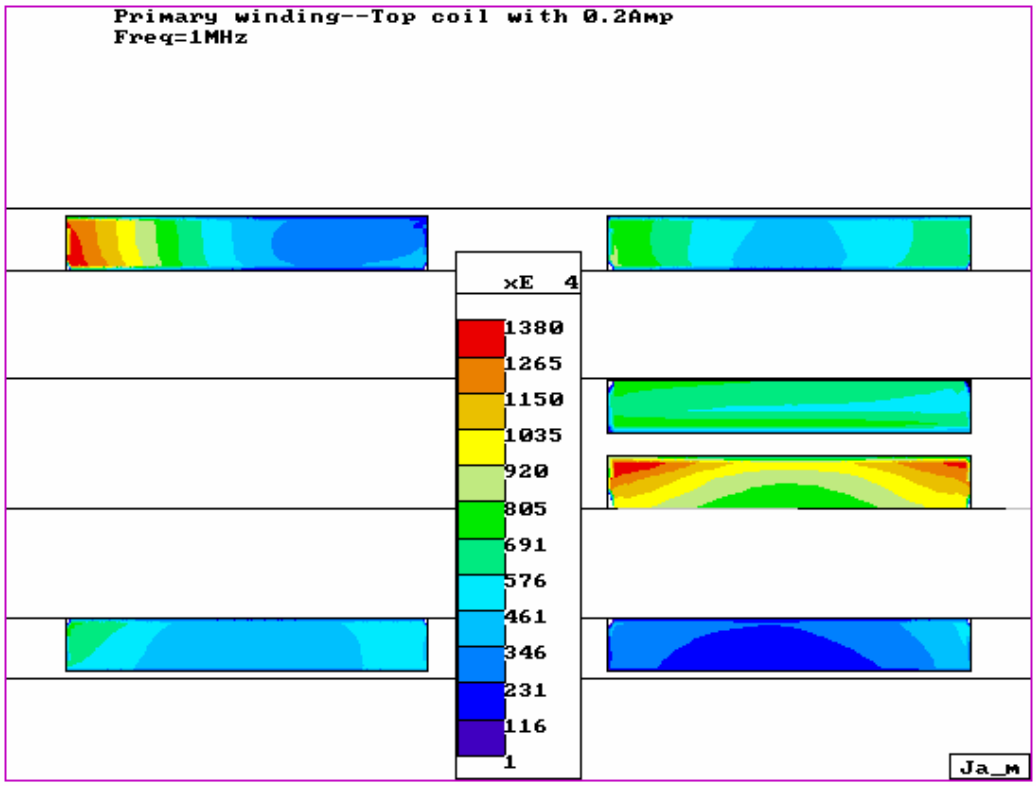

Figure 4.6 Eddy current distribution of the spiral planar transformer.

The maximum eddy current density in these two planar transformers is satisfactory when compared with the conventional winding structure, such as separated pot core winding structure discussed in Chapter 3, Figure 3.3. Table 4.1 lists the maximum eddy current density for these transformers under the same testing conditions, operating frequency of 1 MHz and the excitation current of 0.2 A. However, these planar winding structures can be further improved to have better performance at high frequency applications.

Table 4.1 Maximum eddy current density in transformer windings [A/m^2].

Frequency	1MHz	500kHz	100kHz	50kHz
Spiral	13,800,000	10,410,000	7,170,000	6,910,000
Meander	16,700,000	12,450,000	5,767,000	5,547,000
Conventional	116,900,000	80,510,000	37,240,000	27,110,000

4.3 Basic Principle of Helical Planar Winding Structure

At low frequencies, the magnetic flux generated by the primary winding needs to be concentrated by the magnetic core and coupled with the secondary winding, as mentioned in Chapter 2. Based on Faraday's law, $v = \frac{\partial \Phi}{\partial t}$, the induced voltage in the secondary is proportional to the rate of change of the magnetic flux, more details can be referred to the appendix – Fundamentals of Magnetics at the back of the thesis. When the operating frequency is relatively low, the "∂t" is relatively high, the amount of change of magnetic flux must be also high to maintain the required voltage induced coming from the secondary winding. This is the reason why the transformer magnetic core is needed. Referred back to the basic principle of transformer, transformer cores are not necessarily needed if there is enough rate of change of flux to induce the voltage from the secondary winding.

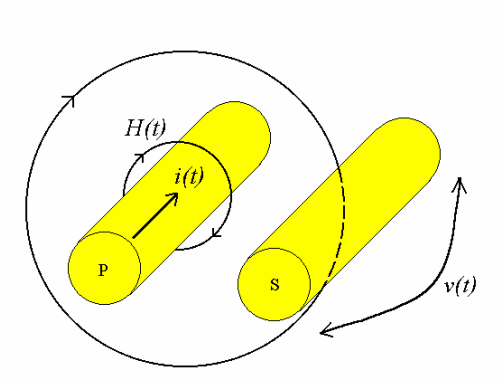

Figure 4.7 Fundamental principle of magnetic induction.

Figure 4.7 shows the fundamental principle of the magnetic induction between two wires. There is no need to have the magnetic core material in between to transfer the energy from primary winding to secondary winding. This fundamental principle of magnetic induction is also the basic principle of the helical winding structure. The magnetic flux generated by the primary wire induces the voltage at the secondary wire directly, without the magnetic material – transformer core. This phenomenon can be effective significantly when the operating frequency is high, say over 500 kHz.

At high frequency transformer operations, leakage flux or leakage inductance is the unwanted magnetic phenomenon in conventional transformer design. According to definition of leakage flux from IEEE Standard Dictionary of Electrical and Electronics Terms, leakage flux is any magnetic flux, produced by current in an instrument transformer winding, which does not link all turns of all windings [10].

In the helical winding structure, each section of the track of the primary winding will couple with the corresponding section of the secondary winding directly, and there is no magnetic material in between. The leakage flux or leakage inductance between the sections of tracks of the primary winding and the secondary winding is much less.

Since winding losses increase dramatically with frequency due to eddy currents and proximity effects, the configuration of wires in high frequency transformer must be deeply considered. The helical winding structure for high frequency transformer has been carefully designed, according to Eqn 4.32 to minimize the eddy current flowing through the windings. Numerical simulation results will strongly verify them from the following sections.

4.4 Structure of Planar Transformer with Helical Winding

The planar transformer with helical winding consists of two pieces of planar magnetic ferrite and one double side printed circuit board (PCB), as shown in Figure 4.8. The ferrite material is Philips soft ferrite – 3F4. The dimension of planar ferrite is 32 mm × 20 mm × 3 mm. The double sided PCB with thickness of 0.2 mm forms an air

core transformer with vertically helical windings. The specification of the transformer is listed in Table 4.2.

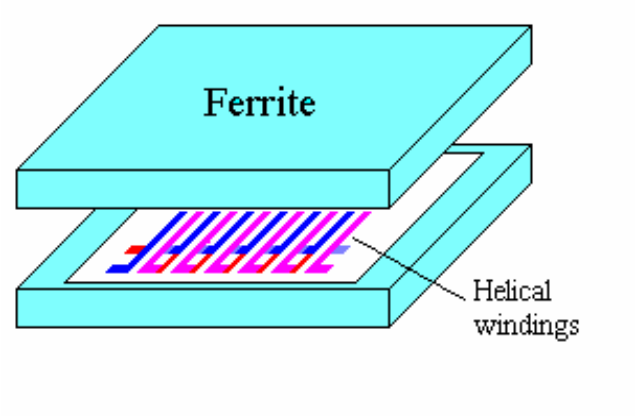

Figure 4.8 Overall structure of the planar transformer with helical winding structure.

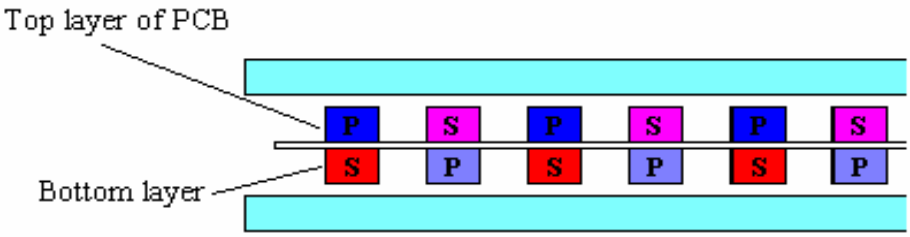

Figure 4.9 Part of the cross section of the transformer.

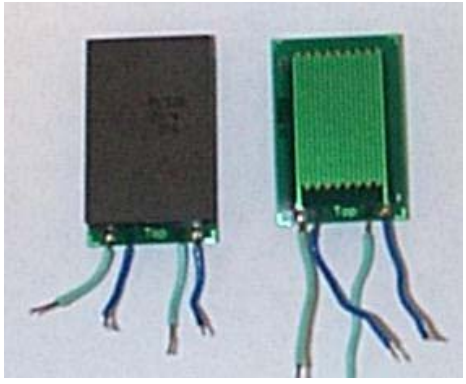

Figure 4.10 Picture of the planar transformer, and the helical winding structure.

Table 4.2 Specification of the transformer winding.

Shape	Rectangular, helical winding with 2 layers
Dimension of the coil area	20 mm x 27.5 mm
Turns	primary 7; secondary 7
Track width	1.0 mm
Track spacing	1.0 mm
Track thickness	35 μm
Substrate thickness	0.15 mm
Total thickness	0.22 mm

The primary winding and secondary winding are looped by connecting the strip lines at each end through the upper layer and bottom layer of the PCB vertically, as shown in Figure 4.8 and Figure 4.9. The plat-through technique is used to connect the strip lines between the upper layer and the bottom layer of the PCB to form a complete helical loop of primary and secondary windings.

Two pieces of planar magnetic ferrite place together to wedge planar helical windings make a completed planar transformer. This planar transformer with such structure can significantly increase the magnetizing impedance and reduce the EMI generated by the planar helical winding (when it was used as an air core transformer). All the flux generated by the coils is enclosed inside the two pieces of ferrite. The primary winding and the secondary winding are separated from each other to minimize the proximity effect and further reduce the eddy current density inside the windings [11-13].

4.5 Numerical Simulation of Planar Transformer with Helical Winding Structure

4.5.1 Flux Distribution

Operating at a frequency of 1 MHz, the magnetic flux distribution of the transformer shows that the magnetic flux is evenly distributed around each track of

primary winding and induces the emf in the secondary winding, shown in Figure 4.11. The problem of unbalance magnetic flux distribution happened in the meander type and the spiral coil of planar transformers is basically solved, shown in the Section 4.2. Two pieces of ferrite enclose all the magnetic flux inside the transformer, which increases magnetic coupling and input impedance, and reduces EMI as produced by an air core transformer.

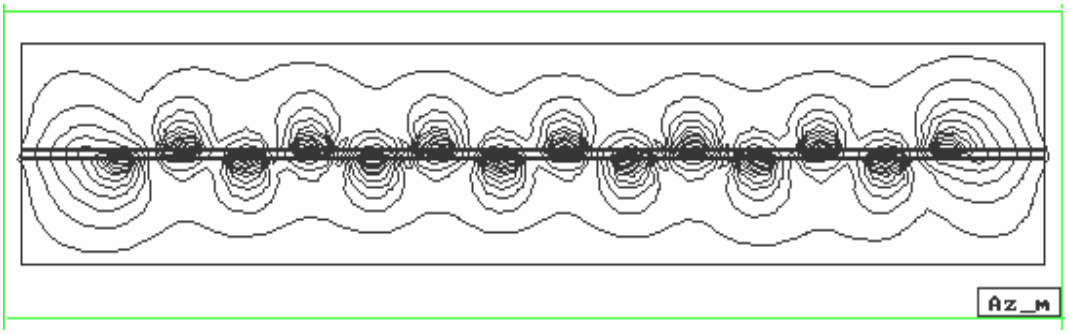

Figure 4.11 Numerical simulation of magnetic flux distribution of the transformer.

Figure 4.12 shows that the details of the flux distribution of the first four pairs of winding of the transformer. The magnetic flux distributions of each pair of tracks are very similar, except the pair of tracks at the both ends. Every strip line of the secondary winding is evenly induced voltage by the adjacent primary line.

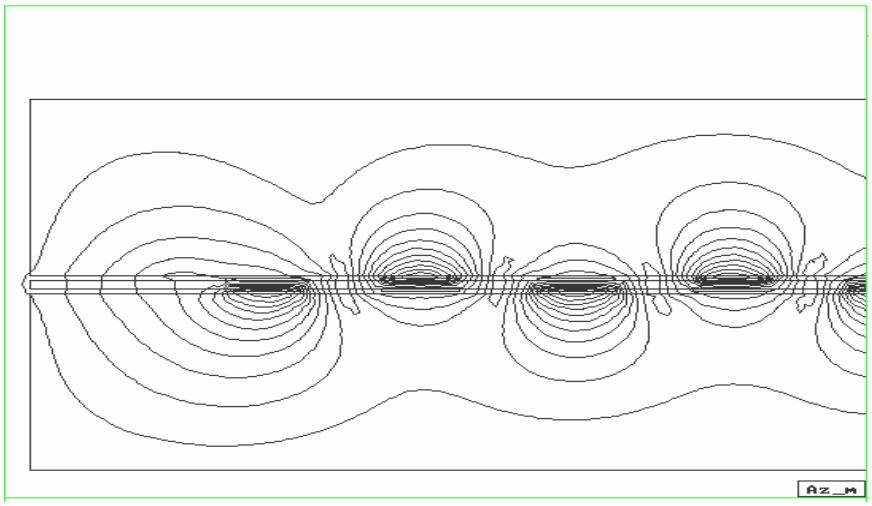

Figure 4.12. Flux distribution of the first four pairs of winding.

Figure 4.13 shows the magnetic flux distribution of the helical winding without ferrite pieces. The flux on the top and under the bottom of the winding can further extend without limitation. The magnetic path of each pair of tracks cannot be well defined.

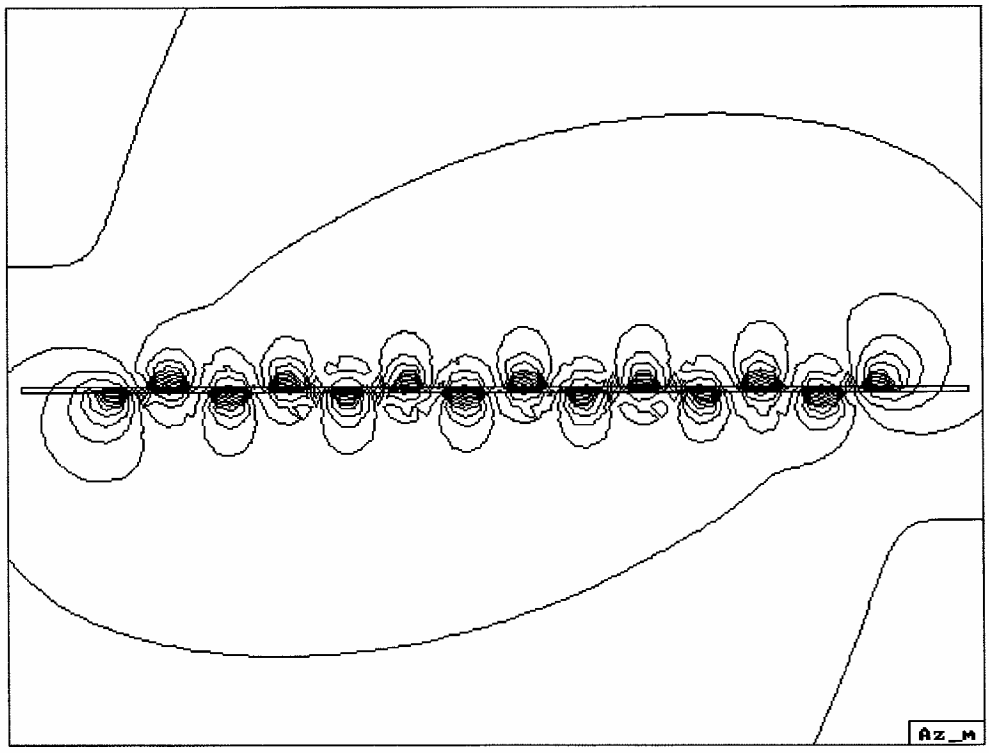

Figure 4.13 Magnetic flux distributions of the transformer without ferrite at 1 MHz.

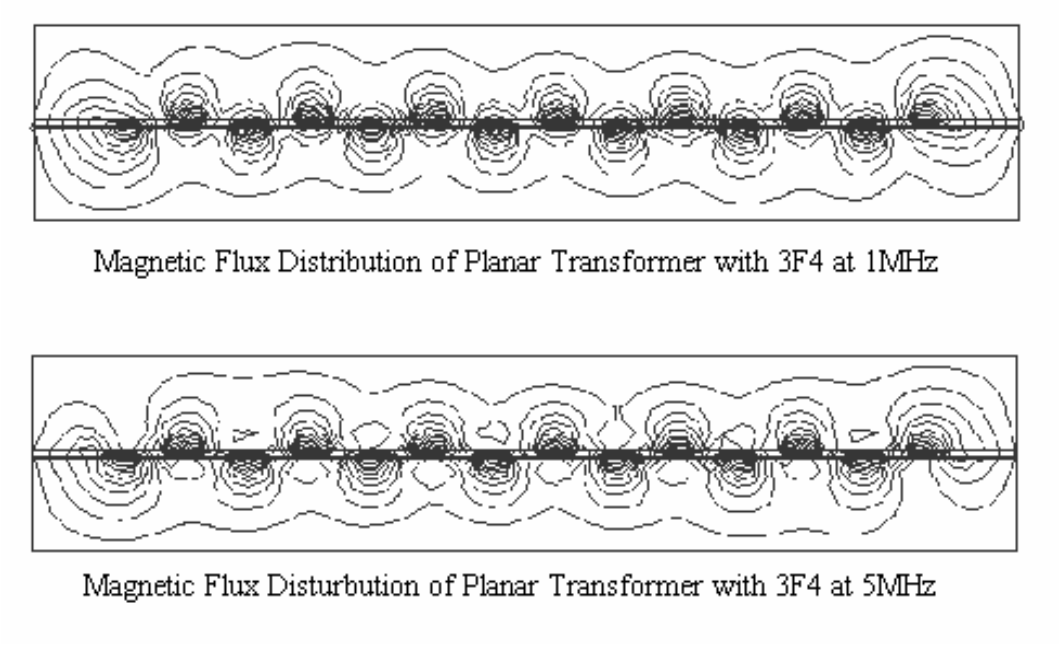

Figure 4.14 Magnetic flux distributions of the planar transformer at 1 MHz and 5 MHz.

Figure 4.14 shows the difference of the magnetic flux distributions of the transformer operating at different frequencies of 1 MHz and 5 MHz. The flux distributions are very similar. The magnetic flux distributes evenly around the windings for both situations.

4.5.2 Eddy Current Distribution

The eddy current distribution inside the transformer windings will effect the leakage inductance and the overall performance of the HF transformer. The eddy current distribution of the helical printed circuit winding of the planar transformer operating at 1 MHz was simulated by BEM-based eddy-current solver [9]. The numerical results are listed in Figures 4.15 to 4.17. From these three figures, the eddy current distributions are found that they are very similar in each two pair of windings. The eddy current is evenly distributed in the whole winding of the HF transformer. It agrees with the flux distribution mentioned in above section. The maximum eddy current flows around the two sides of the strip lines of the secondary winding, because of the magnetic fields generated by the current flowing the strip line [11].

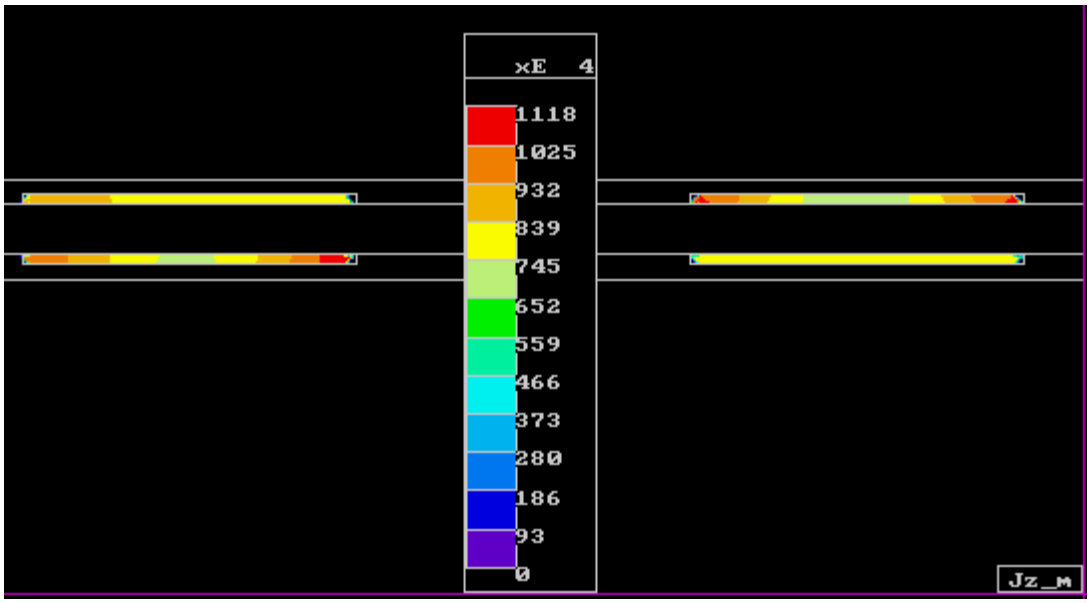

Figure 4.15 Eddy current distribution of the first two pairs of windings.

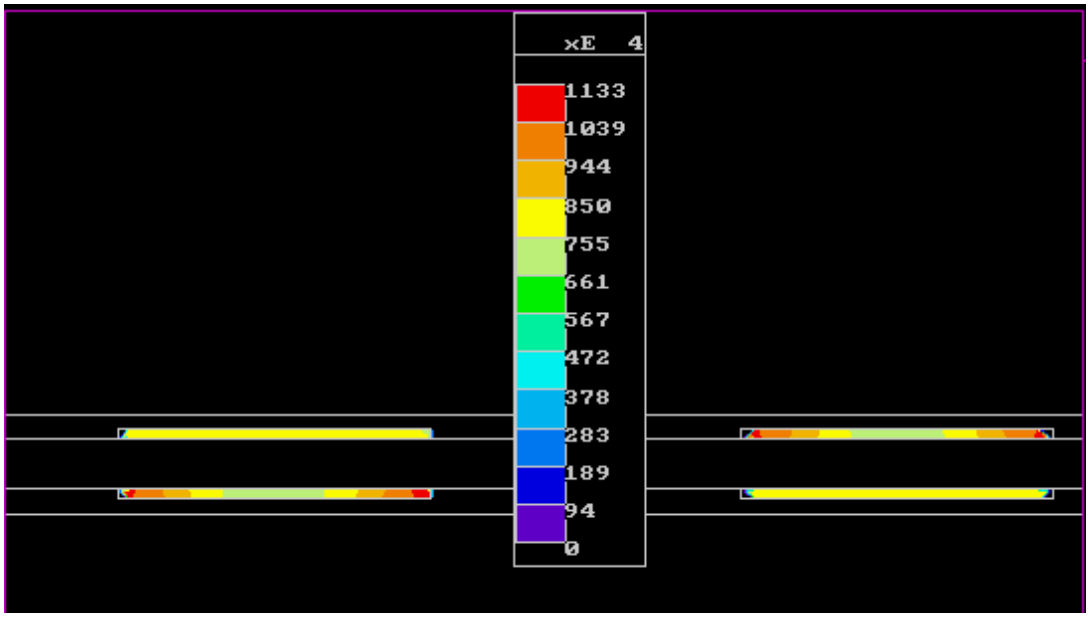

Figure 4.16 Eddy current distribution for the middle two pairs of windings.

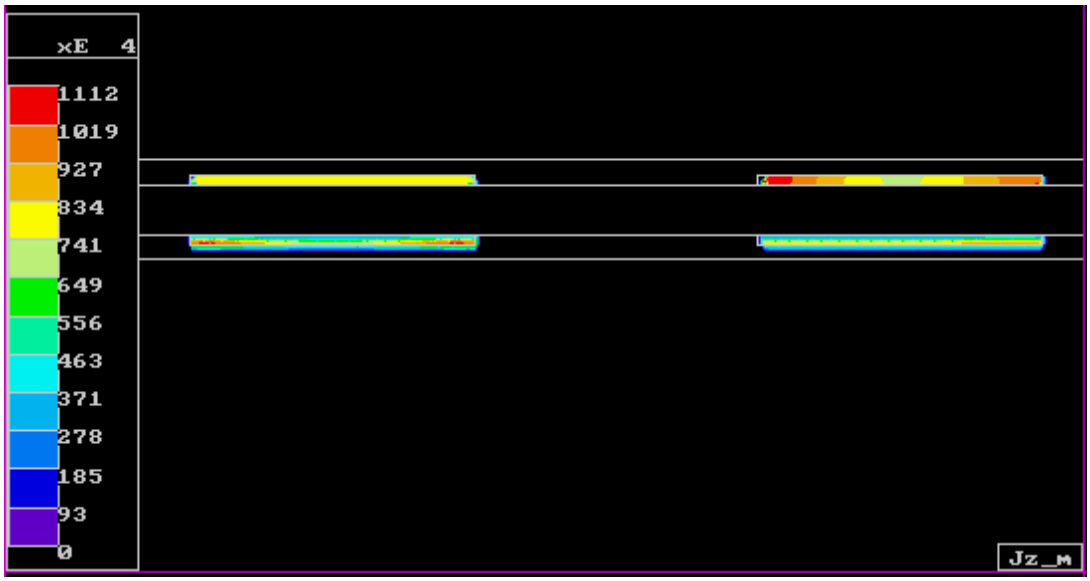

Figure 4.17 Eddy current distribution for the last two pairs of windings.

The maximum eddy current density of the transformer with helical winding is 1133 × 10^4 A/m^2, it is based on the excitation current of 0.5 A in the primary winding, and the operating frequency of 1 MHz. If the eddy current density is recalculated with an excitation current of 0.2 A, the maximum eddy current density will be equal to 453.2 × 10^4 A/m^2. Table 4.3 shows the maximum eddy current density of different transformer windings operating at the frequency of 1 MHz, with the excitation current of 0.2 A.

Table 4.3 Maximum eddy current density in transformer windings [A/m^2].

Transformer winding type	Maximum eddy current density
Helical	**4,532,000**
Spiral	13,800,000
Meander	16,700,000
Conventional	116,900,000

From the Table 4.3, the maximum eddy current density of the helical winding transformer is much less than the other type of winding structures. It is only 27% of the maximum density of meander type winding structure, 33% of the maximum density of spiral type winding structure, and 3.9% of the maximum density of conventional

winding structure. The smallest of the maximum eddy current density is the solid evidence to support the excellent high frequency characteristic of helical winding structure.

Table 4.4 Comparison in percentage of maximum eddy current.

Transformer winding type	Maximum eddy current density comparison
Helical : Spiral	33%
Helical : Meander	27%
Helical : Conventional	3.9%

In this section, the magnetic flux distribution and the eddy current distribution of the planar transformer with helical winding structure have been investigated. According to these simulation results, the planar transformer with helical winding structure has more balanced flux distribution than the existing planar winding structures – meander type winding structure and spiral type winding structure. Furthermore, the eddy current flowing in the tracks of the helical winding structure is much less when it compared with the other two types of winding.

4.6 Experimental Measurements of the Planar Transformer with Helical Winding Structure

4.6.1 Voltage Ratio

Voltage ratio is a very important parameter of a transformer. The voltage ratio of the planar transformer with helical winding has been measured and plotted for the frequency range between 500 kHz to 2 MHz as shown in Figure 4.18. The voltage ratio of the transformer is found between 0.7 to 0.8 within the testing frequency range. The voltage ratio is also the best, comparing with the planar transformers with spiral winding at this frequency range [2, 3]. They are listed in Table 4.5.

The voltage ratio of the transformer with ferrite is double of the voltage ratio of the transformer without ferrite. The voltage ratio of the transformer without ferrite in this frequency range is only up to 0.3. It is much better for the voltage ratio of the transformer with ferrite, comparing with the voltage ratio of its air core counterpart. The voltage ratio within the test frequency range is shown in Figure 4.18.

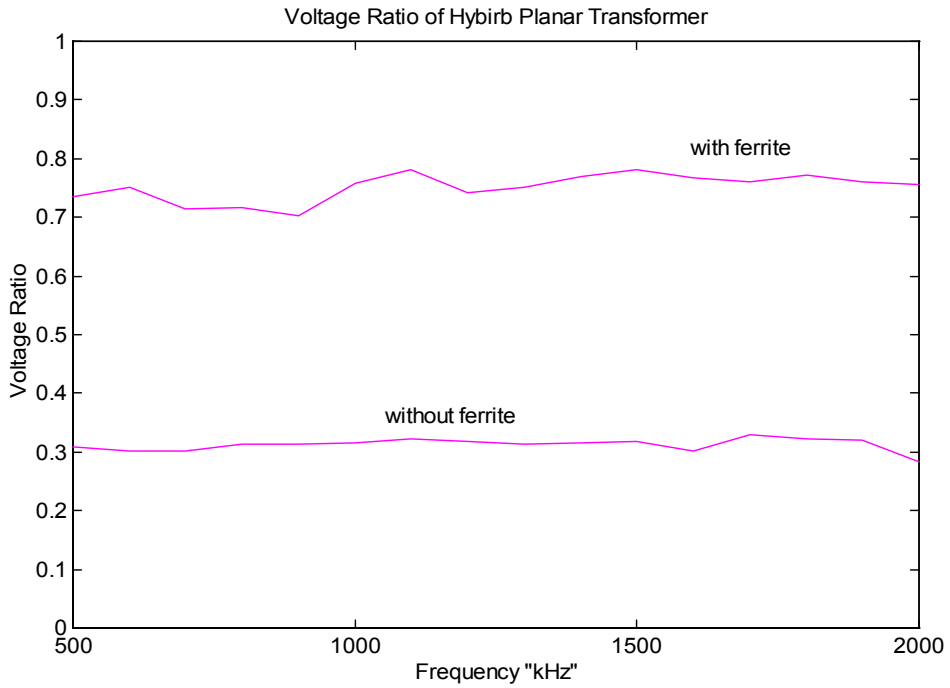

Figure 4.18 Voltage ratio of the planar transformer with helical winding structure.

Table 4.5 Comparison of voltage ratio of planar transformers.

Transformer type	**Helical type**	Type I in [2]	Type II in [2]	In [3]
Voltage ratio $_{(max)}$	**0.8** (<2MHz)	0.5 (<2MHz)	0.4 (<2MHz)	0.6 @1MHz

4.6.2 Input Impedance

The input impedance normalized with its air core counterpart is shown in Figure 4.19. The input impedance of the transformer with magnetic ferrite is twice of the input impedance of the transformer without the ferrite materials. The input impedance keeps increasing form "2" at 500 kHz to "2.4" at 2 MHz, due to the increasing of the permeability of the ferrite material at that frequency range.

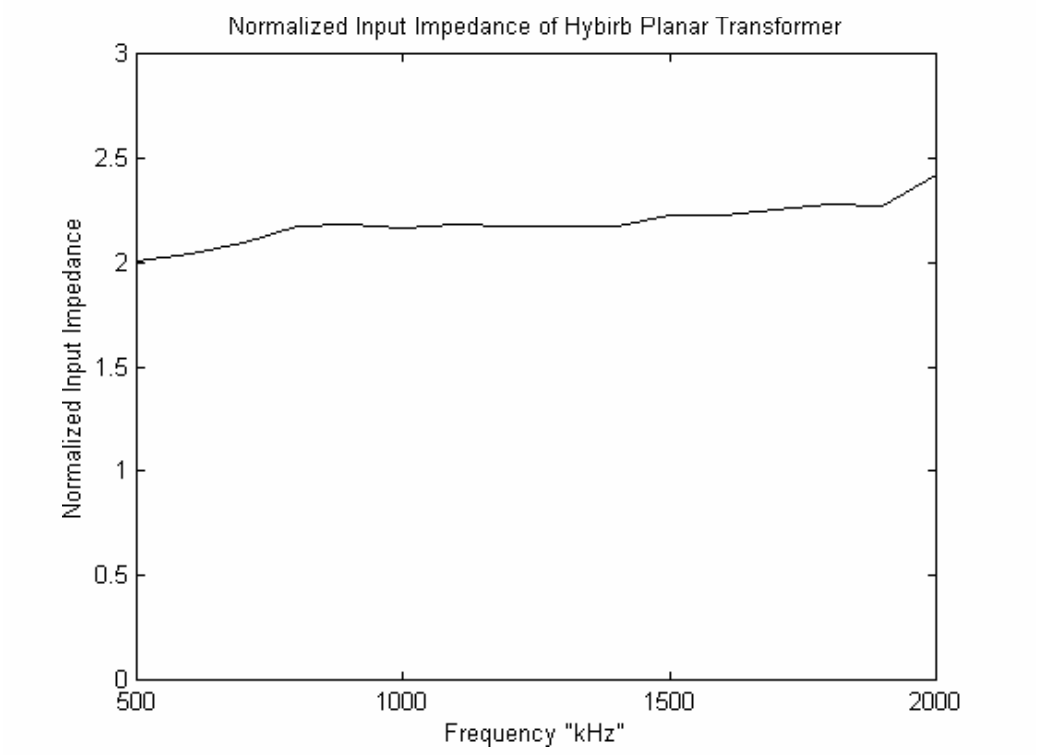

Figure 4.19 Normalized input impedance.

4.6.3 Quality Factor

Quality factor expresses the power losses in a transformer, it can be defined as [14]:

$$Q = \frac{1}{\tan\delta_L}$$

where $\tan\delta_L$ is the loss factor of the coil.

The Q-factor of the transformer with helical winding structure was measured by Agilent 4285A 75 kHz – 30 MHz precision LCR meter over the frequency range from 100 kHz to 30 MHz. Figure 4.20 Shows the Q-factor of the transformer.

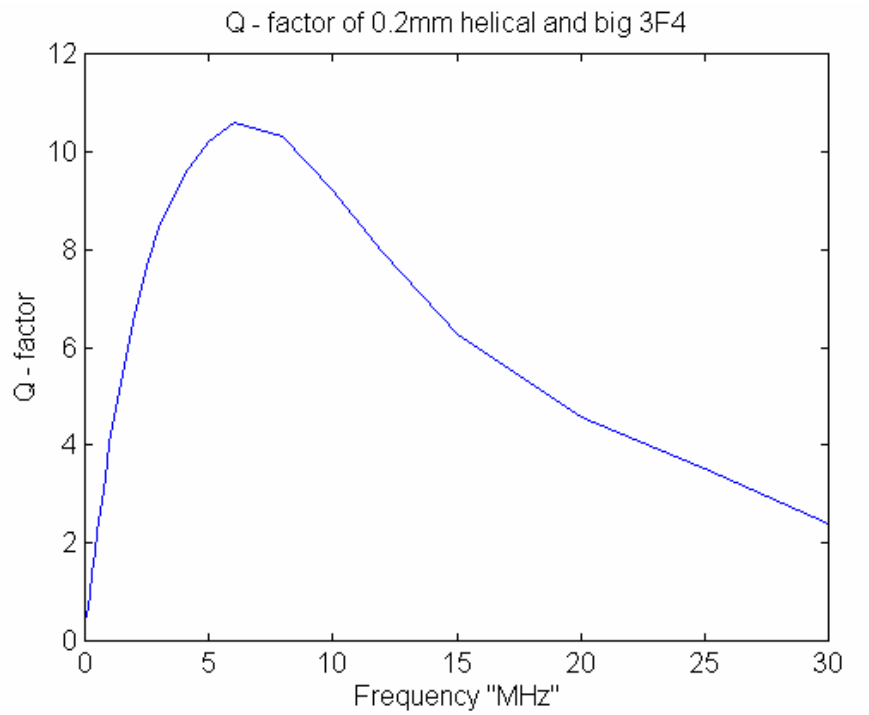

Figure 4.20 Q-factor of the transformer with helical winding structure.

From the figure, Q-factor is equal to 10.6 at the frequency of 6 MHz, as the peak value of the factor. According to the definition of the factor, the power loss of the coil is the minimum when the Q-factor is the maximum. In the other words, the transformer has the minimum power loss in the frequency range around 6 MHz.

4.6.4 Load Test

The planar transformer with helical winding structure has been tested with the load, using single switch forward switching resonant converter configuration, shown in Figure 4.21.

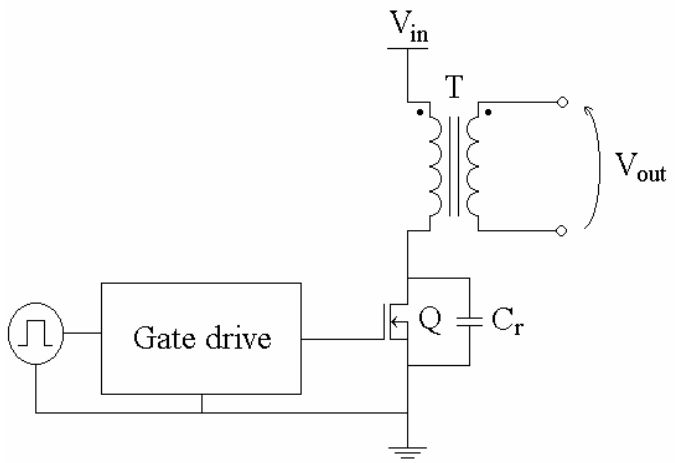

Figure 4.21 Single switch forward switching resonant converter test platform.

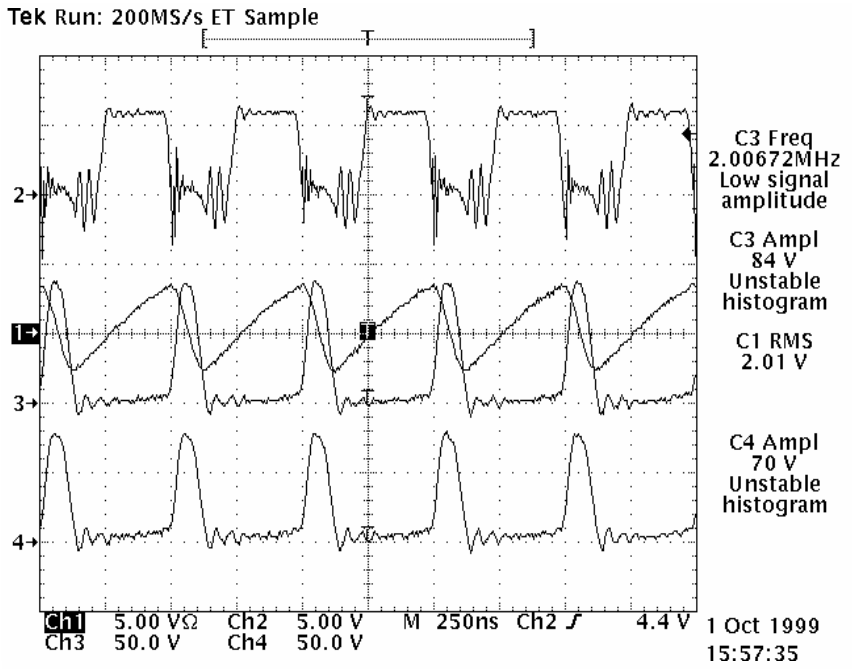

Figure 4.22 Switching waveforms of the planar transformer.

Figure 4.22 shows the switching waveforms of the testing transformer. The waveform at the top of Figure 4.22 is measured between the gate and the source of the switching MOSFET. Channel 3 is the waveform of V_{DS} of the MOSFET. The output from the secondary winding of the testing transformer is monitored by channel 4. The current flowing through the primary winding is indicated by channel 1.The peak to peak voltage ratio is 0.83 with load of 100 Ω at 2 MHz. For the resonant period is less than 150 ns, the switching frequency can be further increased.

4.6.5 Conclusions on the Section

The planar transformer with helical winding structure has been investigated experimentally. The experimental results have shown that the planar transformer performed excellent at frequency range between 500 kHz to 2 MHz. The voltage ratio of the transformer is better than the other two types of winding structure, shown in Table 4.5. The transformer sample performs excellently with loading at the operating frequency up to 2 MHz. With the numerical simulation results, the planar transformer with helical winding structure can be confirmed its outstanding performance at high frequency power transfer applications.

4.7 Analysis of Leakage Inductance

The planar helical winding structure was found to have the best performance at high frequency operations, according the numerical simulation and experimental measurements. Theoretical analysis must be discussed to complete the whole investigation of the helical winding structure for high frequency transformer applications. Perry has stated, “Low frequency phenomena in many cases is manifest as ‘eddy current’ effects in current carrying conductors. In a traditional device such as the power frequency transformer, eddy current losses create additional heating in the windings as well as the flux concentrating core.” [15]. Dowell stated the following words in his famous article of “Effects of eddy currents in transformer windings”. The words are: “The performance of a transformer can be calculated from its equivalent circuit, and methods are available for calculating the values of the equivalent-circuit

elements from the knowledge of the geometry of the transformer and of the materials used in its construction." and "The other elements in the equivalent circuit are the winding resistance and leakage inductance." [11]. Therefore, the leakage inductance is a very important factor to determine the characteristic of a transformer in high frequency operation.

From Chapter 2, Eqn 2.76, $L_g = \mu_0 N_1^2 l_w \frac{1}{M^2} \frac{h_w}{b_w}$, the leakage inductance is proportional to the height of the winding and inversely proportional to the breadth of the winding, i.e. $L_g \propto \frac{h_w}{b_w}$ with the notation is shown in Figure 4.23.

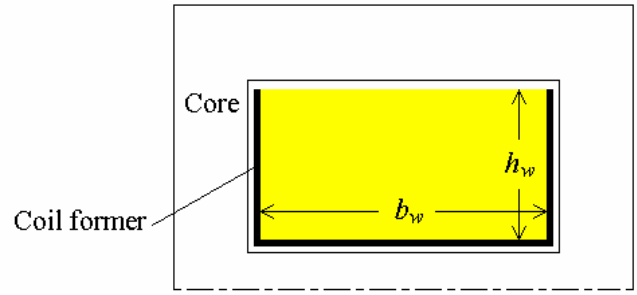

Figure 4.23 Notation for leakage inductance calculation.

The notation of planar transformer with helical winding structure for calculating the leakage inductance is shown in Figure 4.24.

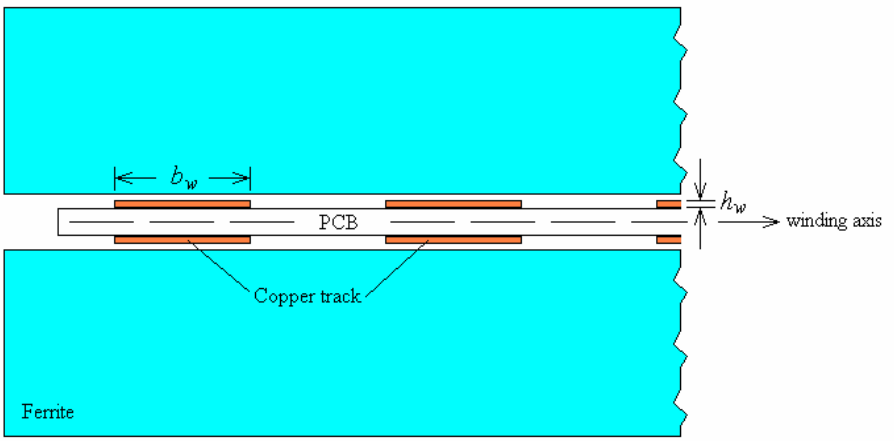

Figure 4.24 Notation of planar helical winding for leakage inductance calculation.

The winding axis is horizontal for planar helical winding structure. The breadth of the winding is much bigger than the height of the winding. Therefore, the ratio of the height to the breadth is much less than 1, i.e.

$$\frac{h_w}{b_w} \ll 1 .$$

If the other parameters are similar, the leakage inductance for planar helical winding structure is much smaller than the other types of winding structure.

The winding axis is vertical for both the spiral winding and meander winding structures. The breadth and height of the winding are interchanged, such that the ratio of them is much bigger than 1 with the same pattern of tracks of winding.

This verifies with the numerical simulation of the maximum eddy current density distributions. The maximum eddy current density of helical winding is only 3.9% of the eddy current density of the conventional winding, and about one-third of the current density of spiral type and meander type windings.

4.8 Design Considerations for the Planar Transformer with Helical Winding Structure

The planar transformer with helical winding structure has been shown to have an excellent performance at high frequencies. It has a relatively uniform distribution of magnetic flux inside the transformer. The maximum eddy current density is only one third of the other two types of planar structures. However, the design methodology for a planar transformer with helical winding structure is the next development point to be considered.

The traditional design formula, $E = kB_{\max} NA_C f \cdot 10^{-8}$, for transformers is not completely suitable for the planar transformers operating in high frequency power transfer applications. The voltage applied to the drive winding, E, is proportion to the effective cross-sectional area of the magnetic core, A_C. However, the effective cross-section area is not well defined for planar transformers.

A new design rule must be developed to fill the gap between the traditional design rule and the design steps of new planar transformers for high frequency power conversion. The design rules for transformers are essential for design engineers working with the high frequency switching mode power supplies. Without new design rules, the design for switching mode power supplies with planar transformers becomes impossible. A new design consideration for planar transformers with helical winding structures should be deeply examined and thus it is the first step towards a new design rule for such transformers.

4.8.1 Comparison of Voltage Ratio

Six new sample transformers have been designed and fabricated. They have been tested in the no-load case, the secondary winding of transformers was open circuit under testing. The voltage ratio between the output voltage and input voltage is an important parameter to describe the fundamental characteristic of a transformer. Figure 4.25 shows the voltage ratio of the six planar transformer samples between 500 kHz to 5

MHz. The voltage ratio of the transformer samples with the same PCB substrate thickness of 0.1 mm but the different ferrite materials (3F4 and 3F3) are found in very similar values of voltage ratio within the test frequency range. The voltage ratios of them at the frequency between 500 kHz to 5 MHz are close to 0.8. Similar situation happened for the samples with 0.2 mm of PCB substrate. The voltage ratio of the sample transformer with 0.2 mm of PCB substrate and ferrite of 3F4, and the sample with ferrite of 3F3 and same thickness of PCB substrate are very close together for the testing frequency range. The voltage ratio at 500 kHz to 5 MHz is close to 0.7.

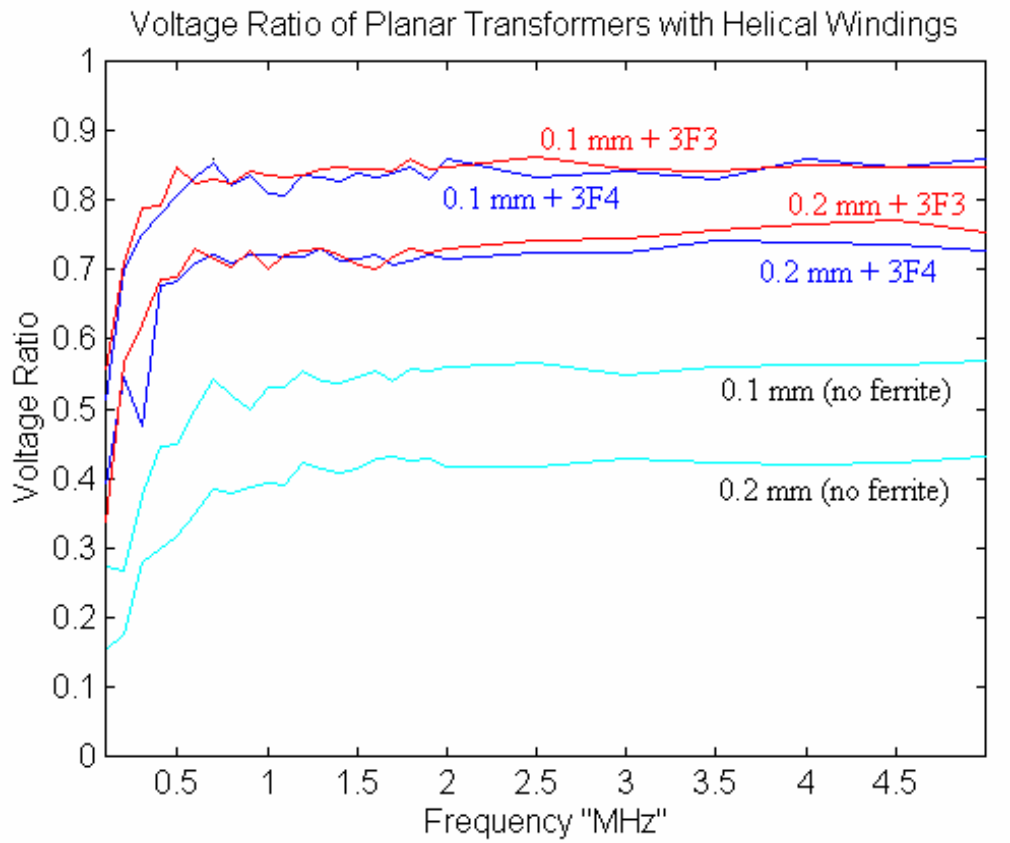

Figure 4.25 Voltage ratio of the six transformer samples.

From the figure, the voltage ratio has been found that it is highly related with the thickness of the PCB substrate, in the other words, it is highly related with the vertical distance between the track of windings. However, the voltage ratio of the transformer samples without ferrite is different, compared with those with ferrite.

The detailed specification of the sample transformers is listed in the following Tables. Table 4.6 lists the different measurements between the transformer samples, and Table 4.7 shows the common specification of the transformer windings.

Table 4.6 The difference between transformer samples.

Sample of transformer	Vertical distance between tracks	Total thickness of the winding	Ferrite used
0.1 mm + 3F4	0.12 mm	0.18 mm	Philips – 3F4
0.1 mm + 3F3	0.12 mm	0.18 mm	Philips – 3F3
0.1 mm (no ferrite)	0.12 mm	0.18 mm	No ferrite used
0.2 mm + 3F4	0.22 mm	0.28 mm	Philips – 3F4
0.2 mm + 3F3	0.22 mm	0.28 mm	Philips – 3F3
0.2 mm (no ferrite)	0.22 mm	0.28 mm	No ferrite used

Table 4.7 Common specification of the transformer winding.

Shape	Rectangular, helical winding with 2 layers
Dimension of the coil area	20 mm x 27.5 mm
Turns	primary 9; secondary 9
Track width	0.5 mm
Track spacing	0.5 mm
Track thickness	30 μm
Substrate thickness	0.15 mm
Total thickness	0.22 mm

4.8.2 Magnetic Flux Distribution of Transformers with Different Ferrite Materials

The flux distributions of the cross-sectional area of the transformer samples have been calculated using a boundary element method (BEM) based software package. The numerical simulation results of magnetic flux distribution and the magnitude of the

magnetic field for different materials (3F3 and 3F4) at two frequencies (1 MHz and 5 MHz) have been shown in Figure 4.26 and Figure 4.27. The magnetic flux distributions for the sample transformers using two different magnetic ferrite at 1 MHz and 5 MHz are almost identical. These flux distributions can show the reason why the voltage ratios of the transformer samples with different ferrite materials are almost the same as well.

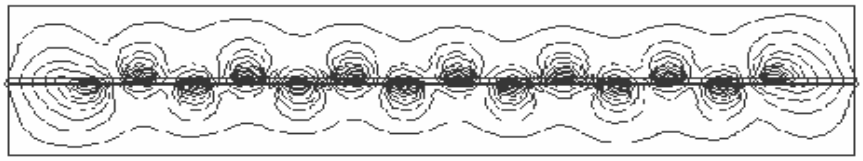

Magnetic Flux Distribution of Planar Transformer with 3F3 at 1MHz

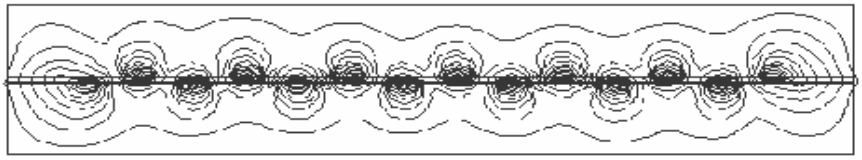

Magnetic Flux Distribution of Planar Transformer with 3F4 at 1MHz

Figure 4.26 Magnetic flux distribution of two samples of planar transformers at 1MHz.

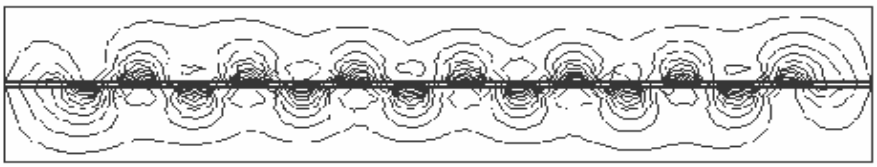

Magnetic Flux Disturbution of Planar Transformer with 3F3 at 5MHz

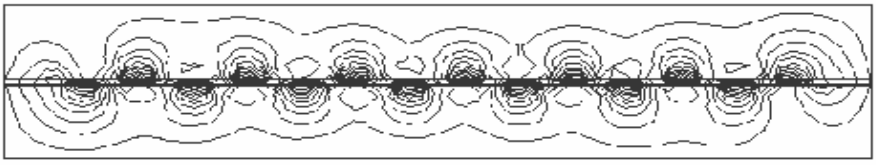

Magnetic Flux Disturbution of Planar Transformer with 3F4 at 5MHz

Figure 4.27 Magnetic flux distribution of two samples of planar transformers at 5MHz.

The permeability of 3F3 and 3F4 are 1800 and 900 respectively. The excitation current for all cases is 0.5 A. The numerical simulation results are solid evidence to

verify the voltage ratio of the transformer samples of the same thickness of helical winding but different ferrite being close together.

Magnetic flux distributions with different ferrite materials, 3F3 and 3F4, are almost the same from the simulation results. The magnetic flux distributes evenly inside the winding structure. Except the most outer pair of tracks, the magnetic flux around each pair of track looks identical. Each track of primary winding generates equal amount of flux, and induces emf to the corresponding track of secondary.

4.8.3 Difference between Transformers with and without Ferrite

Two helical winding transformer samples without ferrite pieces were also investigated, the voltage ratio is found much lower than its magnetic counterpart. It means that magnetic core is essential to form a transformer with higher coupling coefficient. Figure 4.25 shows the voltage ratio of the transformer samples without ferrite and their magnetic counterparts. The voltage ratio of the sample with 0.1 mm PCB substrate is around 0.5 from 500 kHz to 5 MHz of the operating frequency range. It is higher than the voltage ratio of the transformer with a 0.2 mm PCB substrate, it is around 0.4 only from 500 kHz to 5 MHz of operating frequency.

This experimental result points out that the magnetic material – Ferrite, is an essential part of a planar transformer. Without the ferrite, the voltage ratio drops significantly. Furthermore, the ferrite pieces enclose the magnetic flux generated by the primary winding, without the pieces, the flux can be extended unbounded, shown in Figure 4.13. It will increase the electromagnetic interference (EMI) problems around the transformer.

There are some typical advantages for transformer without ferrite pieces – air core transformers, they are no core loss and low manufacturing cost. However drawbacks still exist for air core transformers due to the problems of EMI, low magnetic coupling coefficient and low input impedance.

The planar magnetic core transformer with helical windings can significantly overcome some of these disadvantages while keeping their advantages. The planar magnetic core transformer for low to medium power applications keep all these advantages of low manufacturing cost, low EMI and relatively high coupling coefficient, shown in the previous sections.

4.8.4 Discussion on Design Consideration

To investigate the characteristics of planar transformers with helical winding structure, the thickness of the PCB substrate to form helical winding was thought to be an important factor. From the previous section, it is shown that the thickness of the helical winding affects the voltage ratio of the transformer. However, the following parameters should also be considered in the optimal design:

- The length of the winding
- The width of the winding
- The spacing of the winding
- The number of turns of the winding

If all these parameters have to be considered at the same time, the constancy of the size of the transformer samples is not easy to maintain. The overall size of the samples will be changed significantly, if the width and the spacing of the winding change. To simplify the experimental procedures, the thickness of the winding was the first parameter to be considered. However, all these parameters should be considered to examine the characteristic of the planar transformer with helical winding structure, and the new design rule for the planar transformer with helical winding structure can be completed totally.

4.9 Theoretical Analysis

From the experimental results and the numerical simulation results, the voltage ratio of the high frequency planar transformer with helical winding structure have been found that it is highly related to the reciprocal of the thickness of the printed circuit winding. It agrees with the inductive coupling and the capacitive coupling between two wires.

For inductive coupling [16, 17], the induced *emf* is

$$E_i = \omega BA\cos\theta \tag{4.1}$$

where B is the flux density, A is the area of the flux enclosed by the susceptible conductor and θ is the angle between B and the normal to A.

For extended current distributions, the magnetic field at any point is the sum of the contributions of the individual current elements. In the case of a volume distribution [22],

$$B(r) = \frac{\mu_0}{4\pi}\iiint \frac{J(r')\times(r-r')}{|r-r'|^3} d^3r' \tag{4.2}$$

For an infinitely long strip of foil of width w carries a current I uniformly distributed across its width, shown in the following figure.

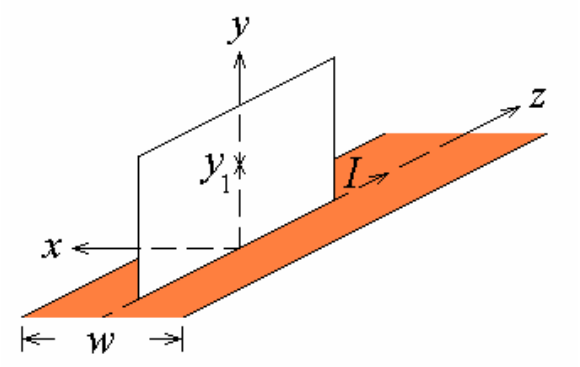

Figure 4.28 Notation of calculation of magnetic flux density of an infinitely long strip.

The magnetic flux density at a point in the plane that perpendicularly bisects the width is defined as

$$B = \frac{\mu_0}{4\pi}\frac{I}{w}\frac{dx'dz'\hat{k}\times(y\hat{j}-x'\hat{i}-z'\hat{k})}{(y^2+x'^2+z'^2)^{3/2}} \tag{4.3}$$

$$B = \frac{\mu_0}{4\pi}\frac{I}{w}\frac{dx'dz'(-y\hat{i}-x'\hat{j})}{(y^2+x'^2+z'^2)^{3/2}} \tag{4.4}$$

The integration over dz' gives

$$B = \frac{\mu_0}{2\pi}\frac{I}{w}\frac{(-y\hat{i}-x'\hat{j})dx'}{(y^2+x'^2)} \tag{4.5}$$

The second integration from $-\frac{w}{2}$ to $\frac{w}{2}$ gives zero for the second term, so

$$B(0,y,0) = \frac{\mu_0}{\pi}\frac{I}{w}\tan^{-1}\frac{w}{2y}(-\hat{i}) \tag{4.6}$$

If the width of the strip is w = 1 mm and the vertical distance between the test point and the strip is y = 0.1 mm, then the magnetic flux

$$B(0,y=0.1,0) = \frac{\mu_0}{\pi}\frac{I}{w}\tan^{-1}\frac{1}{0.2}(-\hat{i}) \tag{4.7}$$

$$B(0,y=0.1,0) = \frac{\mu_0}{\pi}\frac{I}{w}(78.6)(-\hat{i}) \tag{4.8}$$

If the width of the strip is the same, w = 1 mm, but the vertical distance is changing to y = 0.2 mm, then the magnetic flux

$$B(0,y=0.2,0) = \frac{\mu_0}{\pi}\frac{I}{w}\tan^{-1}\frac{1}{0.4}(-\hat{i}) \tag{4.9}$$

$$B(0,y=0.2,0) = \frac{\mu_0}{\pi}\frac{I}{w}(68.1)(-\hat{i}) \tag{4.10}$$

Therefore, $B(0,y = 0.2,0)$ is only 86.64% of $B(0, y = 0.1,0)$. It means that the magnetic flux density is higher if the vertical distance is shorter from the current carrying strip. It matches with the voltage ratio of the transformer samples, shown in Figure 4.25. The voltage ratio of transformer samples of 0.2 mm substrate is about 85%

of the voltage ratio of the samples of 0.1 mm substrate. Two more measurements have been taken with different thickness of the helical winding structure. The voltage ratio has been plotted in Figure 4.29.

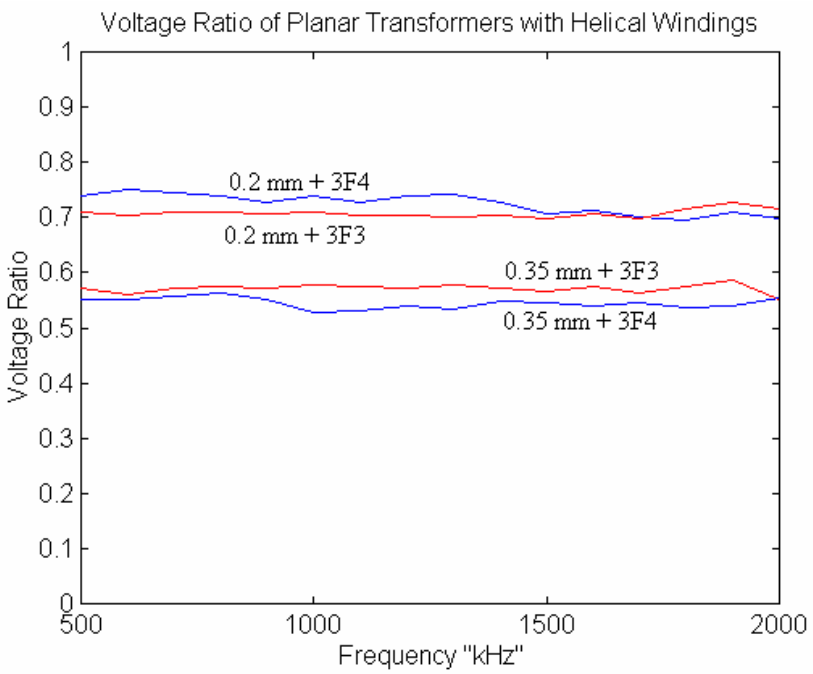

Figure 4.29 Voltage ratio of planar helical winding transformers with different vertical distance.

Compared with Figure 4.25, the voltage ratio of the transformer samples with different vertical distance between primary and secondary winding sections can be tabulated in Table 4.8.

Table 4.8 Voltage ratio of transformer samples with different thickness of substrates at operating frequency of 1.5 MHz.

Vertical distance	Voltage ratio
0.12 mm	0.83
0.22 mm	0.7
0.35 mm	0.55

From Table 4.8, the voltage ratios of transformer samples are decreasing as the

vertical distance between the strips of helical winding increased. It agrees with Eqn. 4.6 derived from previous page.

The flux density is denser if it is closer to the excitation wire. It can also be seen from the magnetic flux distribution, shown in Figures 4.26 and Figure 4.27.

Magnetic coupling is the fundamental principle of transformers. According to the previous calculations, the vertical distance between the primary winding section and the secondary winding of helical winding structure is a critical factor for the magnetic coupling of the high frequency planar transformer.

The other coupling between conductors is the capacitive coupling, it can be defined as [16-18], $E_c \propto \omega C_{12}$, where $C_{12} = \varepsilon \frac{w}{d}$, and d is the separation between the conductors, and w is the width of the conductors. By keeping the width of the conductors as a constant, if the separation between top conductor and bottom conductor is smaller, C_{12} will be larger, and then E_c will be larger as well.

From inductive coupling and capacitive coupling of conductors, it can be found that the separation between the conductors of primary and secondary winding is an important factor to define the coupling of the planar transformers with helical winding. The voltage ratio of a transformer is highly related with the coupling of the transformer. Thus, it is a strong proof that the thickness of the planar helical winding can determine the voltage ratio of such transformers.

4.10 Power Performance

Planar power transformer with helical winding structure has been found to have an excellent performance in no-load case and numerical simulation. It has a very good voltage ratio (VR = 0.9) at Megahertz level of operating frequency, and evenly distributed magnetic flux inside the transformer and less eddy current losses in the winding structure. However, the design target for the transformer is focusing on power

transfer applications, the power test is an unexceptional part for the design of the transformer.

Table 4.9 and Table 4.10 show the experimental data measured by using the testing circuit shown in Figure 4.21. The transformer was loaded with 100 Ω's power resistor. Table 4.9 shows the experimental data of the planar transformer of 0.1 mm thick helical winding structure with the ferrite material of 3F3. Table 4.10 lists the reading taken from the transformer with the same winding structure but different ferrite material, 3F4.

Table 4.9 Power test experimental data of the transformer of 3F3.

Frequency (MHz)	Primary voltage (V_{p-p})	Secondary voltage (V_{p-p})
1	92.8	79.2
1.2	98.4	**85.6**
1.5	87.2	76.8
1.8	76.0	68.0
2.0	68.8	59.2
2.2	62.4	53.6
2.5	54.4	44.8
2.8	48.8	41.6
3.0	44.8	38.4

The peak output current of the planar transformer with ferrite of 3F3 is found as 0.856 A (85.6 V / 100 Ω = 0.856 A). The voltage ratio is plotted and shown in Figure 4.30. The voltage ratio within the testing frequency range can be observed above 0.8, and it is equal to 0.89 at the operating frequency of 1.8 MHz.

Table 4.10 Power test experimental data of the transformer of 3F4.

Frequency (MHz)	Primary voltage (V_{p-p})	Secondary voltage (V_{p-p})
1	96.0	81.6
1.2	100.8	88.0
1.5	88.8	78.4
1.8	75.2	67.2
2.0	68.0	60.8
2.2	62.4	54.4
2.4	57.6	48.8
2.5	53.6	44.0

The peak output current of this transformer sample under the testing condition is found as 0.88 A. The voltage ratio of the planar transformer has been plotted in Figure 4.31. The peak of the voltage ratio was found at the operating frequency of 1.8 MHz, it is the same frequency with the transformer sample of ferrite material of 3F3. The voltage ratio is 0.90, it is very close to the voltage ratio of the transformer of 3F3, 0.89. Further detail measurements has been taken and listed in Table 4.11.

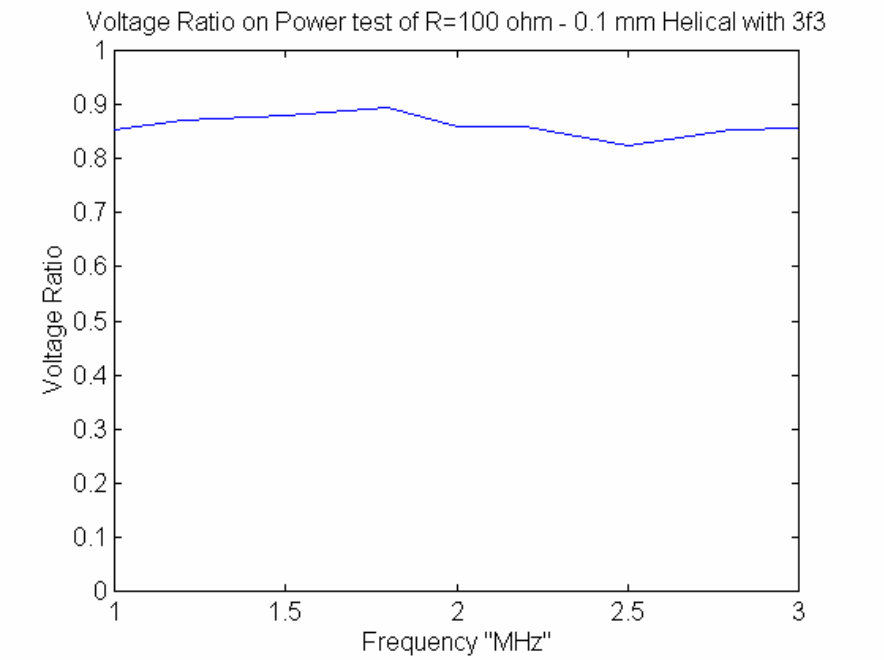

Figure 4.30 Voltage ratio of the transformer sample of ferrite material of 3F3 with load of 100 Ω.

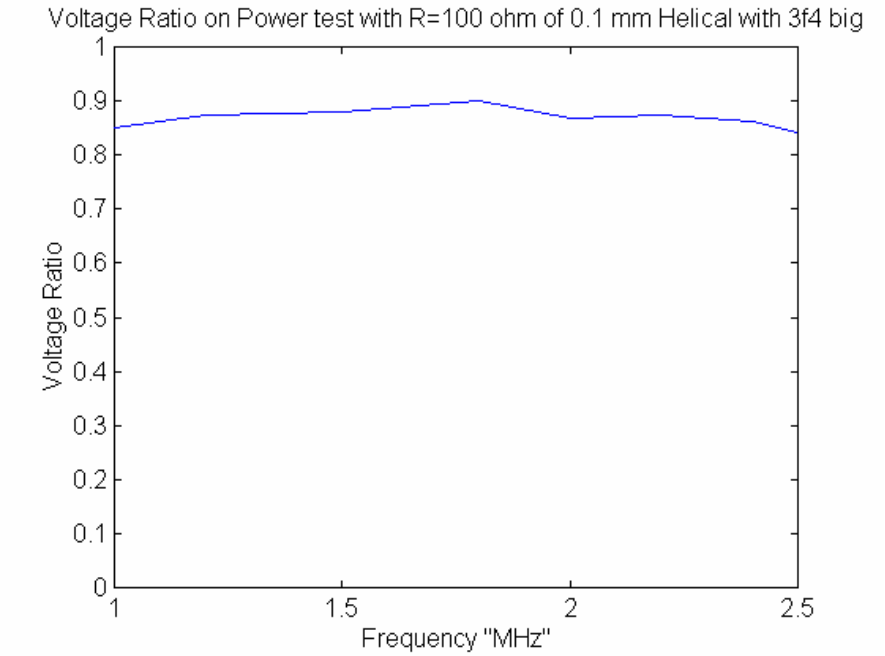

Figure 4.31 Voltage ratio of the transformer sample of ferrite material of 3F4 with load of 100 Ω.

Table 4.11 Detail measurement of the transformer of ferrite material – 3F4.

Frequency (MHz)	Vin (V)	Primary voltage (V)	Secondary voltage (V)	Voltage ratio	Peak o/p current (A)
1	10	69.6	59.2	0.85	0.59
1.2	10	72.8	63.2	0.87	0.63
1.5	10	62.4	55.2	0.88	0.55
1.8	10	53.6	48.0	**0.90**	0.48
2.0	10	48.8	41.6	0.85	0.42
2.2	10	44.8	37.6	0.84	0.38
2.4	10	40.8	34.4	0.84	0.34
2.5	10	39.2	31.2	0.80	0.31
1	15	96.0	81.6	0.85	0.82
1.2	15	100.8	88.0	0.87	0.88
1.5	15	88.8	78.4	0.88	0.78
1.8	15	75.2	67.2	**0.89**	0.67
2.0	15	68.0	60.8	0.89	0.61
2.2	15	62.4	54.4	0.87	0.54
2.4	15	57.6	48.8	0.85	0.49
2.5	15	53.6	44.0	0.82	0.44
1.5	20	112.0	98.4	0.88	0.98
1.8	20	97.6	88.0	**0.90**	0.88
2.0	20	91.2	79.2	0.87	0.79
2.2	20	81.6	71.2	0.87	0.71
2.4	20	75.2	64.8	0.86	0.65
2.5	20	70.4	59.2	0.84	0.59
1.8	25	116.8	104.8	**0.90**	1.05
2.0	25	109.6	94.4	0.86	0.94
2.2	25	100.8	87.2	0.87	0.87
2.4	25	92.0	78.4	0.85	0.78
2.5	25	85.6	72.8	0.85	0.73

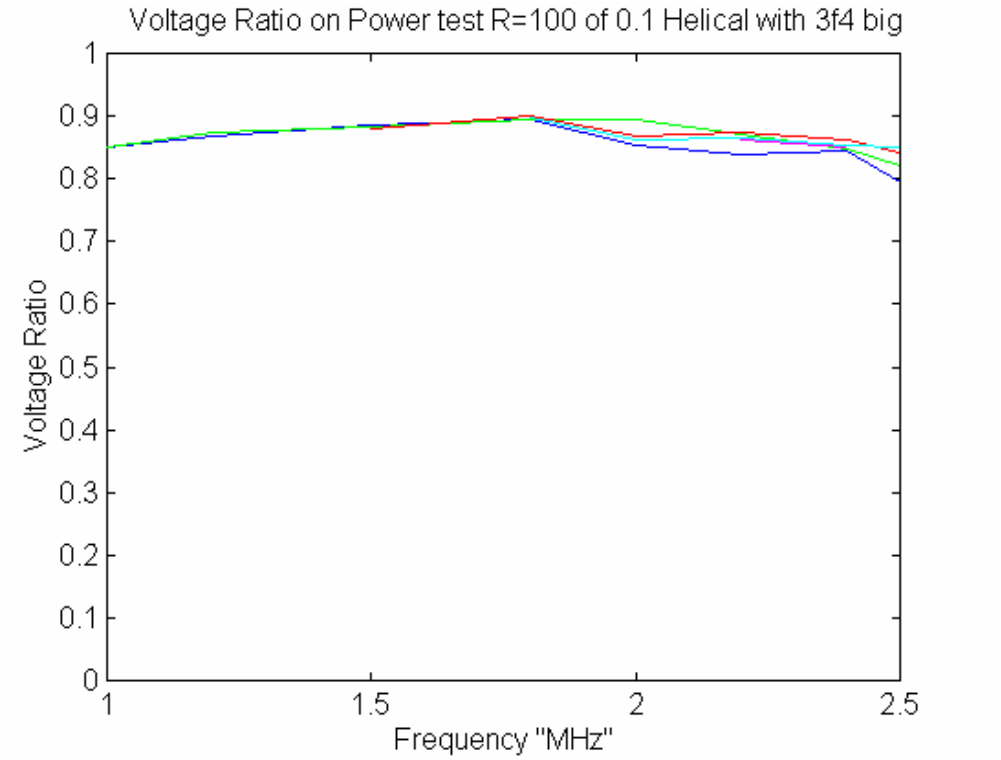

Figure 4.32 Voltage ratio of planar transformer with ferrite material of 3F4.

The voltage ratio of the planar transformer with helical winding of 0.1 mm substrate and ferrite material of 3F4 is found above 0.8 within the testing frequency range from 1 to 2.5 MHz. The peak value of the voltage ratio for all the cases is 0.9 at the frequency of 1.8 MHz with the output loading of 100 Ω. It is similar with different primary voltages from 53.6 V to 104.8 V. The detail of the voltage ratio can be seen in Figure 4.32.

The switching waveform of the testing transformer is shown in Figure 4.33. A 100 Ω power resistor was connected to the output of the transformer. The output voltage of the transformer sample was monitored by the channel 1 of the oscilloscope. The input characteristics of the transformer were observed by channel 2 and 4 for the input voltage and input current respectively. At the operating frequency of 1.8 MHz, the output voltage of the transformer is 88.0 $V_{p\text{-}p}$ and the input voltage is 97.6 $V_{p\text{-}p}$. The voltage ratio is 0.901 and the peak output current is 0.88 A.

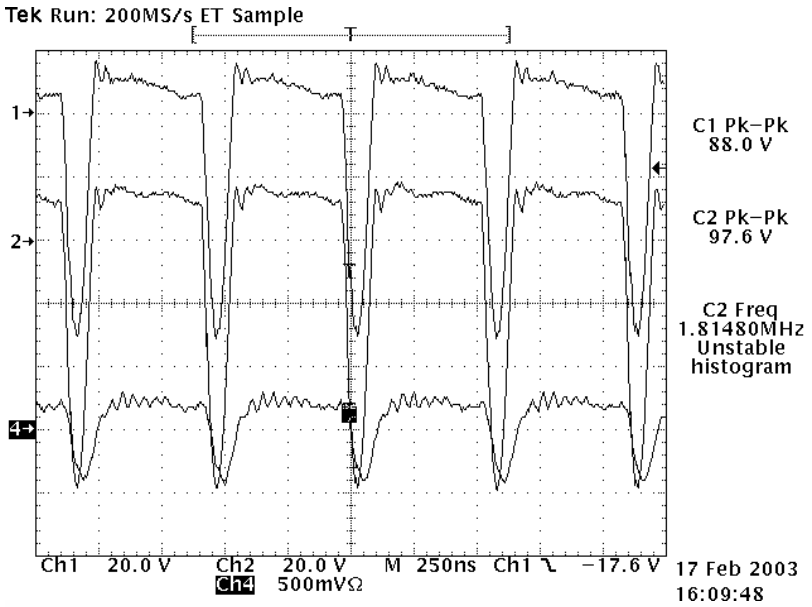

Figure 4.33 Switching waveform of the testing transformer.

The planar transformer with helical winding structure was tested with output loading to demonstrate the power performance. The magnetic flux distribution of the transformer described the characteristic of evenly flux distribution inside the winding structure and low electromagnetic with the planar ferrites. The planar transformer also has advantages of the evenly distributed eddy current and the relatively higher input impedance. The manufacturing cost is much lower than the cost of traditional HF transformers. It improves significantly the ratio of the performance / cost of the HF transformer design. It is an ideal type of switching transformer for high frequency, low to medium power applications.

4.11 References

1. K. Kawabe, H. Koyama and K. Shirae, "Planar Inductor", *IEEE Trans. on Magnetics*, vol. MAG-20, No. 5, September, 1984.

2. J.W. Lu, F.P. Dawson and S. Yamada, "Analysis of High Frequency Planar Sandwich Transformers for Switching Converters", *IEEE Trans. on Magnetics*, vol. 31, No. 6. Nov., 1995, pp.4235-4237.

3. K. Yamaguchi, S. Ohnuma and etc., "Characteristics of a Thin Film Microtransformer with Circular Spiral Coils", *IEEE Trans. On Magnetics*, vol. 29, No. 5, Sep. 1993, pp.2232-2237.

4. H. Tsujimoto and Ieyasu O, "High Frequency Transmission Characteristic of Co-planar Film Transformer Fabricated on Flexible Polyamide Film", *IEEE Trans. on Magnetics*, vol. 31, No. 6. Nov., 1995, pp.4232-4234.

5. M. Mino, T. Yachi and etc., "Planar Microtransformer with Monolithically-Integrated Rectifier Diodes for Micro-Switching Converters", *IEEE Trans. on Magnetics*, vol. 32, No. 2. Mar., 1996, pp.291-296.

6. C. Ahn and M. Allen, "A New Toroidal-Meander Type Integrated Inductor with A Multilevel Meander Magnetic Core", *IEEE Trans. on Magnetics*, vol. 30, No. 1. Jan., 1994, pp.73-79.

7. J. Park, K.Lagorce and M. Allen, "Ferrite-Based Integrated Planar Inductors and Transformers Fabricated at Low Temperature", *IEEE Trans. on Magnetics*, vol. 33, No. 5. Sep., 1997, pp.3322-3324.

8. S. Yamada, H. Fujiki and etc., "Investigation of Printed Wiring Board Testing by Using Planar Coil Type ECT Probe", *IEEE Trans. on Magnetics*, vol. 33, No. 5. Sep., 1997, pp.3376-3378.

9. *Oersted 2D/RS time-harmonic electromagnetic design software manual*, 1995.

10. *IEEE Standard Dictionary of Electrical and Electronics Terms*, 4th Edition, IEEE Inc. New York 1988.

11. P.L. Dowell, "Effect of eddy currents in transformer windings", Proc. IEE, vol. 113, No. 8, pp.1387-1394, Aug. 1966.

12. Fu Wong, J.W. Lu and etc, "Applications of high frequency magnetic components for switching resonant mode power supply", Proc. IEEE-ICIT'96.

13. E.C. Snelling, *Soft ferrites - Properties and applications*, Iliffe Books LTD., 1969.

14. *Ferrite and Accessories Data Book*, Siemens, 1990.

15. Michael P. Perry, *Low Frequency Electromagnetic Design*, Marcel Dekker, Inc. 1985.

16. Lionel Warnes, *Electronic and Electrical Engineering, Principles and Practical*, 2nd ed. Macmillan Press Ltd, 1998.

17. Henry W. Ott, *Noise Reduction Techniques in Electronic System*, 2nd ed. John Wiley & Sons, 1988.

18. David K. Cheng, *Field and Wave Electromagnetics*, 2nd ed. Addison-Wesley Publishing Company, Inc, 1989.

19. Ivan W. Hofsajer, Jan A. Ferreira and J. Daan van Wyk, "Design and Analysis of Planar Integrated L-C-T Components for Converter", *IEEE Trans. on Power Electronics*, vol, 15, No. 6, November 2000, pp. 1221-1227.

20. S. C. Tang, S. Y. Ron Hui and S. H. Chung, "A low-Profile Power Converter Using Printed-Circuit Board (PCB) Power Transformer with Ferrite Polymer Composite", *IEEE Trans. on Power Electronics*, vol. 16, no. 4, July 2001, pp. 493-498.

21. S. Y. (Ron) Hui, S. C. Tang and Henry Shu-Hung Chung, "Some Electromagnetic Aspects Coreless PCB Transformers", *IEEE Trans. on Power Electronics*, vol. 15, no. 4, July 2000, pp. 805-810.

22. Daniel R. Frankl, *Electromagnetic Theory*, Prentice-Hall, Inc., 1986.

Chapter 5

Conclusions and Suggestions for Future Work

5.1 Conclusions

5.2 Suggestions for Future Work

Researchers and engineers of switching mode power supply face challenges to develop new power supplies to meet the requirements of modern electronics in the 21st Century. The design of switching mode power supplies in the new century is an arduous task. With the rapid consumer demand for semiconductors, the technical requirement of power supplies has been set very high.

The high frequency transformer is essential to modern switching mode power supplies. It performs the important task of transferring the pulsed energy from input source to output loads. With the advances in silicon carbide, the switching capability of MOSFET is significantly increased in both the switching frequency and the power handling ability. High power and high frequency pulsed energy can be generated and pumped into the backbone – the high frequency power transformer of switching mode power supplies. High frequency transformers are necessary for handling of extreme heavy power loads. The new power transformer is in enormous demand.

5.1 Conclusions

A planar transformer with helical winding structure offered significant improvement for switching mode power supplies working at high frequency range. It maintains the typical advantages of planar transformers and further improves the unbalanced magnetic flux distribution, as described in Chapter 4. The low eddy current distributed in the helical winding is the principle improvement. The maximum eddy current density of helical winding structure is only 27% of the eddy current density of meander type winding structures and 33% of the eddy current density of spiral type winding structure under the same operating frequency and excitation current. With less eddy current flowing through the winding, there is less leakage inductance.

In addition, the coupling efficiency of the planar transformer with the helical winding structure is the highest of the three planar winding structures. The voltage ratio of the transformer is measured as high as 0.9, shown in Table 4.11. It is 150% of the voltage ratio of the transformer with circular spiral coils, listed in Table 4.5.

The voltage ratio was measured experimentally, and was found to be inversely related to the vertical distance between the copper strips of primary and secondary of the helical winding structure. This is an important design consideration for a planar transformer with helical winding structure.

The planar ferrite pieces are an essential part of the transformer with helical winding structure. They enclose the magnetic flux around the copper strips of the winding and well defined the length of the magnetic path. However, the ferrite materials do not strongly affect the voltage ratio and the magnetic flux distribution of the planar transformer with helical winding structure.

In conclusion, the planar transformer with helical winding structure is excellent for high frequency switching mode power supply applications.

This study has made significant contributions to the application of high frequency transformers for switching mode power supply. The investigation of planar transformers with helical winding structures can be a new step in the development of high frequency magnetics in the 21st Century.

5.2 Suggestions for Future Work

In this thesis, the fundamental investigation of planar transformer with helical winding structure has been performed. However, there is still a long way to go before the transformer design rules are fully mature.

The basic concept of the transformer has been established, and one of the design considerations has been examined. However, there are many conditions that should be further considered, for example, the relationship between the area of the winding and the power handling of the transformer, and the effect of the length of winding and the operating frequency. Now, the transformer is commonly called a high frequency transformer, but it should be correctly classified as a low frequency electromagnetic device, according to the low frequency approximations – the dimension of the device is much less than its wavelength. Unfortunately, if the operating frequency of the transformer is further increased to 100 MHz, according to $\lambda = \frac{c}{f}$, then the wavelength is only 3 m. The dimension of the device is not much less than the wavelength. Therefore, the low frequency approximations applied on the transformer should be revised and more high frequency conditions should be considered.

In addition, the transformer with helical winding structure is a very good match with semiconductor technology. It can be easily adopted by the integrated circuit to form an integrated power modular to be used in the modern portable electronic devices. Therefore, the fabrication technique of a planar transformer with a helical winding structure with the integrated technology should be developed in the near future.

With the continuous effort of researchers, the planar transformer with helical winding structure will become an irreplaceable magnetic component in switching mode power supplies.